THE COPOLYMERIZATION OF CO_2 AND CYCLIC ETHERS AND THEIR

DEGRADATION PATHWAYS

A Dissertation

by

SHENG-HSUAN WEI

Submitted to the Office of Graduate Studies of
Texas A&M University
in partial fulfillment of the requirements for the degree of

DOCTOR OF PHILOSOPHY

Chair of Committee,	Donald J. Darensbourg
Committee Members,	François P. Gabbaï
	Hongcai Zhou
	Hong Liang
Head of Department,	David H. Russell

August 2013

Major Subject: Chemistry

ABSTRACT

      Polycarbonates are found in a variety of common products in daily life due to their favorable mechanical and electrical properties. In addition, they are widely used in biomedical areas due to their stability and biological inertness. Therefore, the production of polycarbonates became an important industrial process in the past decades. However, the current industrial process usually requires toxic phosgene gas as a starting material. Thus, the environmentally benign route by using metal catalyzed couplings of epoxides and CO_2 to produce polycarbonates has received attention from researchers.

      In this dissertation, metal catalyzed CO_2/cyclic ether copolymerization, depolymerization of polycarbonates, and the equilibria between polycarbonate and corresponding six-membered cyclic carbonate will be investigated. First, the Co(III) catalyzed copolymerizations of CO_2 and various epoxides with electron-withdrawing substituents to afford polycarbonates are examined. Comparative kinetic studies were performed via in situ infrared measurements as a function of temperature to assess the activation barriers for the production of cyclic carbonate versus copolymer involving electronically different epoxides: styrene oxide, epichlorohydrin, and propylene oxide.

      Thermodynamically stable cyclic carbonate byproducts are produced during the course of the reaction from the degradations of propagating polymer chains. The depolymerization reactions of several polycarbonates produced from the completely alternating copolymerization of styrene oxide, epichlorohydrin, propylene oxide, cyclohexene oxide, indene oxide, and cyclopentene oxide with carbon dioxide have been

investigated. Various reaction pathways can be found under different reaction conditions, including process involving chain-end backbiting and radical intermediates. Temperature-dependent kinetic studies have provided energy of activation barriers for cyclic carbonate formation. In addition, the generated monomeric materials from the degradation of select polycarbonates show the possibility of chemical recycling of plastic waste.

For the copolymers made from CO_2 and oxetane derivatives, this study focuses on the influence of steric hindrance in the 3-position of the monomer oxetane. The (salen)CrCl/onium salt catalyzed coupling reactions of these oxetane derivatives and carbon dioxide are reported. Depolymerizations of copolymers to their corresponding cyclic carbonates were also studied. In addition, several six-membered cyclic carbonates were synthesized to examine their equilibria between monomeric cyclic carbonates and their corresponding polycarbonates.

DEDICATION

       This dissertation is dedicated to my parents, Tien-Wang Wei and Pai-Yi Song, in thanks for their endless love and support.

ACKNOWLEDGEMENTS

First, I would like to thank my advisor, Prof. Donald J. Darensbourg. He offers us freedom to design creative research projects, although most of our personal ideas are obviously stupid. His patient and careful guidance directs us toward the correct way of targeting problems. Undoubtedly, Don is more than an excellent and super research advisor; he is more like a fantastic uncle to the group as well. His sense of humor and laughter penetrate over the entire hallway and make our lives happier. If I have a chance to be a leader in the future, I will definitely follow his example. In addition, I appreciate my committee members, Prof. François P. Gabbai, Prof. Hongcai Zhou, and Prof. Hong Liang, for serving on my committee and offering their suggestions on my dissertation to make me a better scientist. Next, I would like to acknowledge Prof. Xiaobing Lu and Dr. Guangpeng Wu from Dalian University of Technology for the collaborative project. Thanks to Dr. Joseph H. Reibenspies and Dr. Nattamai Bhuvanesh for their kindness help on refining some complicated X-ray crystal structures.

Without the company of "Taiwanese Mafia at TAMU-CHEM," I would have felt extremely bored during the past five years of living in such a small town. The entertainment that they provided filled my soul outside of the research laboratory. I must express my appreciation to them from the bottom of my heart. For security reasons, their names are confidential.

Special thanks go to Prof. Marcetta Y. Darensbourg. For me, Marcetta is like a mother of mine in College Station, always sharing tea and chatting on various interesting

topics with me. The other important part of my research life that I would like to thank and will never forget is the awesome DJD group members: Dr. Shawn Fitch, Dr. Jeremy Andreatta, Dr. Adriana Moncada, Dr. Osit Karroonnirun (Pop), Dr. Ross Poland, Wan-Chun Chung (Joanna), Andrew Yeung, Sam Kyran, and Yanyan Wang. The one I have to express my extremely special gratitude is to Dr. Stephanie Wilson. Without her help editing my articles, nobody would understand my weird English writing. Also, I appreciate for the discussions between us on everything not only about research, but also those more common talks that are not related to chemistry. Working with a variety of visiting scholars from different countries including Prof. Carla Moura, Prof. Adolfo Horn Jr., Dr. Bo Li, Prof. Binyuan Liu, and Dr. Fu-Te Tsai is really a nice experience in our group that has provided me a broad view of different cultures. As well as all the members in MYD group, I am very thankful for your support. There is still one more person that I must mention − our super powerful administrative assistant, Ms. Ethel Mejia. Thank you!!

The last but not the least, my biggest thanks is given to my dear family in Taiwan. My appreciation to you is more than words. I love you.

NOMENCLATURE

abs	Absorbance
AIBN	Azobisisobutyronitrile
Ar	Argon
ATR	Attenuated Total Reflectance
BF_4	Tetrafluoroborate
b.p.	Boiling Point
BPA	Bisphenol-A
CaF_2	Calcium Fluoride
CaH_2	Calcium Hydride
$CDCl_3$	Deuterated Chloroform
CH_3COONa	Sodium Acetate
CO_2	Carbon Dioxide
$COCl_2$	Phosgene
CPC	Cyclic Propylene Carbonate
DBU	1,8-diazabicyclo[5.4.0]undec-7-ene
DNP	2,4-dinitrophenoxide
DSC	Differential Scanning Calorimetry
Ea	Activation Energy
EA	Ethyl Acetate
ee	Enantiomeric Excess

ESI-MS	Electrospray Ionization Mass Spectrometry
FT-IR	Fourier Transform-Infrared Spectroscopy
GPC	Gel Permeation Chromatography
h or hr	Hour
HCl	Hydrochloric Acid
IR	Infrared Spectroscopy
KOH	Potassium Hydroxide
LALS	Low-Angle Light Scattering
LiAlH$_4$	Lithium Aluminum Hydride
MALDI-TOF	Matrix-Assisted Laser Desorption/Ionization- Time of Flight
min	Minute
MgSO$_4$	Magnesium Sulfate
MMO	3-methoxy-methyl-3-methyloxetane
M$_n$	Number Average Molecular Weight
MPa	Megapascal
MTBD	7-methy-1,5,7-triazabicyclo[4.4.0]dec-5-ene
MTC	5-methoxy-methyl-5-methyl-1,3-dioxan-2-one
M$_w$	Weight Average Molecular Weight
N$_2$	Nitrogen
NaCl	Sodium Chloride
NaH	Sodium Hydride
NaHMDS	Sodium Bis(trimethylsilyl)amide

n-Bu$_4$N	Tetra-n-butyl Ammonium
NMR	Nuclear Magnetic Resonance
NO$_3$	Nitrate
Nu	Nucleophile
OAc	Acetate
-OH	Hydroxy
PDI	Polydispersity Index
PCy$_3$	Tricyclohexylphosphine
PECC	Poly(CO_2-*alt*-epichlorohydrin)
PPC	Poly(propylene carbonate)
ppm	Parts Per Million
PPN	Bis(triphenylphosphine)iminium
PSC	Poly(styrene carbonate)
RALS	Right-Angle Light Scattering
ROP	Ring-opening Polymerization
T	Temperature
t	Time
t-Bu	*tert*-Butyl
TBD	1,5,7-triabicyclo[4,4,0] dec-5-ene
TCE	1,1,2,2-tetrachloroethane
TEMPO	(2,2,6,6-tetramethylpiperidin-1-yl)oxyl
T$_g$	Glass Transition Temperature

THF	Tetrahydrofuran
TMC	Trimethylene Carbonate
tmtaa	Tetramethyltetraazaannulene
TOF	Turnover Frequency

TABLE OF CONTENTS

LIST OF FIGURES

LIST OF TABLES

xviii

CHAPTER I

INTRODUCTION AND LITERATURE REVIEW

Brief review of polycarbonates

Polycarbonates are a class of engineering thermoplastics with high quality and outstanding properties including strength, lightness, durability, high transparency, heat resistance, and good electrical insulation.[1] The properties of polycarbonates can be easily controlled depending on the functionalities of the backbones and side chains, which can be aliphatic, alicyclic, or aromatic groups.

The main advantage of polycarbonates over other types of plastic is their great strength along with light weight. Bulletproof windows and enclosures inside banks are often made of polycarbonates because they are nearly unbreakable.[2] In addition, certain types of environmentally friendly and readily degradable polycarbonates are widely used in biomedical areas due to their biodegradability and biological inertness. Polycarbonates are used to make eyeglasses because of their outstanding transparency, durability, high refractive index, and ease of processing. Polycarbonate lenses can be thinner than glass or conventional plastic, making them the ideal materials for heavy prescriptions. Since polycarbonates can be easily colored and compatible with other materials, sunglasses manufacturers choose polycarbonates as materials. They can be facilely shaped without splitting or cracking, resulting in extremely lightweight, distortion-free, fashionable glasses that feature all of the health benefits doctors recommend. Furthermore, the toughness, shatter-resistance and heat-resistance of

polycarbonates make them excellent choices for tableware, reusable bottles, and food storage containers that can be conveniently used in the refrigerator and microwave. The electronics industry uses polycarbonates to create transparent colored computer cases, cell phones, pagers, and laptops for daily life.

Due to these advantages, polycarbonates are currently used for a wide variety of common products including water bottles, automobile headlights, bulletproof windows, sports equipment, construction glazing, various household electronics, data storage devices like CDs and DVDs, et al.[3]

Industrial routes to polycarbonate

Annual market growth for polycarbonates has been more than 10 % from the late 1990s.[4] Nowadays, about 2.7 million tons of polycarbonates are produced in industry every year all over the world.[5] The commercial productions of polycarbonates are mostly by an interfacial polycondensation between diols and phosgene ($COCl_2$), and thus have been called "phosgene process" (**Figure 1**).[6, 7]
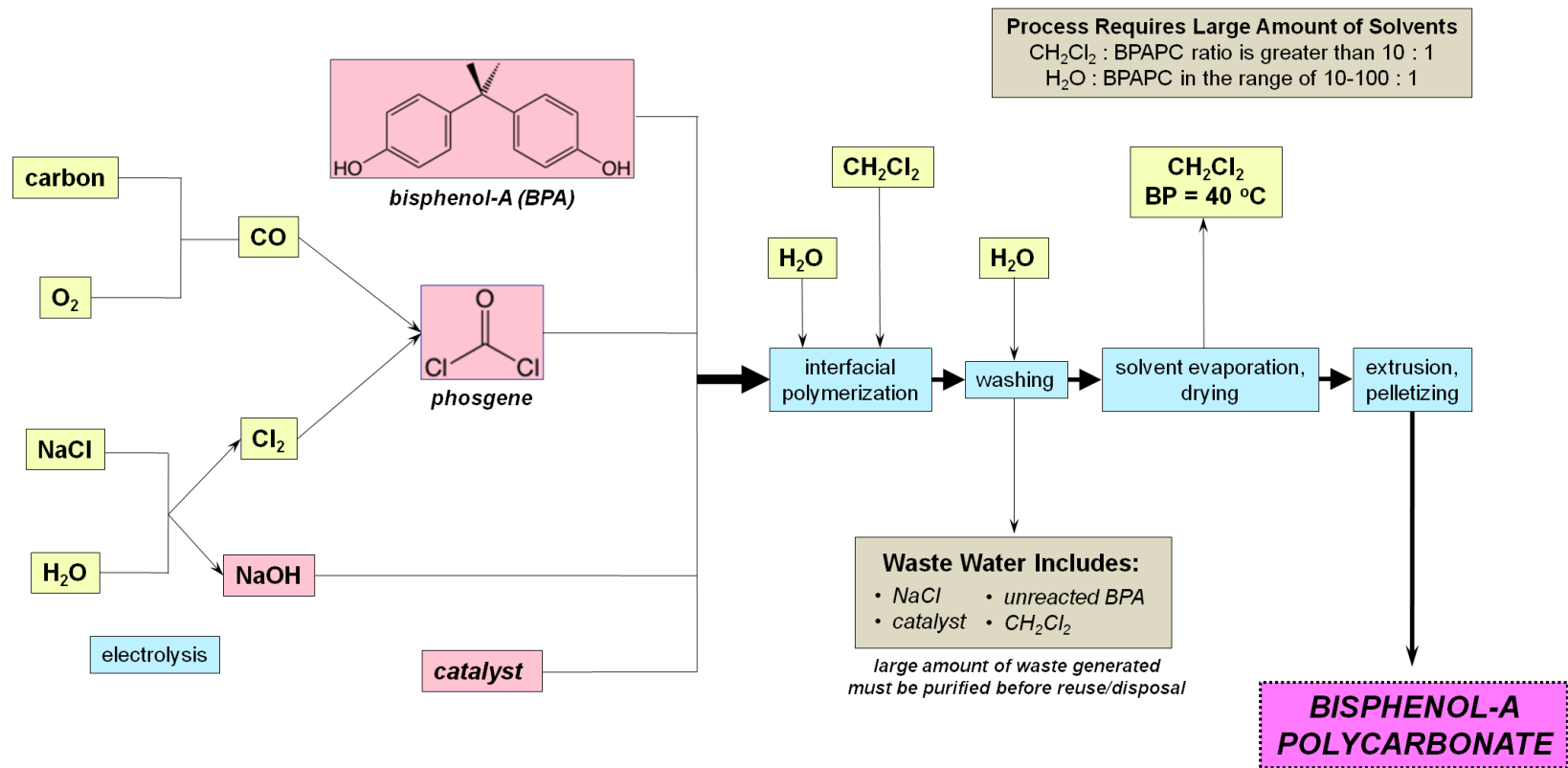
Figure 1. Phosgene process for polycarbonates production.[5]

The polycarbonate made from 2,2-bis-(4-hydroxyphenyl)-propane (bisphenol-A) became the most important industrial plastic since 1950s due to its mechanical and electrical properties. It was discovered by Schnell, Bottenbruch, and Krimm in 1953 at Bayer, and independently by Fox at General Electric Company shortly afterwards.[3] This polymer, known as Lexan®, Makrolon®, Makroclear® and others, is optically transparent and has strong impact strength. It has wide usable temperature from -100 $^{\circ}$C to 135 $^{\circ}$C with a high glass transition temperature of 145 to 150 $^{\circ}$C.[8] With these properties of clarity, strength, and workability of poly(bisphenol-A) make it useful in a variety of applications. The industrial process to produce poly(bisphenol-A carbonate) was first commercialized by General Electric Company using bisphenol-A and phosgene in the presence of pyridine.[5] All the industrial phosgene methods are carried out in an interfacial system with two immiscible solvents, mostly water and a chlorinated solvent such as dichloromethane. The reaction occurs between the aqueous phase with di-sodium salt of bisphenol-A dissolved and the organic portion with phosgene under a strong agitation. The generated polycarbonate can be separated by extraction into the chlorinated organic solvent, which is usually CH_2Cl_2 is used due to polycarbpnates' high solubility in it.

Despite the many advancements that have been made since the 1950s, there are still a number of downsides to the phosgene process, especially in terms of health and economic issues.[5]

(1) A large amount of dangerous and corrosive phosgene is required for this process. However, phosgene is a highly toxic gas and is known as a chemical

weapon dating back to World War I. Therefore, the production of phosgene has been very restricted worldwide.

(2) 10 weight equivalents of CH_2Cl_2 solvent are used to produce 1 equivalent of polycarbonate. CH_2Cl_2 is a low boiling point solvent and also a well known carcinogen. Thus, long terms of exposure will cause health issues for people involved in the process. Also, it is hard to completely prevent releasing CH_2Cl_2 into atmosphere since the boiling point is low.

(3) A very large amount of water is used for purification of polycarbonate in CH_2Cl_2 by extraction to remove water soluble salts, oligomers, and catalyst used in polymerization. This water must undergo costly purification before reuse or reentering into public waterways.

(4) Industrial equipment used in the production process can be easily corroded due to reactions with chloride anion and chlorine gas. Almost all systems have contact with chlorine, methylene chloride, and hydrochloric acid, which are highly corrosive to metal. Thus, a great cost is needed to maintain facilities for replacing corroded parts.

(5) Unavoidable chlorinated impurities within the final polycarbonate product have a detrimental effect on polymer properties.

Non-phosgene process was designed to reduce the use of toxic phosgene by running a melt polymerization of diols and safer phosgene substitutes, such as diphenyl carbonate. However, this pathway needs to be run in a very high temperature (280 to 310 ℃) under a high vacuum of 1 mmHg or less, consuming much more energy.[6] Also,

high reaction temperature causes the high possibility of undesired side reactions. The purification process becomes more complicated to remove byproducts generated from the method involving phosgene substitutes. For example, high temperature and high vacuum are needed to remove generated phenol from highly viscous polycarbonates. Thus, more cost must be spent on the alternative route replacing phosgene. In addition, ultra high pure diphenyl carbonate with low cost is usually conventionally produced from the reaction of phosgene with phenol.[5] Therefore, the use of these safer replacements does not completely solve the problem of handling toxic phosgene.

Although many advancements have been made to make the phosgene process safer, cleaner, and have a higher yield, it still inherently has poor atom economy, is time consuming, produces large quantities of solvent waste, and poses several health and environmental concerns.[9] Thus, there is a need to find an alternative route for affording this type of useful plastics. It would be a great advance and assist in improving the industrial method employing a more environmental-friendly synthetic pathway for polycarbonates production.

Copolymerization of CO_2/cyclic ether

In 1969, a remarkable discovery that provided an environmentally benign route to polycarbonate was made by Inoue using the metal catalyzed copolymerization of carbon dioxide, CO_2, and epoxides in the presence of a heterogeneous catalyst made from the mixture of diethylzinc and water (**equation 1**).[10] Although the catalytic activity was very low, it demonstrated another pathway to make polycarbonates and opened a new research area of polymer chemistry. Using this method, cyclic carbonate can be

afforded as a byproduct and some ether linkages can be found in the polymer chain. Polycarbonate is formed by the alternating insertion of epoxide and CO_2. Ether linkages can be generated due to the consecutive ring opening of epoxide. The byproduct cyclic carbonate is an intramolecular backbiting product, and this backbiting mechanism will be further discussed in the following section. By the new synthetic route, CO_2 works as both solvent and as a reagent. CO_2 is a nontoxic, nonflammable, cheap and naturally abundant C1 feedstock, resulting in a safer way to produce polycarbonates than phosgene process. CO_2 is considered one of the major greenhouse gases that can absorb and emit infrared radiation within the thermal infrared range. In recent years, technologies have been developed not only to reduce but also to capture the 37 Gton per year of the total anthropogenic CO_2 emissions. This coupling reaction provided a constructive use of a greenhouse gas to make daily used products. It represents environmentally-friendly and potentially less expensive route to make polycarbonates than the current industrial processes.

$$CO_2 \quad + \quad \overset{O}{\underset{R_1 \quad R_2}{\triangle}} \quad \xrightarrow{\text{catalyst}} \quad \left(\!\!\left(O\!\!\begin{array}{c}R_1\\\\R_2\end{array}\!\!O\!\!\begin{array}{c}O\\\\\end{array}\!\!\right)_n\!\!\left(O\!\!\begin{array}{c}R_2\\\\R_1\end{array}\!\!\right)_m\right) \quad + \quad \overset{O}{\underset{R_1 \quad R_2}{O\!\!\bigtriangleup\!\!O}} \tag{1}$$
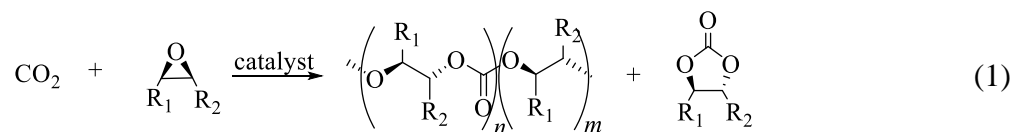
After Inoue's first example, numerous of Zn-based catalysts were developed for copolymerizing epoxide and CO_2 while the turnover frequency (TOF) is still low. Lots of effort was put into looking for new catalytic system, including the study of aluminum

tetraphenyl porphyin, the first homogeneous catalyst for copolymerizing CO_2 and epoxide, reported by Inoue in 1978.[7b, 11]   The major advance came in 1995 while Darensbourg group discovered the homogeneous well-defined zinc bis-phenoxide catalysts providing a significant increase in activity over the previously catalysts reported for copolymerization of CO_2 and cyclohexene oxide.[12]   The active species were believed in a dimeric structure supported by the lack of catalytic activity in the presence of 1 equiv of PCy_3 per zinc center.   NMR experiments support that the nucleophilic addition to epoxide is involved in the initiation step.   After that, Beckman has developed a similar Zn-based compound for cyclohexene oxide copolymerization in supercritical CO_2.[13] Along with Darensbourg's work of zinc phenoxide catalysts, these studies demonstrated that the initiator for polymerization is part of the ligand in the catalysts.

The following breakthrough of the zinc-based catalyst is the use of a new class of well-defined, high-activity Zn β-diiminates investigated by Coates in 1998, representing some of the most active catalysts reported under mile condition.[14]   A bimetallic mechanism was proposed based on a series of stoichiometric insertion reactions, and rate studies.[15]   In the later study by Chisholm, the initial ring-opening step involving sterical bulky anionic initiators probably undergoes a monometallic transition state for copolymerization of cyclohexene oxide and CO_2.[16]   In addition, the β-diiminate zinc catalysts were highly active for the other living ring-opening polymerization of lactide,[17] ε-caporlactone, and β-butyrolactone.[18]

In 2000, Holmes reported that tetrakis(pentafluorophenyl)porphyrin chromium(III) chloride showed catalytic activity for the alternating copolymerization of cyclohexene oxide and CO_2 in the presence of an organic base.[19] Another year later, Darensbourg and coworker developed the use of salen chromium(III) complex, where H_2salen = *N,N'*-bis(3,5-di-*tert*-butyl-salicylidene) -1,2-cyclohexene diamine, to be an effective catalyst for the coupling of cyclohexene oxide and carbon dioxide making poly(cyclohexenylene carbonate) in high yields along with a small quantity of *trans*-cyclic carbonate byproduct.[20] This series of developments for catalysts was inspired by Jacoben's study which found salen chromium complexes are highly active for the asymmetric nucleophilic ring-opening of epoxides.[21] The Schiff base ligands can be easily synthesized, and the catalytic activity can be tuned by changing the sterics and electronics on ligand architecture. In most cases, cocatalysts can be applied to enhance the catalytic activity.

The catalytic reaction mechanism has been proposed. The cocatalyst will first bind to metal salen complex to form an anionic species. Epoxide will then coordinate onto the metal center, followed by a nucleophilic attack to ring open the epoxide. The next step is CO_2 insertion, thus forming the carbonate group in the growing chain. Polycarbonates are then made by repeating the epoxide coordination, ring opening, and CO_2 insertion steps (**Scheme 1**).[22]

Scheme 1. Reaction mechanism of copolymerization of CO_2 and epoxides.

$\rightsquigarrow P$ = growing polymer chain
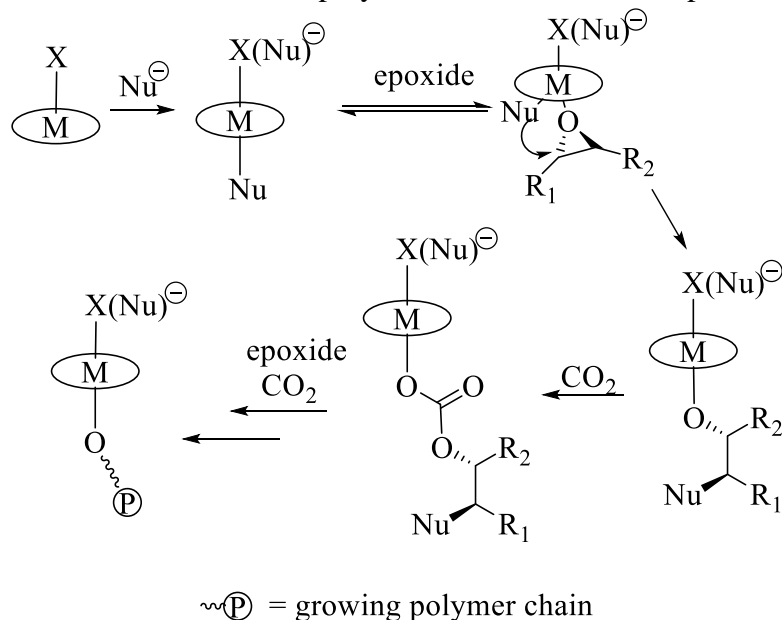
Darensbourg and Fitch have proved only one polymer chain propagation occurs on each metal center by using tetramethyltetraazaannulene (tmtaa) chromium complexes with one side protected by side arm of the ligand and the other side is free.[23] Comparing with chromium complex without strapped ligand, both catalysts show similar catalytic activities and formation rates on both polycarbonate and cyclic carbonate.

Salen chromium(III) catalyst system works not only in three-membered epoxides but also in four-membered ring oxetane derivatives.[24] The low-level of ether linkage found in this type of copolymer can be mechanical explained. Oxetane and CO_2 can be copolymerized directly in a similar manner to CO_2/epoxide copolymerization or they can generate six-membered cyclic carbonates. The kinetic product, cyclic carbonate, then undergoes ring-opening to afford the thermodynamic product, polycarbonate, without ether linkages (**Scheme 2**).[24] This ring-opening process of six-membered cyclic

10

carbonates retains all of the carbonate linkages and produces alternating copolymer, effectively reducing the undesired ether linkages within the polymer chain.

Scheme 2. Mechanism of copolymerization of CO_2 and oxetane.
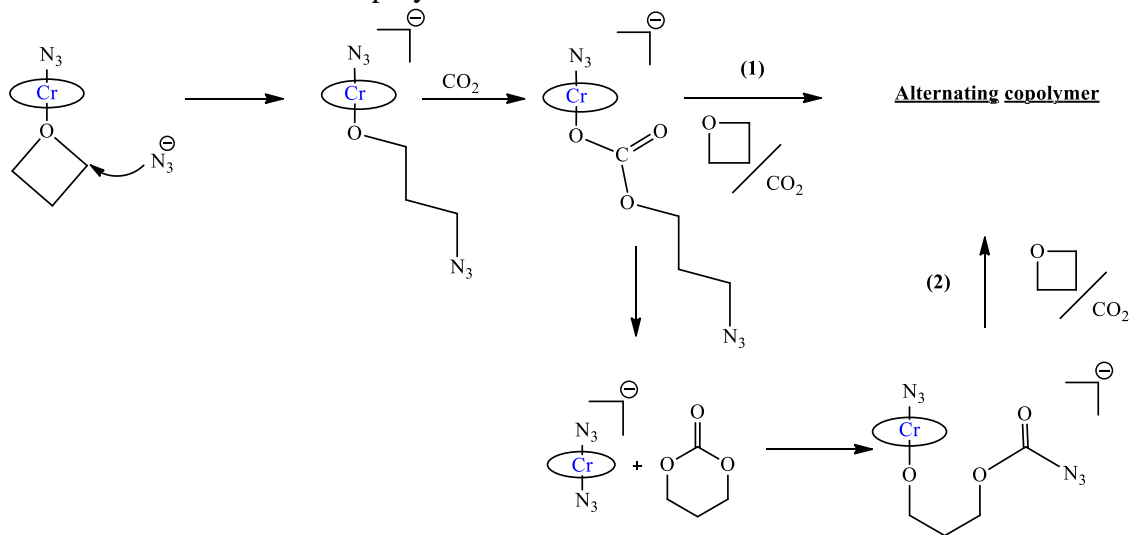
Although notable successes on Coates's Zn β-diiminates catalysts were achieved for the copolymerization of CO_2 with alicyclic epoxides (such as cyclohexene oxide), their high activities with aliphatic epoxides (such as propylene oxide), have not been reported. (Salen)Co(III) complex developed by Coates successfully solved this difficulty, catalyzing the copolymerization of propylene oxide and CO_2 to produce polycarbonate and preformed high selectivity to polymer with excellent regioselectivity.[25] Designing this type of catalysts opens a new window for related research area in the following decades.

Inspired by Coates's dimetallic mechanism of Zn β-diiminates and highly efficient salen metal complexes, Williams developed a special catalytic system combining two salan units with di- or tri- zinc metal centers.[26] Similarly, other metals were applied in this ligand showing high catalytic activities, such as Co,[27] Fe,[28] Mg.[29]

Problems for CO_2/cyclic ether copolymers

Although several different catalyst systems have been developed, the main difficulty for the epoxide/CO_2 copolymerization is the polycarbonates generated from this process do not have an excellent working temperature range. The glass transition temperatures are not as high as the most useful industrial polycarbonate, poly(bisphenol-A carbonate) which has a T_g of 145 to 150 ^{o}C.[8] Cyclohexene oxide and propylene oxide are the most studied monomers in this area, and the T_gs of the polycarbonate formed are 115 ^{o}C and 35 ^{o}C, respectively. The low T_g limits the applications for these polycarbonates. It is found that the regioregularity of CO_2/epoxide copolymers also has a critical influence on their T_gs. Several reports shows that increasing regioregularity of of poly(propylene carbonate) results in an increase in the T_g from 37 ^{o}C to 47 ^{o}C, 10–12 ^{o}C higher than that of atactic polymer. [30] Furthermore, a novel stereogradient poly(propylene carbonate) was reported with a higher thermal stability than the irregular poly(propylene carbonate).[31] A similar observation was also found for the copolymerization of cyclohexene oxide and CO_2 showing that stereoregular poly(cyclohexene carbonate) is a semicrystalline thermoplastic, and possesses a high melting point of 215–230 ^{o}C and increase the T_g to 122 ^{o}C.[32] It is also true in the copolymer from CO_2 and epichlorohydrin resulting that the T_g of the isotatic copolymer

with a 94% *ee* is found at 42 $^{\circ}$C, which is 11°C higher than atatic poly(CO$_2$-*alt*-epichlorohydrin).[33]

On the other hand, strategy of choosing different monomer to afford highly thermal stable polycarbonate was also reported. Darensbourg and Wilson have published the synthesis of poly(indene carbonate) made from indene oxide and CO$_2$ in the presence of salenCo(III) binary catalyst system, giving the highest T$_g$ at 134 $^{\circ}$C ever reported by epoxide/CO$_2$ copolymerizations.[34] This might show a potential great leap to reach the goal of making polycarbonates by epoxide/CO$_2$ copolymerization with higher T$_g$.

Backbiting of polycarbonates

In addition to the catalytic activity toward polymer production, the other large challenge is to avoid the formation of cyclic carbonate. The cyclic carbonate is formed during polymerization *via* the backbiting mechanism. The nucleophilic attack is able to occur from both alkoxide anion and the carbonate unit (**Scheme 3**). In addition, the intramolecular backbiting process could take place on free anionic polymer chain or be aided by a metal center. Additionally, the backbiting from the free anion will be assisted by excess amount of cocatalyst and adventitious water in the system. Generally, it is very difficult to avoid significant formation of thermally stable cyclic carbonates *via* two concurrent backbiting pathways, one aided by the central metal ion and one taking place on the free anionic polymer chain.[35] Due to the electron-withdrawing nature of the group such as the chloromethyl of epichlorohydrin, it is possible that cyclic carbonate is

predominantly produced *via* backbiting of the propagating polycarbonate anion to the chloromethyl carbon of the adjacent carbonate unit.

Scheme 3. Intramolecular backbiting to generate cyclic carbonate.

(P) = propagating polymer-chain
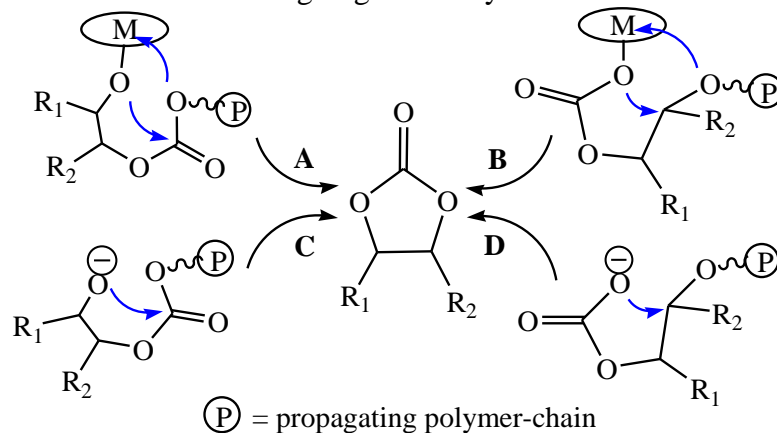
In order to get a better understanding of the backbiting process during polymerization, the activation energy barriers of polycarbonate and cyclic carbonate formations can be calculated. The kinetic studies on the copolymerization of epoxides and CO_2 were monitored by *in situ* infrared spectroscopy (**Figure 2**). The rates of polycarbonate and cyclic carbonate formations at different temperature can be determined (**Figure 3**). Thus, activation energies can be calculated and the reaction coordinate diagram can be obtained (**Figure 4**).[36] In the reaction coordinate diagram, the cyclic carbonate formation is considered to be happening after the polymer chain starts growing.
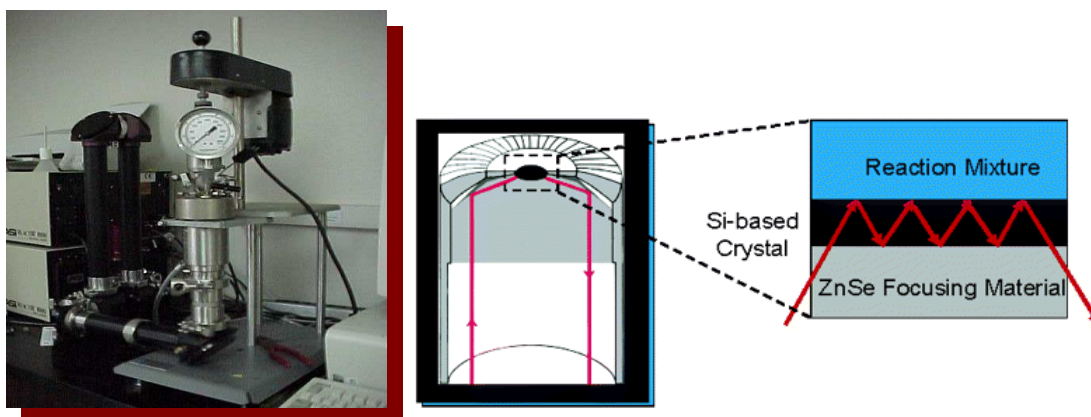
Figure 2. The ASI ReactIR 1000 system modified with a high pressure Parr® autoclave for the use of studying high pressure reaction system (left) and a diagram illustrating ATR-FTIR (right).
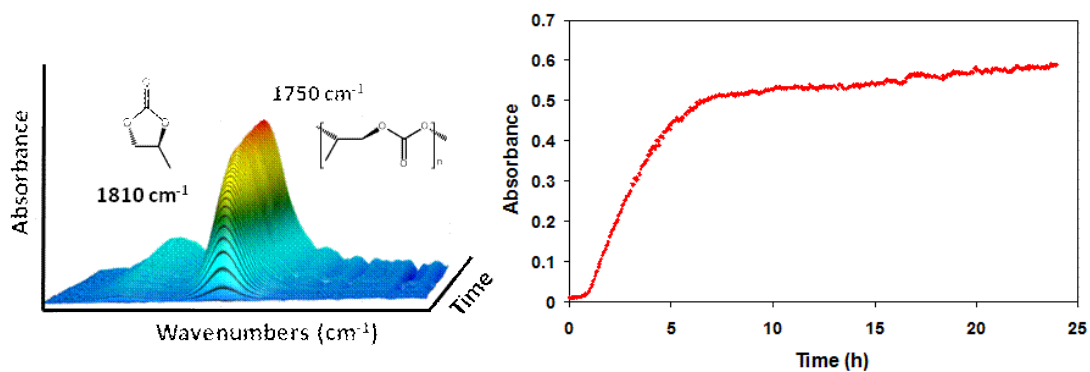
Figure 3. Three-dimensional stack plot of the IR spectra collected every 2 min, during the reaction of CO_2 and propylene oxide. (b) Time profile of the absorbance at 1750 cm^{-1} (corresponding to the poly(propylene carbonate)).[36a]
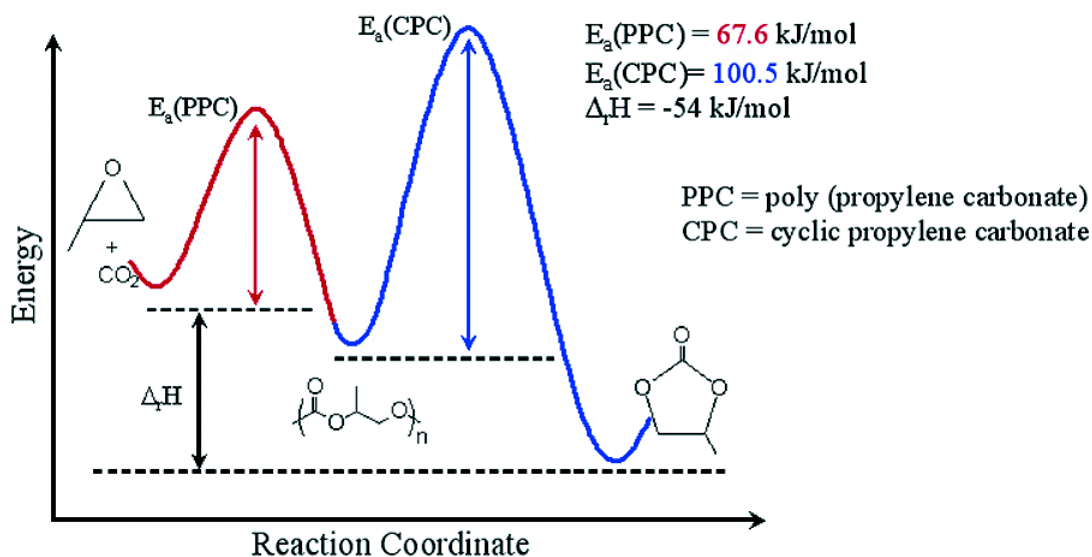
Figure 4. Reaction coordinate diagram for the coupling of CO_2 and propylene oxide.[36a]

In 2007, Darensbourg and coworkers have shown the activation energy of backbiting of poly(cyclohexene carbonate) *via* a metal-alkoxide polymer chain end intermediate of 105 ± 7 kJ/mol.[35] This energy barrier is much lower than the reported activation energy (133 kJ/mol) for the formation of cyclic carbonate during the copolymerization of cyclohexene oxide and high pressure CO_2, representing presumably *via* a metal-carbonate polymer chain end intermediate.[36a] This suggests the backbiting pathway from carbonate polymer chain end (**Scheme 3**, route B) to afford corresponding cyclic carbonate is higher than that from an alkoxide chain end (**Scheme 3**, route A) by about 28 kJ/mol. This also implies that the pressurized CO_2 is required during copolymerization process to reduce the formation of cyclic carbonate byproduct due to the higher energy barrier of carbonate backbiting pathway.

In order to prevent from cyclic carbonate formation via backbiting pathways, studies of several catalysts with specific ligand designs were developed, and therefore the selectivity of polycarbonate over cyclic carbonate byproduct was increased. The first example was reported by Nozaki in 2006 for CO_2 and propylene oxide copolymeriation in the presence of a Co(III) catalyst with a piperidinium end-capping arm at 3-position of salen ligand.[37] The piperidinyl groups offer a chance for protons shuffle between the amine and the propagating polymer chain end, controlling chain transfer reaction and backbiting (**Figure 5**). The proton protected polymer chain end mechanism successfully maintains a 90% polycarbonate selectivity over cyclic carbonate at the comparatively high temperature of 60 ℃, a temperature where most Co catalysts are no longer effective or selective for poly(propylene carbonate) production. The piperidinyl group on the ligand also performs the function of cocatalyst, thus this is considered the first example of bifunctional catalyst. This work led to a serious of studies on bifunctional catalyst designs combining the nature of metal catalysts and the characteristics of cocatalysts that could successfully hinder the cyclic carbonate formation *via* backbiting process.
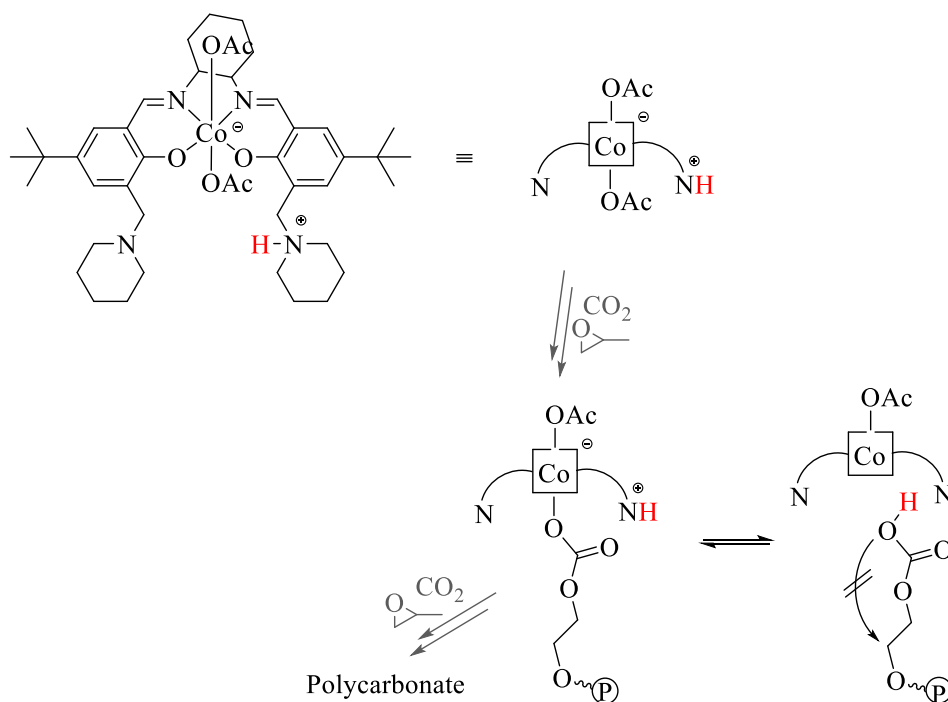
Figure 5. The first bifunctional catalyst design to suppress the production of cyclic carbonate.[37]

After that, the next breakthrough is Lee's design for Co(III) catalyst with an ammonium salt arm at the 5-positon of phenyl ring of salen ligand being able to operate at 90°C and affording a high TOF to 3500 h^{-1} with 90% selectivity (**Scheme 4**).[38] The catalyst loading can be lowered to 50000:1 without an induction period, which is more than ten times lower than traditional binary catalyst system. Later, the superactive salen Co(III) catalysts were then synthesized by Lee containing four quaternary ammoniums salts at the 5-position of phenyl rings.[39] This series of catalysts are considered some of the most active catalyst to date. The unusual binding mode around Co center, was proven by ^{1}HNMR experiments, increases the catalytic activity (TOF > 20000h^{-1}).

Scheme 4. Lee's bifunctional catalysts.

$$\overset{\ominus}{Y} = 2,4\text{-dinitrophenoxide}$$
$$\overset{\ominus}{Z} = \overset{\ominus}{Y}\text{--}\overset{\oplus}{H}\text{--}\overset{\ominus}{Y}$$
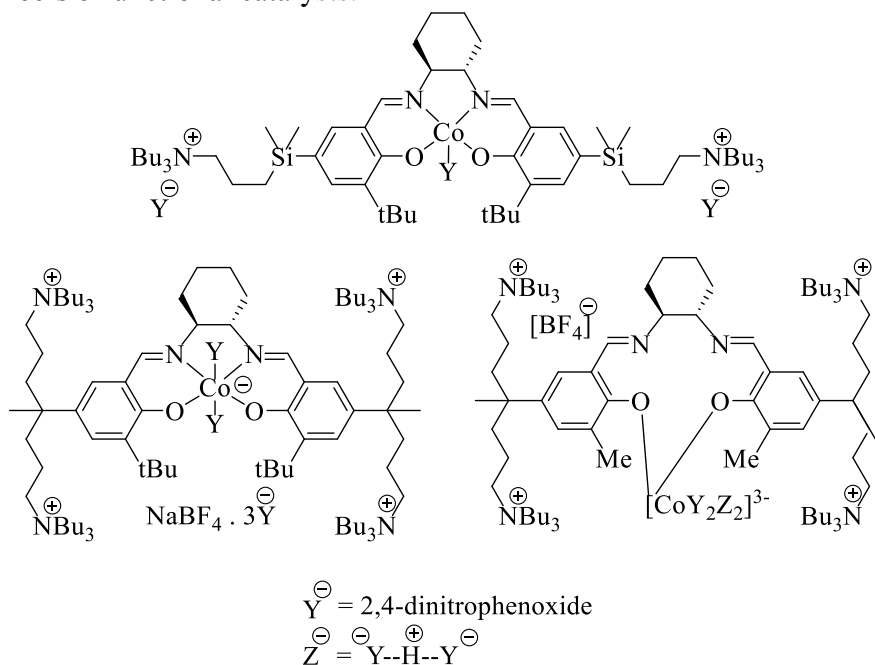
The other major series of active catalysts, asymmetric salenCo(III)X complexes, were developed by the Lu group of Dalian University of Technology. First published in 2009, they display an additional arm anchoring bulky amine or ammonium salt at the 3-position of phenyl ring on salen ligand playing an important role in maintaining thermal stability and high activity of the catalyst (**Scheme 5**).[40] The attached quaternary ammonium salt stabilizes the free growing polymer chain by electrostatic attraction to suppress the backbiting process resulting in high polymer selectivity (**Scheme 6**). Darensbourg has also shown that this bifunctional Co(III) catalyst successfully prohibits the cyclic carbonate generation and increases the selectivity of polycarbonate from 59% to > 99% in the copolymerization of indene oxide and CO_2.[41]

Scheme 5. Lu's bifunctional catalysts.

Where X = OAc, NO₃, BF₄
Y = 2,4-dinitrophenoxide
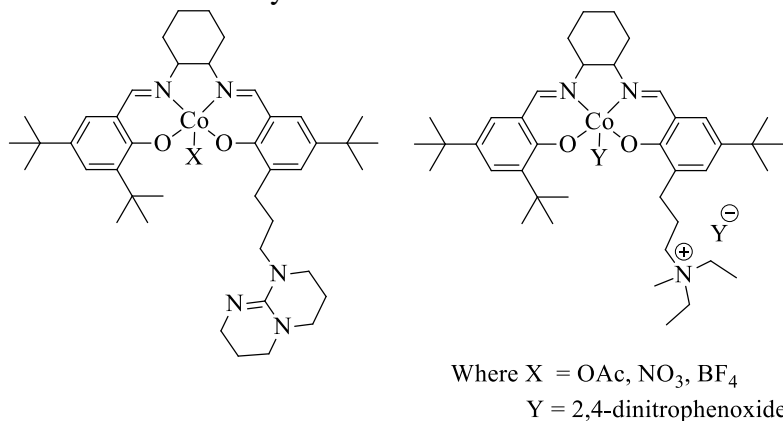
Scheme 6. Proposed mechanism for preventing backbiting to cyclic carbonate by Lu's bifunctional catalyst.
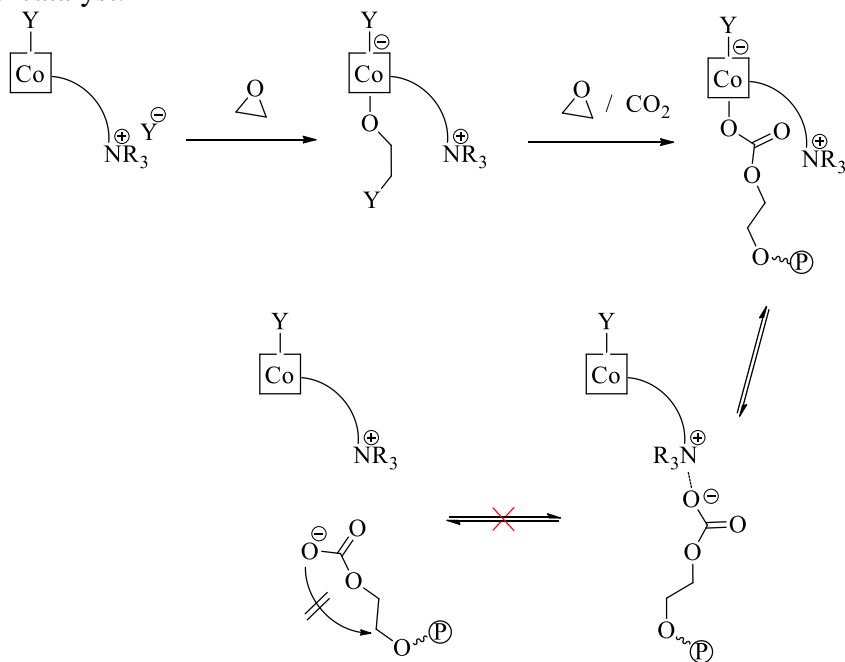
Another reported special pathway for cyclic carbonate generation during the polymerization process was proposed by Williams in the presence of their di-iron catalyst, which *cis*-cyclohexene carbonate was observed in the CO₂/cyclohexene oxide

20

copolymerization.[28] A mechanism involving a double-inversion of cyclohexene oxide stereochemistry rationalizes the generation of the unusual *cis*-isomer (**Scheme 7**). The cocatalyst helps exchange reactions between the initiating iron carbonate species and chloride ions. The anionic carbonate species would be significantly more nucleophilic than the metal bound carbonate, and then the intramolecular nucleophilic substitution takes place to form the *cis*-cyclohexene carbonate.

Scheme 7. Proposed mechanism for *cis*-cyclohexene carbonate formation in the coupling of cyclohexene oxide and CO_2.
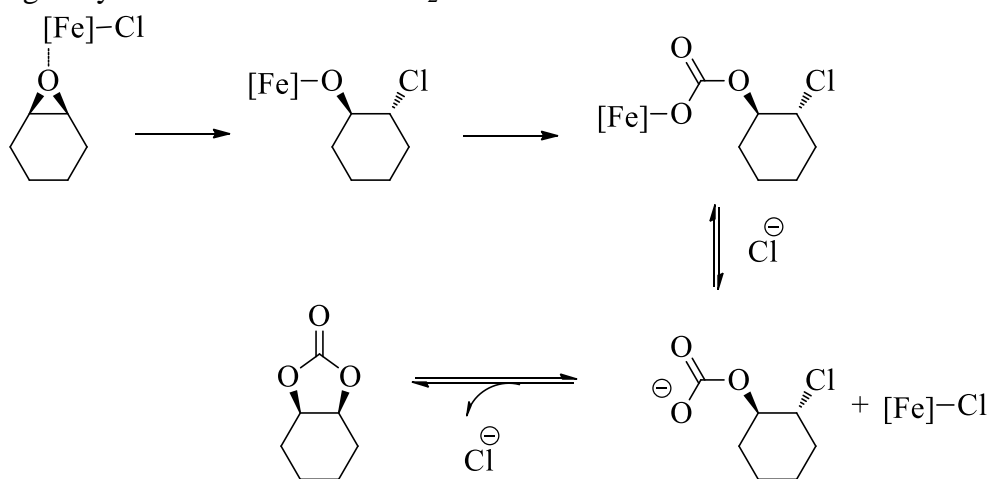
Plastic recycling

Plastic, one of the most significant innovations of 20th century, is a ubiquitous material. The consumption of plastic products has increased many folds over the past several decades.[42] Plastic wastes and their disposal generate environmental problems along with economic loss.

Since plastic is composed of organic hydrocarbons, its high calorific value can be used for incineration or in other high temperature processes. But, burning plastics generates a variety of poisonous chemicals which are released into the air. Included among these are dioxins, which are some of the most toxic substrates. Recycling plastics is a possible way to solve the pollution issue. Plastic recycling has been studied not only on the laboratory scale, but also in practical applications.

Recycling codes are used to identify the material from which an item is made, to facilitate easier recycling or other reprocessing, including batteries, biomatter/organic material, glass, metals, paper, and plastics. For plastic recyclings, the SPI Resin Identification Code (RIC) system, also known as Plastic Recycling Codes, is a set of symbols placed on plastics to identify the polymer type (**Table 1**).[43] The Society of the Plastics Industry, Inc. (SPI) introduced this system in 1988 at the urging of recyclers around the world. The symbols used in the code consist of arrows that cycle clockwise to form a rounded triangle the symbol known as the universal Recycling Symbol and enclosing a number, often with an acronym representing the plastic below the triangle. It identifies the resin/plastic content of bottles and containers commonly found in the residential waste stream listed in **Table 1**. For polycarbonates discussed in this dissertation, they do not have a unique resin identification code and are identified as other, 7.

Table 1. Resin identification codes.[44]

Resin code	Polymer name (Abbreviation)	Resin code	Polymer name (Abbreviation)
1 PET	Polyethylene terephthalate (PETE)	5 PP	Polypropylene (PP)
2 HDPE	High density polyethylene (HDPE)	6 PS	Polystyrene (PS)
3 V	Polyvinyl chloride (PVC or V)	7 OTHER	Other
4 LDPE	Low density polyethylene (LDPE)		

The reuse and various of recycling of waste residues can lead to reductions in the use of non-renewable materials and energy sources, with the energy saving generally ranked as follows: reuse > material recovery > energy recovery.[45] Energy recycling is the recovery of the energy bound in the plastic by combustion, economizing on fossil fuels. However, this type of process has been recently excluded from normal concept of recycling and mentioned only as a form of energy recovery. For a modern recycling concept, there are three basic types of recycling processes.[46] In primary recycling, plastics are melted down and reintroduced into the same type of product depending on use. For secondary recycling, plastics are melted down, repelletized, and reintroduced into different types of production. These two recycling process are called mechanical recycling, consisting of the reprocessing of plastic resides into new products. They may be different from or similar to the original products. The waste plastic may come from

the manufacturing or from the post-consumer products. This is the simplest way for recycling plastic waste, requiring the lowest initial investments.

In tertiary recycling, known as chemical or feedstock recycling, plastics are brokendown into monomer or fuel chemicals *via* heat or chemical treatments. It is considered as the ideal recycling process. Useful starting materials are recovered and clean monomers can then be repolymerized or used for other applications. Therefore, plastic waste can also be used to produce new plastic based products after processing.[47] In chemical recycling, polymers are converted into low molecular-weight products by using depolymerization and decomposition reactions. A variety of raw materials can be generated in several sectors depending on the type of reaction employed. It is usually divided into two categories: thermolysis and solvolysis. Thermolysis works with high temperature based on three main processes: pyrolysis, gasification, and hydrogenation.[48] Solvolysis is a general expression comprising processes like glycolysis, methanolysis, hydrolysis, acidolysis and alcoholysis. Preferentially, these processes are utilized when the polymers are classified and precleaned manufacturing wastes. Unfortunately, only a limited amount of research has been conducted on these processes.

In this dissertation, metal catalyzed copolymerizations of CO_2 and various cyclic ethers to afford polycarbonates will be discussed. The studies of polycarbonate degradation pathways have been investigated for the possibility of chemical recycling of plastic by generating monomeric starting materials. For the copolymers made from oxetane derivatives, the study will cover the crystal structures of several six-membered

cyclic carbonates to examine their equilibria between monomeric cyclic carbonates and

their corresponding polycarbonates.

ALTERNATING COPOLYMERIZATION OF CO_2 AND EPOXIDES WITH

ELECTRON-WITHDRAWING SUBSTITUENT USING COBALT(III)-BASED

CATALYST SYSTEMS[*]

Introduction

The catalytic transformation of carbon dioxide into degradable polycarbonates via the alternating copolymerization with epoxides has received considerable attention during the last decades.[15, 28, 49] Numerous catalyst systems have been developed for this reaction.[12a, 13a, 14, 50,51,52,20, 53,54,25, 55,37-38, 40] Much progress has been made in the formation of polycarbonates from aliphatic terminal epoxides or cyclohexene oxide derivatives, very limited literature exists concerning the synthesis of CO_2 copolymers from epoxides with electron-withdrawing groups, such as styrene oxide. Furthermore, these reported processes generally suffered from poor copolymer selectivity and the concomitant production of ether linkage units in the resulting polymers.[10, 56] Although

---

[*] Reprinted (adapted) with permission from "Highly Selective Synthesis of CO_2 Copolymer from Styrene Oxide." Wu, G.-P.; Wei, S.-H.; Lu, X.-B.; Ren, W.-M.; Darensbourg, D. J. *Macromolecules* **2010**, *43*, 9202–9204. Copyright 2010 American Chemical Society. "Perfectly Alternating Copolymerization of CO_2 and Epichlorohydrin Using Cobalt(III)-Based Catalyst Systems." Wu, G.-P.; Wei, S.-H.; Ren, W.-M.; Lu, X.-B.; Xu, T.-Q.; Darensbourg, D. J. *J. Am. Chem. Soc.* **2011**, *133*, 15191–15199. Copyright 2011 American Chemical Society. "Alternating Copolymerization of CO_2 and Styrene Oxide with Co(III)-based Catalyst Systems: Differences Between Styrene Oxide and Propylene Oxide." Wu, G.-P.; Wei, S.-H.; Ren, W.-M.; Lu, X.-B.; Li, B.; Zu, Y.-P.; Darensbourg, D. J. *Energy Environ. Sci.* **2011**, *4*, 5084–5092. – Reproduced by permission of The Royal Society of Chemistry. http://dx.doi.org/10.1039/C1EE02566J.

some zinc-based catalyst systems were applied to the coupling of CO_2 and styrene oxide, they generally suffered from low activity, poor polymer selectivity and the concomitant production of ether linkage units.[56b, 56c, 57]   Well-defined β-diiminate zinc complexes proved to be efficient in catalyzing this reaction at ambient temperature and 2.0 MPa, but the selectivity for copolymer was only 35%.[56d] Increasing the CO_2 pressure did not improve the selectivity for copolymer.

Being distinct from the terminal epoxides with electron-donating groups such as propylene oxide, the nucleophilic ring-opening of styrene oxide predominantly occurs at the methine C_α-O bond rather than the methylene C_β-O bond (**Scheme 8**).[58] As a result, it is very difficult to avoid the formation of styrene carbonate by intramolecularly cyclic elimination via two concurrent backbite mechanisms, one aided by the central metal ion and one taking place on the free anionic polymer chain. The latter process is believed to have a lower activation barrier and to be assisted in the presence of an excess of nucleophilic cocatalyst or adventurous water, which serves to displace the growing polymer chain from the metal center.[37-38, 40,35]

Scheme 8. The difference in nucleophilic ring-opening between styrene oxide and propylene oxide.
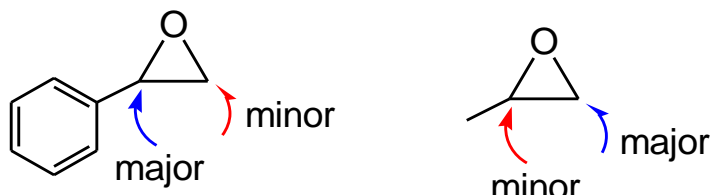
Copolymerization processes involving epoxides containing electron-donating substituents, e.g., propylene oxide, are thought to proceed to cyclic carbonates predominantly by way of routes **A** and **C** in **Scheme 9**, where the alkoxide chain end attacks the carbonyl carbon of the adjacent carbonate unit. Because of the electron-withdrawing nature of the aromatic ring, it is possible that cyclic styrene carbonate is predominantly produced via backbiting of the propagating polycarbonate anion to the benzyl carbon of the adjacent carbonate unit (**Scheme 9**, routes **B** and **D**). In addition, the isomerization of styrene oxide into hyacinthin easily occurs at enhanced temperatures.[59] Compared with the low glass-transition temperatures (T_g) associated with aliphatic polycarbonates, the polymer from the alternating copolymerization of CO_2 and styrene oxide should exhibit an enhanced T_g value.[56c, 56d, 57] Therefore, selective synthesis of the corresponding polycarbonate from styrene oxide is highly desirable.

Scheme 9. The formation of styrene carbonate by intramolecular cyclic elimination of the propagating polymer-chains involving the carbonate unit associated with ring-opening of styrene oxide at the methine C_α-O bond.
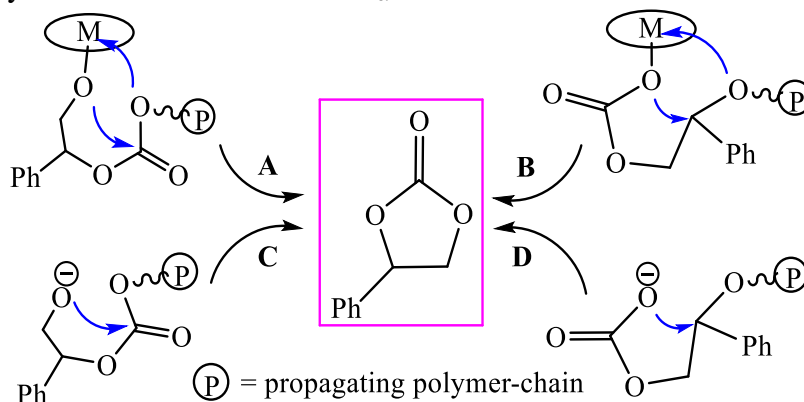
Another important functionalized epoxide, epichlorohydrin is widely used in chemical industry such as epoxy resins, adhesive, and starting material for organic synthesis.[7b, 60] It has been used in the random copolymerization with maleic anhydride in the presence of coordination catalysts such as rare earth metal complexes, producing copolymers with low molecular weights.[7a, 61] Although epichlorohydrin is a highly reactive epoxide in the coupling reactions with CO_2, the corresponding cyclic carbonate rather than the polycarbonate usually is the sole product.[10, 56a, 56b, 56d, 56e] A heterogeneous catalyst system based on rare earth phosphonates and triisobutyl aluminum was reported by Shen and coworkers for the copolymerization of epichlorohydrin and CO_2, but the strong Lewis acidity of the catalyst systems resulted in the formation of polymers having more than 70% ether linkages.[56f] Thus, it would be worthwhile to develop a selective synthesis of a completely alternating copolymer from CO_2 and epichlorohydrin.

In the present report, we communicate studies aimed at a selective synthesis of a perfectly alternating copolymer between CO_2 and epoxides with electron-withdrawing groups, styrene oxide and epichlorohydrin, utilizing cobalt-based catalyst systems. The investigation provided herein also involves temperature-dependent kinetic studies of the relative propensity of these catalyst systems for producing copolymer *versus* cyclic carbonate as a function of the nature of the epoxide.

Experimental section

Reagents and methods. All manipulations involving air- and/or water-sensitive compounds were carried out in a glove box under argon atmosphere or with the standard

Schlenk techniques under dry nitrogen. Styrene oxide was purchased from Alfa Aesar and distilled ($< 40\ ^{o}C$) under reduced pressure over CaH_2. Carbon dioxide (99.995%) was used as received. (*R*)- and (*S*)-styrene oxide were prepared according to the literature.[62] Methanol was distilled under nitrogen from magnesium. Epichlorohydrin, methylene chloride and chloroform were distilled from CaH_2 under nitrogen. PPNCl [PPN$^+$ = bis(triphenylphosphine)iminium] was purchased from Aldrich and recrystallized from dry methylene chloride and diethyl ether under nitrogen before use. N, N'-Bis(3, 5-di-tert-butylsalicylidene)-1, 2-cyclohexanediamino cobalt(II) SalcyCo(II) and SalcyCo(III)X (X = Cl, Br, 2, 4-dinitrophenoxy) were synthesized according to the literature method.[55c] Catalyst **2** and **3**was synthesized according to the literature method.[40]

^{1}H and ^{13}C NMR spectra were recorded on Varian INOVA-400 MHz type (^{1}H, 400 MHz), and a Bruker 500 MHz type (^{13}C, 125 MHz) spectrometer, respectively. Their peak frequencies were referenced versus an internal standard (TMS) shifts at 0 ppm for ^{1}H NMR and against the solvent, chloroform-*d* at 77.0 ppm for ^{13}C NMR, respectively. Molecular weight determinations (M_n and M_w) were carried out with with a PL-GPC 220 high temperature chromatograph (Polymer Laboratories Ltd.) equipped with the HP 1100 series pump from Agilent Technologies. The GPC columns were eluted with tetrahydrofuran at 35 °C at 1.00 ml/min. The sample concentration was about 0.1%, and the injection volume was 100 μL. The curve was calibrated using monodisperse polystyrene standards covering the molecular weight rage from 580 to

460000 Da. Infrared spectra were recorded on a Bruker Tensor 27 FTIR spectrometer in CaF_2 solution cells of 0.1 mm pathlength.

Mass spectrometry. A Micromass Q-Tof (Micromass, Wythenshawe, UK) mass spectrometer equipped with an orthogonal electrospray source (Z-spray) used for the cobalt complexes in positive ion mode (Capillary = 2000V, Sample cone = 20V).

MALDI-TOF mass spectroscopy. MALDI-TOF mass spectrometric measurements were performed on a Shimadzu Axima CFR MALDI-TOF MS mass spectrometer, equipped with a nitrogen laser delivering 3 ns laser pulses at 337 nm. α-Cyano-4-hydroxycinnamic acid (J&K, 97%), was used as a a matrix. CH_3COONa (Aldrich, 98%) was added for ion formation.

Synthesis of PPNY (Y = 2,4-dinitrophenoxy). To a stirred mixture of PPNCl (0.574g, 1 mmol) in CH_2Cl_2 (20 ml) in a 40 ml Schlenk vial was added 2, 4-dinitrophenol sodium salt (0.205 g, 1 mmol, 1 equive). The mixture was stirred for 24h, and then filtered for removing the NaCl byproduct. Precipitation from dry methylene chloride and diethyl ether under N_2 afforded PPN-2, 4-dinitrophenoxide as yellow powder. ^1H NMR (CDCl$_3$, 400 MHz): δ 6.57 (d, J = 9.6 Hz, 1H), 7.41-7.46 (m, 24H), 7.62-7.66 (m, 6H), 7.83 (q, 1H), 8.85 (d, J = 3.2 Hz, 1H); 13C NMR (CDCl$_3$, 100 MHz): δ 126.5 (CH), 127.4 (CH), 127.6 (CH), 127.9 (C), 129.7 (6C), 132.2 (15CH), 134.0 (15CH), 136.4 (C), 172.5 (C); Elemental analysis calcd. (%) for $C_{42}H_{33}N_3O_5P_2$: C, 69.90; H, 4.58; N, 5.82; found: C, 69.74; H, 4.58, N, 5.76.

Representative procedures for the copolymerization CO_2 with neat epoxide. A 25 mL Parr autoclave was heated to 120 ^{o}C under vacuum for 8 h, then cooled under

vacuum to room temperature and moved to a glove box. Complex (19.6 mg, 0.025 mmol), PPN-2, 4-dinitrophenoxide (18.0 mg, 0.025 mmol) and epoxide (12.5 mmol, 500 equiv) were placed in autoclave equipped with a magnetic stirrer. The autoclave was put into a bath of desired temperature, and then pressurized to appropriate pressure with CO_2. After the allotted reaction time, a small amount of the resultant polymerization mixture was removed from the autoclave for ^{1}H NMR analysis to quantitatively give the conversation and also used for GPC analysis. The crude polymer was dissolved in a 10 mL $CHCl_3$/MeOH (5/1, v/v) mixture with 0.5% HCl solution and precipitated from methanol. This process was repeated 3-5 times to completely remove the catalyst, and white polymer was obtained by vacuum-drying.

Kinetic studies for CO_2/epoxide couplings monitored by *in situ* ATR-FTIR spectroscopy. Temperature dependent kinetic measurements of the copolymerization processes were obtained employing the respective epoxides in the presence of catalyst 1 and PPNY under solventless conditions. The epoxide/CO_2 copolymerization reactions were carried out in a 300 mL stainless steel Parr autoclave reactor that was previously dried in vacuo overnight at 80 °C. The autoclave is modified with a 30 bounce SiComp window to allow for the use of an ASI ReactIR 1000 system equipped with a MCT detector.[63] Because the above in situ system is not readily adapted to monitor reaction below ambient temperature, the copolymerization reactions between epichlorohydrin and CO_2 were followed in a 50 mL Parr autoclave cooled by a circulating bath using a Mettler Toledo iC10 ReactIR with an AgX fiber conduit probe.

Results and discussion

Stimulated by the success with binary catalyst systems of a metal salen complex in conjunction with a bulky onium salt or sterically hindered organic base for the alternating copolymerization of aliphatic epoxides and CO_2,[20, 25, 53, 55] we have tested these systems for the coupling reaction of styrene oxide with CO_2. Previously, few catalyst systems based on the salenCo(III)X complex have shown activity for this coupling reaction at ambient temperature with moderate to good selectivity for polymer formation (**Table 2**). Most systems predominately afforded cyclic styrene carbonate at various temperatures. However, the judicious choice of axial X anions on salenCo(III)X and Y anions of PPNY significantly impacts the catalytic activity and selectivity for copolymer formation (**Table 2**, entries 1-4). The screening revealed that salenCo(III) complex **1a** in conjunction with 1 equiv. PPNY [Y = 2,4-dinitrophenoxy] was the most effective binary catalyst to provide polycarbonate with a narrow polydispersity (M_w/M_n ratio) in 99% selectivity. This is a rare example of the selective synthesis of a copolymer from CO_2 and an epoxide with an electron-withdrawing group.
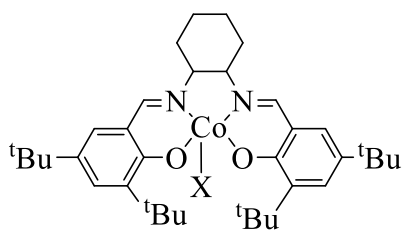
1a: X = 2,4-dinitrophenoxy
1b: X = Cl
1c: X = Br
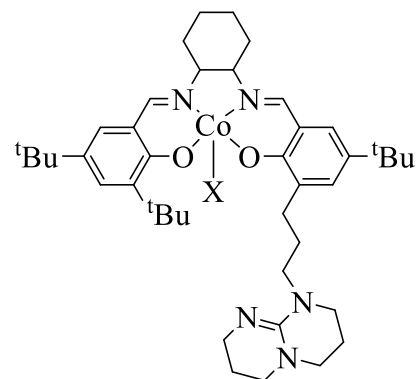
2: X = 2,4-dinitrophenoxy
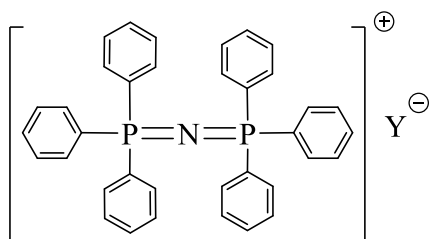
PPNY
Y = Cl, 2,4-dinitrophenoxy

MTBD
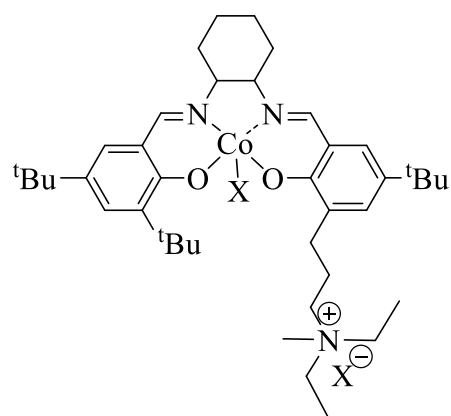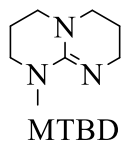
3: X = 2,4-dinitrophenoxy

Table 2. The coupling reaction of styrene oxide with CO_2.[a]
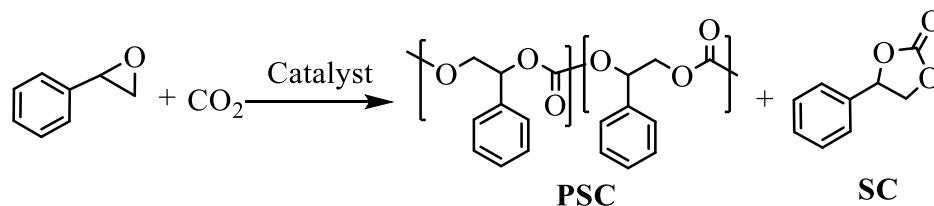
Entry	Catalyst	T (°C)	t (h)	TOF[b] (h^{-1})	PSC/SC[c]	Mn[d] (Kg/mol)	PDI[d]
1	**1a**/PPNCl[e]	25	3	62	90/10	12.9	1.04
2	**1b**/PPNCl	25	3	61	58/42	7.4	1.12
3	**1c**/PPNCl	25	3	94	5/95	-	-
4	**1a**/PPNY[f]	25	3	75	99/1	15.7	1.05
5	**1a**/PPNY[f]	50	2	160	91/9	20.4	1.05
6[g]	**2**	25	12	60	100/0	76.4	1.03
7[g]	**2**	50	6	134	99/1	86.0	1.10
8[h]	**2**	25	12	13	99/1	16.2	1.07

[a]The coupling reaction was performed in neat styrene oxide (100 mmol) in 50 ml autoclave at 2.0 MPa CO_2 pressure. Catalyst/cocatalyst/epoxide = 1/1/500 (molar ratio). Epoxide/Catalyst Carbonate linkages of the resulted polymers are >99% based on ^{1}H NMR spectroscopy. [b]Turnover frequency of styrene oxide to products [poly(styrene carbonate) and cyclic styrene carbonate]. [c]Determined by using ^{1}H NMR spectroscopy. [d]Determined by gel permeation chromatography in THF, calibrated with polystyrene. [e]PPN = bis(triphenylphosphine)iminium. [f]Y = 2,4-dinitrophenoxy anion. [g]Catalyst/epoxide = 1/3000 (molar ratio). [h]The reaction was performed at 0.1 MPa CO_2 pressure.

During the optimization of the catalyst systems, we were gratified to discover that a novel cobalt-based catalyst **2** with 1,5,7-triabicyclo[4,4,0] dec-5-ene (designated as TBD, a sterically hindered organic base) anchored on the ligand framework was highly active for catalyzing CO_2/styrene oxide copolymerization to selectively give the corresponding polycarbonates with more than 99% carbonate linkages even at a low catalyst loading (entry 6). However, the activity for CO_2/styrene oxide coupling is less than one tenth that of CO_2/propylene oxide copolymerization under the same reaction conditions.[40] Of importance, the catalyst proved to be effective at 0.1 MPa CO_2 pressure and at enhanced temperature of 50 °C with 99% polymer selectivity (entries 7 and 8).

The isolated polymers have narrow molecular-weight distributions less than 1.1 and exhibit monomodal distribution, which is very different from the bimodal distributions generally found in the copolymerization of CO_2 and propylene oxide using these same binary catalyst systems. Notably, the M_n values are close to the expected values, and also exhibit a linear relationship with the % conversion (**Figure 6**). This is consistent with a living polymerization process.
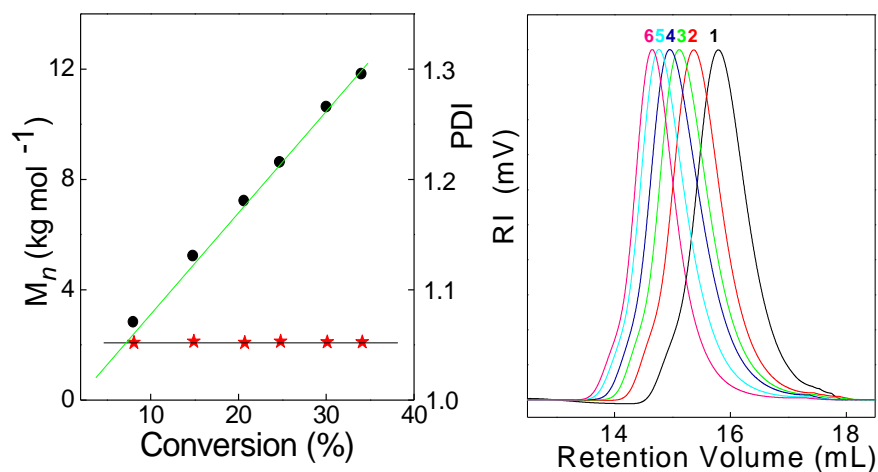
Figure 6. Plots of Mn ($\bullet$) and PDI ($*$) versus the % conversion (left), and GPC traces of poly(styrene carbonate)s obtained at various conversions (right). [Reaction conditions: epoxide / 1a / PPNY (Y = 2,4-dinitrophenoxy) catalyst = 500/1/1; 25 ^{o}C; 2.0 MPa CO_2 pressure]

As expected, the resulting polymer exhibits excellent thermal stability with a thermolysis temperature up to 300 ^{o}C, which is about 60°C higher than that of the copolymer obtained with zinc glutarate as catalyst reported by Lee et al.,[56c] and has a relatively high glass-transition temperature of 80 ^{o}C (**Figure 7**).
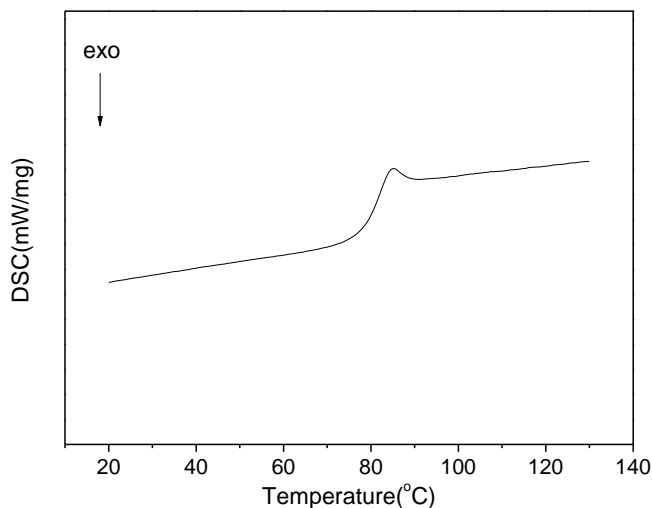
Figure 7. DSC thermogram of poly(styrene carbonate).

The main chain sequence of the resulting polycarbonate was confirmed by ^{1}H and ^{13}C NMR spectroscopy, as well as MALDI-TOF. In the ^{1}H NMR spectrum of the resulting copolymer in CDCl₃, the resonance of methine CH in styrene carbonate unit is found at 5.87 ppm, due to the electron-withdrawing effect of the aromatic ring. No signal at δ = 3.3 to 3.6 ppm assignable to ether linkage units was observed in this spectrum,[64] demonstrating that the copolymer has >99% carbonate linkages. MALDI-TOF spectroscopy also confirmed the highly alternating nature of the resulting polymer. The ^{13}C NMR spectrum suggests that the resulting copolymer has a head-to-tail content of 51% (**Figure 8**), indicating that ring-opening of styrene oxide during the copolymerization with CO_2 occurs almost equally at both C_{α}-O and C_{β}-O bonds. Even for the copolymerization (*S*)-styrene oxide (98% *ee*) with CO_2 using the binary catalyst system of *1R,2R*-**1a** and PPNY (Y = 2,4-dinitrophenoxy), the resulting copolymer has a head-to-tail content of 82% and its hydrolysis product has a enantioselectivity of 87%

37

with a (*S*)-configuration, suggesting that this reaction proceeds with 11% inversion at the benzyl carbon. The result is in sharp contrast with the copolymerization of optically active styrene oxide and CO_2 using a diethylzinc/water system as catalyst, in which the ring-opening predominantly takes place at the methine-oxygen bond cleavage accompanying 96% inversion at the benzyl carbon.[65]
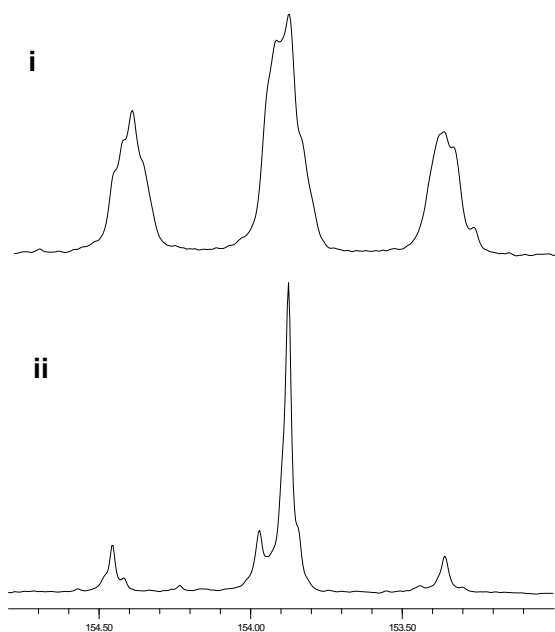
Figure 8. Carbonyl region of ^{13}C NMR spectra of poly(styrene carbonate)s obtained with catalyst system: (i) racemic 1a/PPNY(Y = 2,4-dinitrophenoxy)/racemic styrene oxide (1/1/500, molar ratio); (ii) (*1R,2R*)-1a/ PPNY(Y = 2,4-dinitrophenoxy)/(*S*)-styrene oxide (1/1/500, molar ratio).

In order to clearly understand the difference in reactivity exhibited by these two types of epoxides in their copolymerization reactions with CO_2, we have carried out parallel studies with styrene oxide and propylene oxide. The binary cobalt(III) catalyst

systems of complexes **1a** in conjunction with onium salts was employed in these studies. Comparative investigations of the copolymerization reactions of propylene oxide or styrene oxide and its derivatives with CO_2 were performed under identical reaction conditions with complex **1a** in the presence of PPNY, where Y = 2,4-dinitrophenoxy. These results are summarized in **Table 3**.

Table 3. The coupling of CO_2 with epoxides catalyzed by complex 1a in conjunction with PPNY.[a]

R = CH₃, Ph,

Polycarbonate   Cyclic carbonate
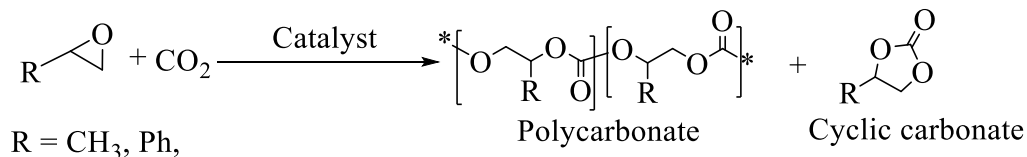
Entry	Epoxide (R)	Temp (°C)	Pressure (MPa)	Time (h)	TOF^b (h^{-1})	Polymer selectivity^c	Mn^d (Kg/mol)	PDI^d
1	Ph	25	2.0	3.0	75	99	15.7	1.04
2^e	Ph	50	7.0	2.0	160	91	20.4	1.09
3	Ph	25	1.0	3.0	60	99	14.2	1.05
4	Ph	25	3.0	3.0	82	99	19.9	1.05
5	CH₃	25	1.0	1.5	530	> 99	31.4	1.15
6	CH₃	50	2.0	0.5	1560	99	27.9	1.19
7	CH₃	25	2.0	1.5	540	> 99	32.5	1.08
8	CH₃	25	3.0	1.5	536	> 99	33.1	1.10

[a]The coupling reaction was performed in neat epoxide (100 mmol) in a 50 ml autoclave. Catalyst/cocatalyst/epoxide is 1/1/500 (molar ratio) for styrene oxide cases, and 1/1/2000 (molar ratio) for propylene oxide case. PPN = bis(triphenylphosphine)iminium; Y = 2,4-dinitrophenoxy anion. Carbonate linkages of the resultant polymers are >99% based on ^{1}H NMR spectroscopy. [b]Turnover frequency of styrene oxide to products (polycarbonate and cyclic styrene carbonate). [c]Determined by using ^{1}H NMR spectroscopy. [d]Determined by gel permeation chromatography in THF, calibrated with polystyrene. [e]When the reaction was performed at 50 °C and 2.0 MPa CO_2 pressure, complete loss in polymer selectivity was observed.

As noted in **Table 3** (entries 3 and 5) the activity for CO_2/styrene oxide coupling is about one tenth that of the corresponding process involving CO_2/propylene oxide. In

both instances the resulting polycarbonates were found to have polydispersity indices < 1.10, and were perfectly alternating copolymers as confirmed by ^{1}H NMR and MALDI-TOF spectroscopies. Although this binary catalyst system is highly effective at producing regioregular poly(propylene carbonate), it is inefficient at controlling the stereochemistry in the copolymerization of styrene oxide and carbon dioxide. This may in part be due to steric hindrance in the ring-opening process of styrene oxide at the methine C_α–O bond. The axial X anion in (salen)CoX and the Y anion in PPNY significantly impact the selectivity for copolymer formation. When both X and Y are chlorides, cyclic styrene carbonate is predominantly formed at ambient temperature. On the contrary, in the CO_2/propylene oxide coupling reaction under this condition the selectivity for copolymer formation is greater than 99%. In general the production of cyclic carbonates over copolymer is enhanced as the reaction temperature is increased. Nevertheless, the product distribution for the styrene oxide/CO_2 process is more sensitive to an increase in temperature than the propylene oxide/CO_2 coupling process. This is best illustrated upon examining the relative activation barriers obtained from temperature dependent rate data for these two CO_2 coupling processes using complex **1a** and PPNY, and this study will be discussed later in this chapter.

Another difference between the styrene oxide and propylene oxide coupling reactions with CO_2 emerged upon examining the CO_2 pressure dependence of these two processes (**Table 3**, entries 1, 3, and 4). Whereas there was no observable change in rate of the propylene oxide/CO_2 coupling process beyond 1.0 MPa CO_2 pressure, the corresponding styrene oxide/CO_2 process underwent a 26% increase in rate upon

increasing the CO_2 pressure from 1.0 to 3.0 MPa. This difference is ascribed to the relatively lower solubility of CO_2 in styrene oxide as compared to propylene oxide. Indeed, it was found that the solubility of CO_2 in styrene oxide was only about one-third that in propylene oxide.

The activity of this system for catalyzing the coupling reaction of epichlorohydrin with CO_2 using binary catalyst system consisting of complex **1a** and PPN-2,4-dinitrophenoxide was also investigated (**Table 4**). It was gratifying to find that the binary catalyst system in 0.1 mol% loading showed an excellent activity for this coupling process with a TOF of 300 h^{-1} at 25 ^{o}C, however the selectivity for copolymer formation was only 10%. Alternatively, a reduction in the reaction temperature suppressed the formation of cyclic carbonate and concomitantly increased the selectivity for copolymer formation. A similar temperature-dependent for product selectivity was observed in the binary catalyst system of complex **1a** in conjunction with 7-methy-1,5,7-triazabicyclo[4.4.0]dec-5-ene (MTBD, a sterically hindered strong organic base). During the optimization of the catalyst systems, it was found that the cobalt-based catalyst **2** with TBD anchored to the ligand framework and bifunctional catalyst **3** bearing an appended quaternary ammonium salt were highly active for catalyzing CO_2/epichlorohydrin copolymerization to selectively give the corresponding polycarbonates even at a low catalyst loading (entries 6 and 8).

41

Table 4. The coupling reaction of epichlorohydrin with CO_2 by salenCoX complexes.[a]

Polycarbonate   Cyclic carbonate
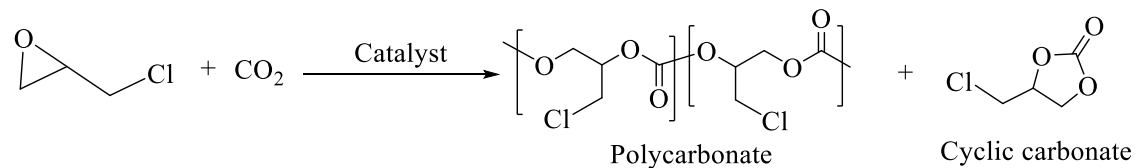
Entry	Catalyst	Cocatalyst	Temp. (°C)	Time (h)	TOF[b] (h^{-1})	Selectivity[c] (Polymer %)	Carbonate linkages[c] (%)	M_n[d] (Kg/mol)	PDI[d] (Mw/Mn)	T_g (°C)
1	**1**	PPNY	25	1	300	10	--	--	--	
2	**1**	PPNY	0	12	31	61	>99	4.7	1.22	
3	**1**	MTBD	25	1	246	10	--	--	--	
4	**1**	MTBD	0	24	15	65	>99	4.4	1.21	
5	**2**	--	25	1	640	72	>99	8.6	1.10	27
6	**2**	--	0	24	36	>99	>99	22.3	1.12	31
7	**3**	--	25	1	580	75	>99	7.9	1.09	27
8	**3**	--	0	24	37	>99	>99	25.9	1.07	31

[a]The coupling reaction was performed in neat epichlorohydrin in 25 mL autoclave at 2.0 MPa CO_2 pressure. Catalyst/cocatalyst/epichlorohydrin = 1/1/1000 (molar ratio) for entries 1-4; catalyst/epichlorohydrin = 1/2000 (molar ratio) for entries 5-8. [b]Turnover frequency of epichlorohydrin to products (polycarbonate and cyclic carbonate). [c]Based on ^1H NMR spectroscopy. [d]Determined by gel permeation chromatography in THF, calibrated with polystyrene.

Notably, the resulting polycarbonates have more than 99% carbonate content as confirmed by ^{1}H NMR and MALDI-TOF spectroscopy. As shown in the ^{1}H NMR spectrum in CDCl$_3$ of the resultant copolymer in **Figure 9**, the signals at δ = 3.6-3.8 ppm are assigned to the hydrogens of the CH$_2$Cl group, while the signals at 5.1 ppm and 4.5 ppm originate from the resonances of the methine CH and the methylene CH$_2$ of the carbonate unit, respectively. Although only one peak at 3.7 ppm was observed in the ^{1}H NMR spectrum of the homopolymer of epichlorohydrin, the well-proportional relationship of the CH, CH$_2$ and CH$_2$Cl integrated areas (1/2.01/2.04), as well as MALDI-TOF and ESI-MS analyses confirmed the perfectly alternating nature of the copolymer.
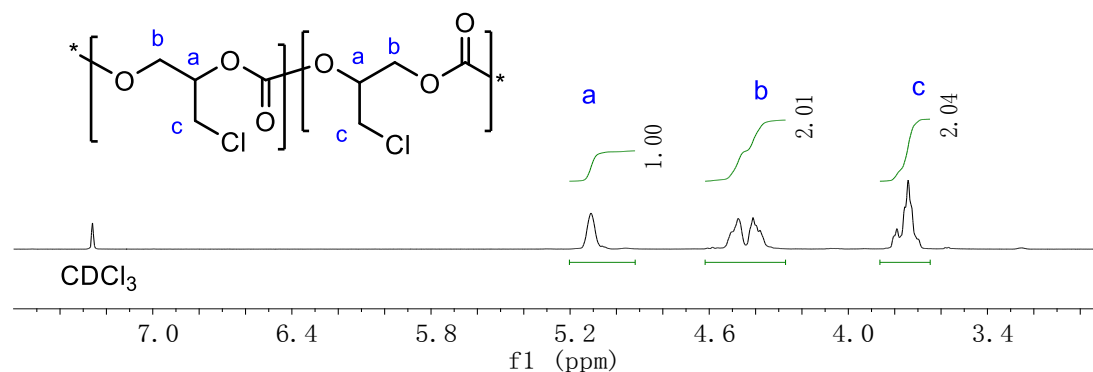
Figure 9. Representative ^{1}H NMR spectrum of CO$_2$ copolymer from epichlorohydrin in CDCl$_3$.

In order to better ascertain the influence of the chloromethyl group of epichlorohydrin on the catalytic activity and selectivity for copolymer *versus* cyclic

carbonate formation, comparative kinetic experiments between epichlorohydrin and propylene oxide were conducted for the copolymerization with CO_2, using the binary catalyst system of complex **1a** and PPNY (Y = 2,4-dinitrophenoxy). **Table 5** lists the initial reaction rates for production of copolymer and cyclic carbonate for both epoxide monomers as a function of temperature. **Figure 10** illustrates the reaction profiles for the propylene oxide/CO_2 and epichlorohydrin/CO_2 copolymerization processes at two different temperatures as monitored by *in situ* infrared spectroscopy. Even at the very low temperature of -5 ^{o}C for epichlorohydrin/CO_2 copolymerization, cyclic carbonate was produced to a significant extent. On the contrary, only weak ν_{CO_2} absorptions at 1800 cm^{-1} assigned to cyclic propylene carbonate were detected at an enhanced temperature of 40 ^{o}C in the copolymerization of CO_2 and propylene oxide. The energies of activation for copolymer and cyclic carbonate formation for both propylene oxide and epichlorohydrin were derived from the plots of ln(initial rate) *vs* 1/T. Using these activation parameters, we obtained the reaction coordinate diagrams for each process as depicted in **Figure 11**. It is important to note that although the diagrams in **Figure 11** present the production of cyclic carbonates *via* pathways involving a metal bound copolymer chain, the energy of activation barriers measured for cyclic carbonate formation actually reflects a composite of mechanistic pathways. That is, we are not able to resolve the energy barriers for the three routes to cyclic carbonate production as depicted in **Scheme 10**. The difference in activation energy barriers employing this catalyst system for cyclic carbonate *vs* copolymer formation for the epichlorohydrin process is less than that of propylene oxide, 45.4 *vs* 53.5 kJ/mol. In addition, the relative

rates of production of cyclic carbonate *vs* copolymer becomes greater than one for epichlorohydrin/CO_2 coupling above 5 °C, whereas this is projected to occur at a much higher temperature (>80 °C) for the propylene oxide/CO_2 process (Table 5). In other words, cyclic carbonate formation during the epichlorohydrin/CO_2 coupling process is *entropically* favored as well over the corresponding process involving propylene oxide and CO_2, with the former case being under thermodynamic control at temperatures above 5 °C. This explains the tendency to produce large quantities of cyclic carbonate in the coupling reaction of epichlorohydrin and CO_2 even at rather low temperatures.

Table 5. Reaction conditions and variable temperature rate data for copolymerization reactions.[a]

Temperature (K)	Epoxide	Rate(abs/s $\times$ 10^6)	
		Cyclic carbonate	Polymer
298	Propylene oxide	1.7	96.3
315	Propylene oxide	10.6	218.9
323	Propylene oxide	27.3	277.7
269	Epichlorohydrin	1.7	3.3
277	Epichlorohydrin	7.6	7.9
283	Epichlorohydrin	14.5	10.5

[a]Each experiment was performed under 2.0 MPa in CO_2, 14 mL of the appropriate epoxide, and complex1a/PPNY/epoxide = 1/1/2000 (molar ratio), Y = 2,4-dinitrophenoxy.
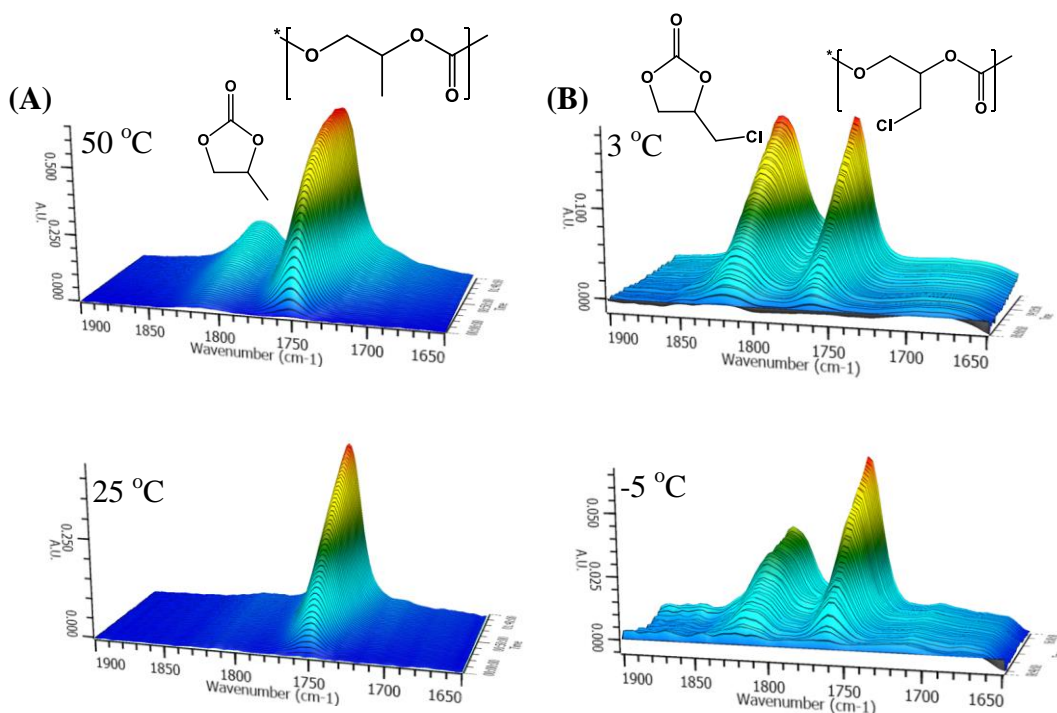
Figure 10. Three-dimensional stack plots for the epoxide/CO_2 coupling reactions utilizing complex 1a and PPNY as catalysts. (A) Propylene oxide and CO_2. (B) Epichlorohydrin and CO_2.
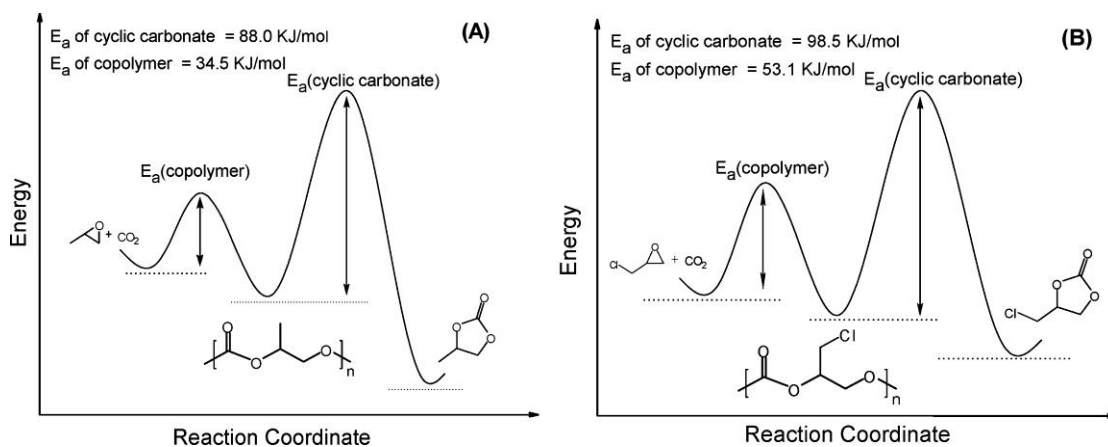
Figure 11. Reaction coordinate diagrams for (A) CO_2/propylene oxide, and (B) CO_2/epichlorohydrin coupling reactions.

46

Scheme 10. Three modes for cyclic carbonate production.

$(P)\sim$ = growing polymer chain
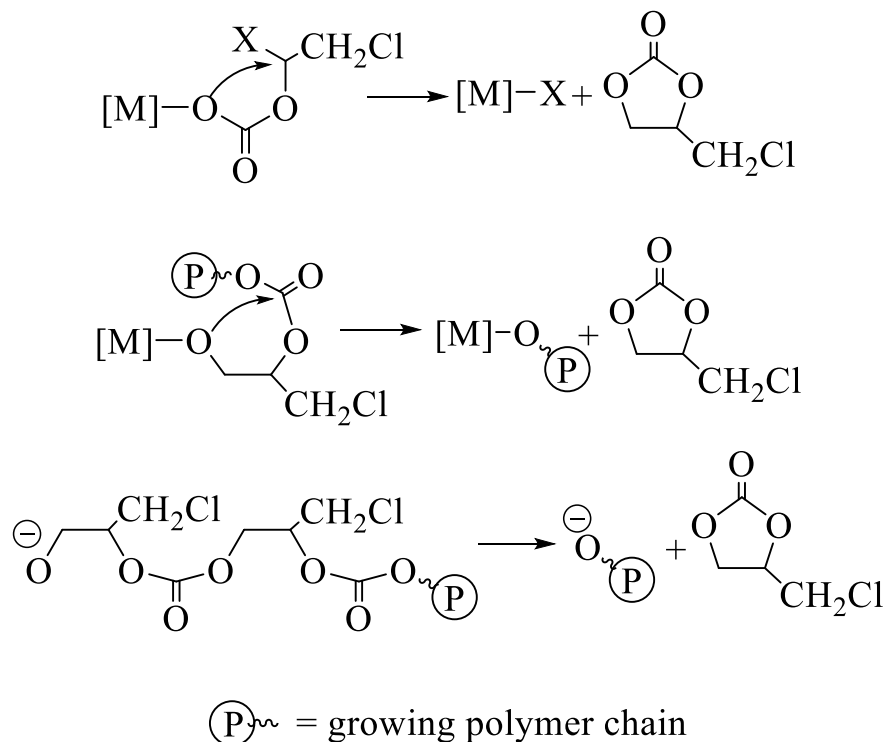
Similarity, the activation barriers for styrene oxide/CO_2 coupling to afford the two products are more closely matched than those for the propylene oxide/CO_2 process (**Figure 12**). In particular for the propylene oxide/CO_2 reaction, cycloaddition occurs with significantly higher activation energy over that for copolymer formation (**Figure 11A**). It is important to note here that in the temperature regime studied (273-303 K), the propylene oxide/CO_2 cycloaddition process most likely proceeds principally *via* the metal-coordinated process, whereas for the styrene oxide/CO_2 reaction the activation barrier for cyclic carbonate production is a composite of metal-assisted and free anionic polymer chain backbiting pathways (**Scheme 10**). Support for this is obtained from

examining the styrene oxide/CO_2 reaction in the higher temperature regime (315-332 K) where *no* copolymer was formed and cyclic carbonate formation most likely takes place away from the metal center. In this instance an E_a value for cyclic carbonate production was found to be significantly lower at 34.1 kJ/mol.
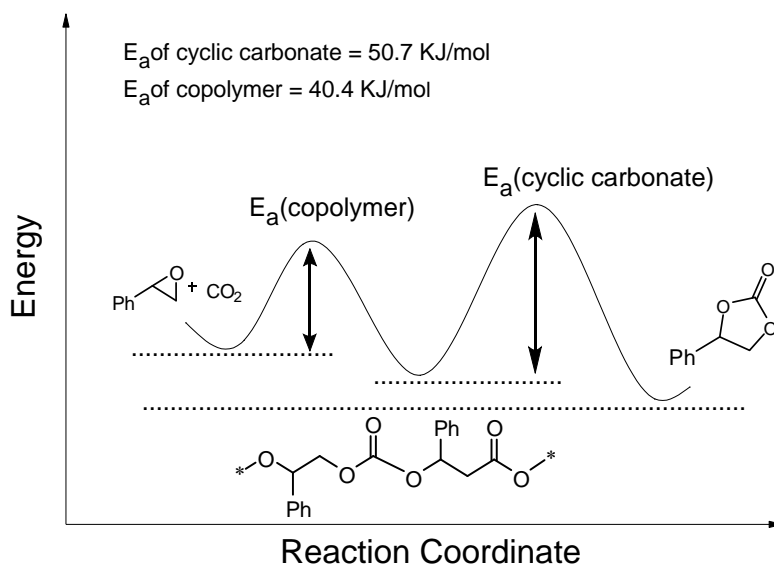
Figure 12. Reaction coordinate diagram for CO_2/styrene oxide copolymerization.

Concluding remarks

In summary, the alternating copolymerization of CO_2 and styrene oxide to afford the corresponding polycarbonate with more than 99% carbonate linkages was achieved with the use of cobalt-based catalyst systems. The completely alternating polycarbonate exhibits excellent thermal stability and has a relatively high glass-transition temperature of 80 ^{o}C.

In addition, we have reported perfectly alternating copolymerization of CO_2 and epichlorohydrin using cobalt(III)-based catalyst systems. Single component cobalt(III)-based complexes bearing an appended TBD or quaternary ammonium salt on the ligand framework have been shown to be highly active for catalyzing CO_2/epichlorohydrin copolymerization to selectively provide the corresponding polycarbonates with more than 99% carbonate linkages even at a low catalyst loading. A more sensitive temperature-dependent product distribution, with cyclic carbonate readily formed at enhanced temperatures, was observed in the coupling reaction of CO_2 and epichlorohydrin in comparison with the propylene oxide/CO_2 process. In part, this is ascribed to the lower activation energy barrier for cyclic carbonate production *via* the backbiting mechanism for epichlorohydrin *versus* propylene oxide.

Another more sensitive temperature-dependent product distribution was observed for the CO_2 coupling reaction with styrene oxide as compared to that with propylene oxide, with styrene carbonate being the sole product at elevated reaction temperatures. This difference in product selectivity is in part attributed to backbiting of the propagating carbonate anion on the enhanced electrophilic nature of the methine carbon center in styrene oxide. The preferential ring-opening of propylene oxide at the methylene carbon as compared to styrene oxide at the sterically hindered methine carbon accounts for the much slower rate of epoxide/CO_2 copolymerization in the styrene oxide case.

DEPOLYMERIZATION OF POLYCARBONATES DERIVED FROM CARBON DIOXIDE AND EPOXIDES TO PROVIDE CYCLIC CARBONATES – A KINETIC STUDY[*]

Introduction

The utilization of carbon dioxide as a comonomer with epoxides in the synthesis of polycarbonates is presently seen as a viable method for producing useful materials made in part from sustainable resources (**equation 2**).[15, 49, 66]

polycarbonate   **cyclic carbonate**   (2)
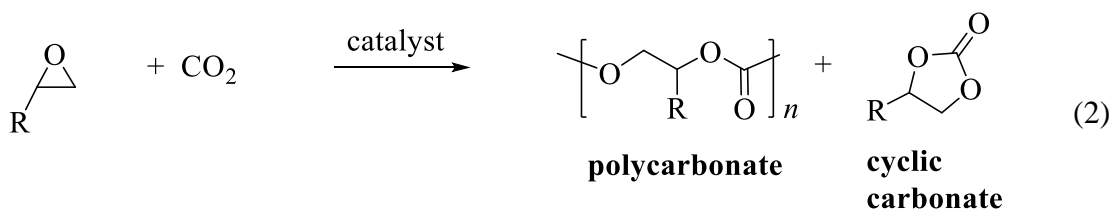
A major impediment to the selective production of copolymer from the coupling reaction of epoxides and CO_2 is the ease of the backbiting process from the free anionic growing polymer chain to provide cyclic carbonate. This process is illustrated below starting from either the carbonate or alkoxide end group for the copolymer formed from

---

ethylene oxide and CO_2 with formation of ethylene carbonate (**Scheme 11**). These copolymer chains are terminated in general by protons resulting in polycarbonates with –OH end groups. Similarly, the copolymer is stabilized while bound to the metal catalyst during monomer enchainment processes.[35, 67]

Scheme 11. Backbiting from either the carbonate or alkoxide end group.

$$\text{~P} = \text{growing polymer-chain}$$
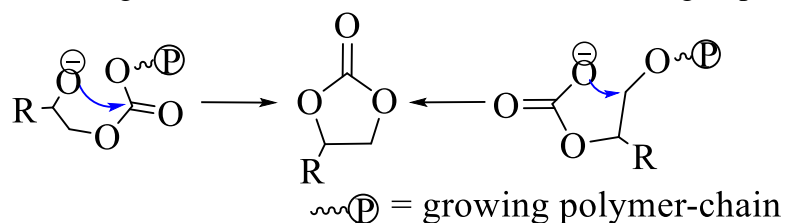
It has become increasingly evident that for many epoxide/CO_2 generated polycarbonates, low reaction temperatures, which generally translate to long reaction time, are required to afford selective formation of copolymer *vs* cyclic carbonate.[68, 69] Herein, we wish to report on kinetic studies of the thermal anaerobic decomposition of these anionic copolymer chains derived from epoxides bearing both electron donating and electron withdrawing substituents.

Experimental section

Reagents and methods. Toluene and tetrahydrofuran were freshly distilled from sodium/benzophenone. Tetra-*n*-butylammonium chloride and tetra-*n*-butylammonium bromide (Aldrich) was recrystallized from acetone/diethyl ether before use. (2,2,6,6-Tetramethylpiperidin-1-yl)oxyl (Aldrich) was stored in the glovebox. Tetra-*n*-butylammonium azide (TCI) was stored in the freezer of the glovebox upon arrival.

Poly(styrene carbonate),[68] poly(CO_2-*alt*-epichlorohydrin),[69] poly(propylene carbonate),[70] and poly(cyclohexene carbonate)[71] were prepared as reported in the literature.

^{1}H NMR spectra were acquired on Unity+ 300 MHz and VXR 300 MHz superconducting NMR spectrometers. Molecular weight determinations (M_n and M_w) were carried out with a Viscotek Modular GPC apparatus equipped with ViscoGEL I-series columns (H + L) and a model 270 dual detector comprised of refractive index (RI), low angle light scattering (LALS), and right angle light scattering (RALS) with THF as eluent. *In situ* infrared experiments were performed using a ReactIR ic10 reaction analysis system with a SiComp ATR crystal (purchased from Mettler Toledo). Infrared spectra were recorded on a Bruker Tensor 27 FTIR spectrometer in CaF_2 solution cells of 0.1 mm pathlength.

X-ray crystal study. Crystals of cyclic cyclohexene carbonate were obtained by slowly evaporating the reaction solution. For the crystal structure, a Bausch and Lomb 10x microscope was used to identify suitable crystals. A single crystal sample was coated in mineral oil, affixed to a Nylon loop, and placed under streaming N_2 (110 K) in a single-crystal APEXii CCD diffractometer. X-ray diffraction data were collected by covering a hemisphere of space upon combination of three sets of exposures. The structure was solved by direct methods. H atoms were placed at idealized positions and refined with fixed isotropic displacement parameters and anisotropic displacement parameters were employed for all non-hydrogen atoms. The following programs were used: for data collection and cell refinement, APEX2;[72] data reductions, SAINTPLUS,

version 6.63;[73] absorption correction, SADABS;[74] structure solutions, SHELXS-97;[75] structure refinement, SHELXL-97.[76]

Depolymerization of polycarbonates monitored by ^{1}H NMR. Polycarbonate (carbonate repeating unit = 0.3 mmol), (R,R′)-(*N*,*N*′-bis-(3,5-di-*tert*-butylsalicylidene)-1,2-cyclohexenediimine chromium(III) chloride (3.85 mg, 0.006 mmol, (salen)CrCl), and *n*-Bu$_4$NN$_3$ (3.47 mg, 0.012 mmol) were dissolved in 1 mL of *d*-toluene. The solution was prepared in an Ar-filled glove box and transferred into a J-Young tube (0.5 mL). The J-Young tubes were placed in a 110 ^{o}C oil bath and the reactions were monitored by ^{1}H NMR and shown to quantitatively produce cyclic carbonate (see ^{1}H NMR spectra in Apendix B). Similar experiments were carried out in the absence of metal complex.

Basicity depended depolymerization reaction monitored by *in situ* ATR-FTIR spectroscopy. Anionic initiators (*n*-Bu$_4$NX, X = N$_3$ or halide), and poly(styrene carbonate) (250 mg) were dissolved in 5 mL of toluene. The repeating units-to-initiator ratio was maintained at 25:1. The infrared spectrometer was set to collect one spectrum every 1 min over the corresponding reaction time. Profiles of the absorbance at 1760 cm$^-$^{1} (polymer) and at 1830 cm^{-1} (cyclic carbonate) with time were recorded after baseline correction.

Kinetic studies of depolymerization monitored by *in situ* ATR-FTIR spectroscopy. Polycarbonate (carbonate repeating unit = 1.5 mmol) was dissolved in 4 mL of toluene and heated up to the appropriate temperature. (R,R′)-(*N*,*N*′-bis-(3,5-di-*tert*-butylsalicylidene)-1,2-cyclohexenediimine chromium(III) chloride (19.3 mg, 0.03 mmol), and *n*-Bu$_4$NN$_3$ (17.4 mg, 0.06 mmol) were dissolved in 1 mL of toluene. The

mixture was transferred into the heated polycarbonate solution. The infrared spectrometer was set to collect one spectrum every 1 min over the corresponding reaction time. Profiles of the absorbance at 1760 cm^{-1} (polymer) and at 1830 cm^{-1} (cyclic carbonate) with time were recorded after baseline correction.

Preparation of acetate end-capping poly(styrene carbonate). Triethylamine (0.3 mL, 2 mmol) and hydroxy-end poly(styrene carbonate) (400 mg, 0.01 mmol) were dissolved in 5 mL of anhydrous THF. Acetyl chloride (0.1 mL, 1.4 mmol) was added dropwise to the THF solution maintained at 0 ^{o}C. Following warm up to ambient temperature, the reaction was stirred overnight, during which NH_4Cl precipitated from solution. The ammonium salt was removed by filtration through silica gel, and the filtrate was concentrated to remove excess triethylamine. Upon adding diethyl ether, the acetate end-capping poly(styrene carbonate) was precipitated from solution, isolated by filtration, and dried under reduced pressure.

Depolymerization of acetate end-capping poly(styrene carbonate) monitored by ^{1}H NMR. Acetate end-capping poly(styrene carbonate) (carbonate repeating unit = 0.3 mmol), and *n*-Bu$_4$NN$_3$ (3.47 mg, 0.012 mmol) were dissolved in 1 mL of d-toluene in an Ar-filled glove box and transferred into a J-Young tube (0.5 mL). The J-Young tube was heated to the appropriate temperature and the reaction was monitored by ^{1}H NMR.

Results and discussion

Influence of anions on depolymerization. Initially we chose poly(styrene carbonate), made from CO_2 and styrene oxide employing a (salen)CoX catalyst,[68] to test

54

the decomposition of polycarbonate in the presence of various anionic initiators. *It is of importance to note that the poly(styrene carbonate) sample employed in this study is very well characterized and contained >99% carbonate linkages.[77] Its molecular weight distribution was narrow and monomodal over various conversion levels, hence the end groups of the copolymer chain are the initiating anion and an –OH group.[53c, 78] Furthermore, the sample's M_n values were close to the calculated values and exhibited a linear relationship with % conversion as anticipated for a living polymerization process.* Tetra-*n*-butylammonium salts (*n*-Bu₄NX) were selected to examine the depolymerization process, where X equals azide, chloride, and bromide anions, since these are common cocatalysts used along with metal salen catalysts in the copolymerization reactions. Tetra-*n*-butylammonium salts were chosen rather than the more commonly used *bis*(triphenylphosphine)iminium salts (PPNX) due to their solubility in toluene. Reactions were carried out in a 0.3 M toluene solution of copolymer at 70 $^{\circ}$C in a molar ratio of repeating unit: anion equal to 25: 1. The reaction was monitored by *in situ* infrared spectroscopy. Upon treating a toluene solution of poly(styrene carbonate) with *n*-Bu₄NN₃, the depolymerization reaction began after a 10 minute induction period and was completed within 10 minutes (**Figure 13A**). When X = Cl, the reaction took more than 10 hours to initiate the depolymerization and another 4 hours to complete the process (**Figure 13B**). No reaction was observed after 1.5 days in the presence of bromide anion, even upon increasing the temperature to 90 degrees for another day (**Figure 13C**). This suggests, as anticipated, that the initiation of depolymerization process, i.e., deprotonation of the polymer –OH end group, highly depends on the

55

basicity of the anions of the initiator. Similarly, the initiation step depends on the concentration of the anion, e.g., note the decrease in depolymerization rate at 70 $^{\circ}$C upon decreasing the azide loading in **Figure 13A** to that in **Figure 14**. **Equation 3** illustrates this as an equilibrium process where all copolymer chains are not deprotonated, hence leading to a broadening of the molecular weight distribution as the reaction proceeds to completion (*vide infra*). On the other hand, employing a stronger, non-nucleophilic base like DBU (1,8-diazabicyclo[5.4.0]undec-7-ene) leads to complete depolymerization of poly(styrene carbonate) to styrene carbonate at 22 $^{\circ}$C in less than an hour.

$$P\sim\!\!\!\sim OH \ + \ N_3^- \ \rightleftharpoons \ P\sim\!\!\!\sim O^- \ + \ HN_3$$

$$\Downarrow$$

cyclic carbonate

(3)

(A)   (B)   (C)
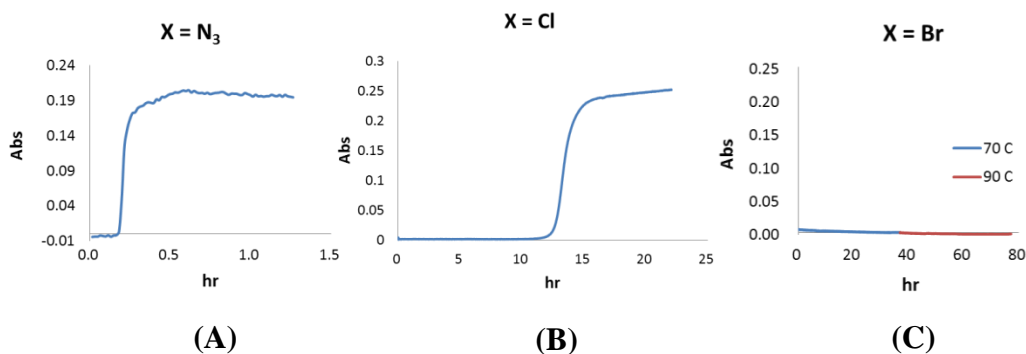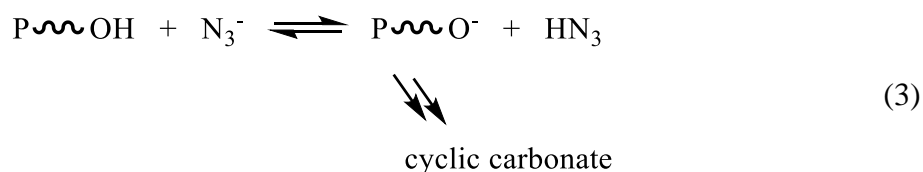
Figure 13. ReactIR profiles of cyclic styrene carbonate formation in the depolymerizations of poly(styrene carbonate) employing different anions (A) *n*-Bu$_4$NN$_3$ (B) *n*-Bu$_4$NCl (C) *n*-Bu$_4$NBr. Reactions were carried out in 0.3 M toluene solutions of copolymer (mole ratio of repeating unit: anion = 25:1) at 70 $^{\circ}$C.

Having established the azide anion from the soluble n-Bu$_4$NN$_3$ salt as the most effective reagent surveyed for deprotonating the –OH polymer end group, all future studies reported upon herein will utilize this initiator for polymer degradation.

Reaction mechanism. In order to study the mechanism of the depolymerization process, the changes in the copolymer's molecular weight and polydispersity were monitored during the process. For this investigation, poly(styrene carbonate) was treated with n-Bu$_4$NN$_3$ in toluene at 70 $^{\circ}$C and the reaction was monitored by *in situ* infrared spectroscopy. Once the depolymerization reaction began, small aliquots (~ 0.5 mL) of reaction solution were periodically withdrawn and added to acidified methanol to isolate the copolymer by precipitation. The solid poly(styrene carbonate) samples were dissolved in THF and their molecular weights were determined by gel permeation chromatography. If the depolymerization occurs *via* backbiting from the polymer chain end, the molecular weight will slowly decrease. Furthermore, the PDI of the chains should remain narrow throughout the depolymerization process (**Scheme 12A**). In contrast, if the polymer chain is randomly cut during the reaction, the molecular weight will dramatically drop, and broad molecular weight distributions should be observed (**Scheme 12B**).

Scheme 12.

(A)

(B)
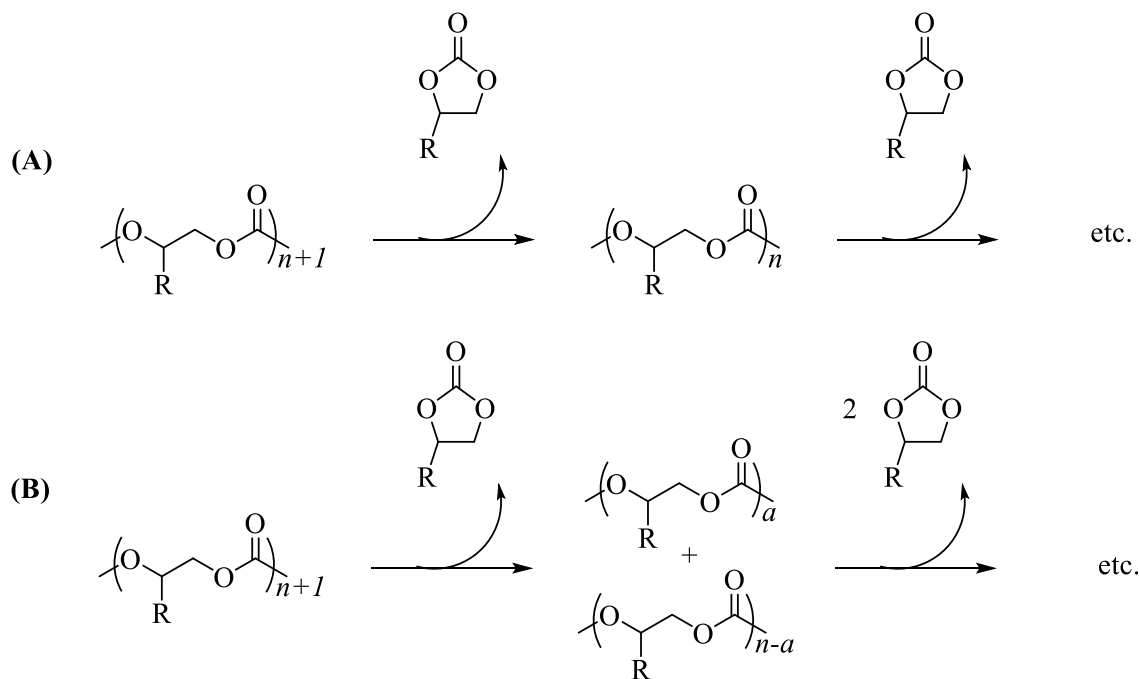
The depolymerization of poly(styrene carbonate) was carried out on a pure sample of molecular weight 32,600 Da and a polydispersity index of 1.03, and the reaction was monitored by *in situ* infrared spectroscopy. The reaction profile for the formation of cyclic styrene carbonate at 70 ^{o}C is depicted in **Figure 14**, where the copolymer repeating unit:azide anion ratio was 1000:1. As noted in Figure 14, cyclic carbonate formation started slowly over the initial stages of the process and then proceeded to completion over a few hours. The molecular weight of the unreacted copolymer slowly decreased over the course of the reaction with small increases in PDI being observed. Hence, the depolymerization process is highly ordered and proposed to follow the backbiting process illustrated in **Scheme 12A**. It is thus assumed that the depolymerization process is initiated by deprotonation of the hydroxyl chain end by the

anion followed by backbiting from the anionic copolymer chain as illustrated in **Scheme 11**. This reaction pathway is *strongly* supported by end-capping the copolymer with an acetate group. In this instance, for a reaction carried out under identical conditions as in **Figure 13A**, the copolymer is perfectly stable for over 1.5 hrs at 70 $^{\circ}$C. If the reaction temperature is increased to 90 $^{\circ}$C, complete depolymerization to cyclic carbonate occurs over an extended period of time, i.e., over 12 hours. Presumably, this involves a higher energy route where the azide ion randomly attacks carbonyl units in the copolymer chain, thereby subdividing the polymer into smaller macromolecular units.

Time (hr)	Mn	PDI
0	32600	1.03
2.2	32500	1.04
2.5	31300	1.04
2.8	28400	1.05
3.1	20800	1.11
3.4	15100	1.24
3.6	8400	1.34
3.9	7200	1.49
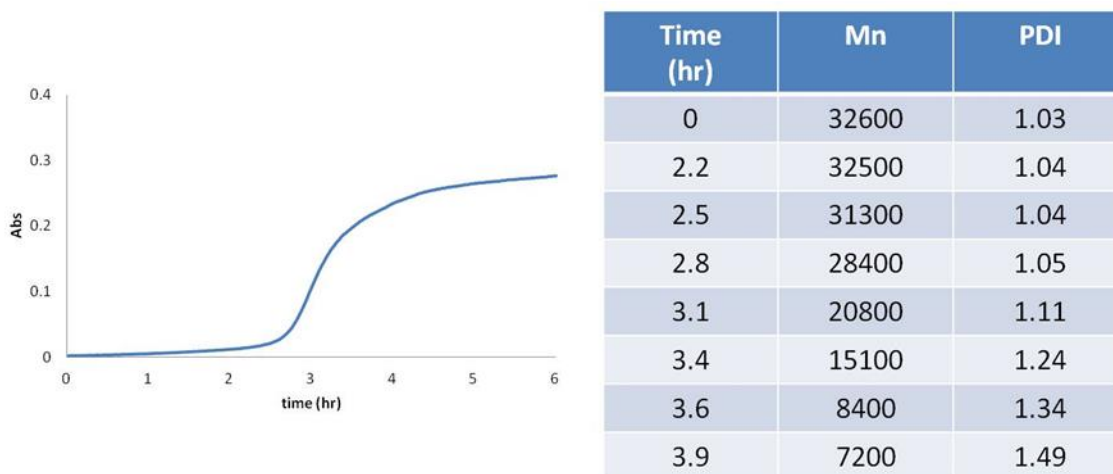
Figure 14. The reaction profile for cyclic styrene carbonate formation initiated by azide, along with the molecular weight data for the remaining copolymer chain. Reactions were carried out in 0.3 M toluene solutions of copolymer (mole ratio of repeating unit: anion = 1000:1) at 70 $^{\circ}$C.

In order to analyze the influence of metal binding of the growing polymer chain on the depolymerization process, several aliphatic polycarbonates were selected for

further investigations. Initially, depolymerization of the copolymer poly(styrene carbonate) was examined in the presence of (salen)CrCl/n-Bu$_4$NN$_3$ at a polymer repeating unit:metal:anion ratio of 50:1:2. The (salen)Co(III) analog is unstable with regard to reduction to (salen)Co(II) under the reaction conditions. The reactions were monitored by ^{1}H NMR spectroscopy in d-toluene at 110 ^{o}C under an argon atmosphere. The results are summarized in Table 6, along with comparable studies for the copolymers poly(CO$_2$-alt-epichlorohydrin) and poly(propylene carbonate). Control experiments carried out under identical reaction conditions in the absence of (salen)CrCl are reported as well, where the depolymerization processes were shown to occur on a much faster time scale.

As noted in **Table 6**, depolymerization of poly(styrene carbonate) to styrene carbonate occurs to only 18% conversion after one hour in the presence of (salen)CrCl, whereas, the process is 100% complete in the absence of the chromium complex. That is, depolymerization is significantly *retarded* presumably due to the anionic copolymer chain end binding to the metal center. Analogous behavior is observed for the depolymerization of poly(CO$_2$-alt-epichlorohydrin) where in the absence of metal catalyst the process is complete within two hours compared to 8-10 hours with addition of (salen)CrCl. Similarly, whereas poly(propylene carbonate) completely depolymerizes to cyclic propylene carbonate in one hour in the presence of n-Bu$_4$NN$_3$ alone, it requires over 30 hours upon adding the chromium catalyst. Hence, these experimental results clearly demonstrate that similar to capping the copolymer chain ends with protons, metal

binding of the anionic polymer chain greatly diminishes the rate of depolymerization of copolymer to cyclic carbonate.

It has previously been noted in numerous reports employing a wide range of catalyst systems that the coupling of cyclohexene oxide and carbon dioxide is generally highly selective for copolymer *vs* cyclic carbonate formation.[36a] Indeed, studies involving the production of poly(cyclohexene carbonate) are the most widely investigated to date. Consequently, it is important to investigate the depolymerization of poly(cyclohexene carbonate) both in the presence and absence of (salen)CrCl. Unlike our previous observations for aliphatic polycarbonates, poly(cyclohexene carbonate) exhibited unusually high stability toward depolymerization in its anionic form (**Table 7**). That is, no cyclic carbonate was observed after 20 days at 110 ^{o}C. On the other hand, upon adding (salen)CrCl, cyclic cyclohexene carbonate formed slowly with 100% conversion noted at 170 hours.

Table 6. Depolymerization of polycarbonates.
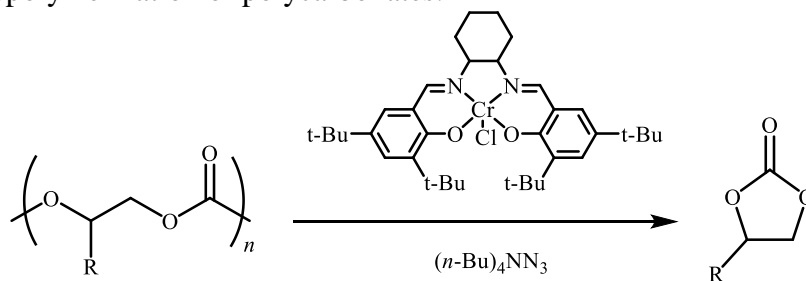
R	Time (h)	Yield of cyclic carbonate (%)[a]	
		Metal-involved[b]	Anion-assisted[c]
Ph	1	18	100
	2	67	
	3	100	
CH$_2$Cl	1	-	90
	2	68	100
	4	91	
	6	95	
	8	99	
	10	100	
Me	1	0	100
	6	0	
	10	6	
	12	18	
	24	82	
	28	93	
	32	100	

[a]Determined by ^{1}H NMR.
[b]Reaction condition: polycarbonate repeating unit: Cr: n-Bu$_4$NN$_3$ = 50: 1: 2. 0.3M of repeating unit solution in d-toluene, 110 °C.
[c]Reaction condition: polycarbonate repeating unit: n-Bu$_4$NN$_3$ = 50: 2. 0.3M of repeating unit solution in d-toluene, 110 °C.

Table 7. Depolymerization of poly(cyclohexene carbonates).

Time (h)	Yield of cyclic carbonate (%)[a]	
	Metal-involved[b]	Anion-assisted[c]
82	0	0
100	3	0
120	63	0
144	91	0
170	100	0
480	-	0

[a]Determined by ^{1}H NMR.
[b]Reaction condition: polycarbonate repeating unit: Cr: n-Bu$_4$NN$_3$ = 50: 1: 2. 0.3M of repeating unit solution in d-toluene, 110 ^{o}C.
[c]Reaction condition: polycarbonate repeating unit: n-Bu$_4$NN$_3$ = 50: 2. 0.3M of repeating unit solution in d-toluene, 110 ^{o}C.

In an effort to better assess the significant difference observed for this alicyclic epoxide copolymer, the degradation product, cyclohexene carbonate was fully characterized. Although the infrared bands in the carbonate region at 1800 and 1830 cm$^-$^{1} in methylene chloride strongly suggested the *trans* conformation (**Figure 15**),[36b, 79] we carried out an X-ray structural analysis of the cyclic carbonate. As seen in **Figure 16**, the structure is indeed that of the *trans* isomer.
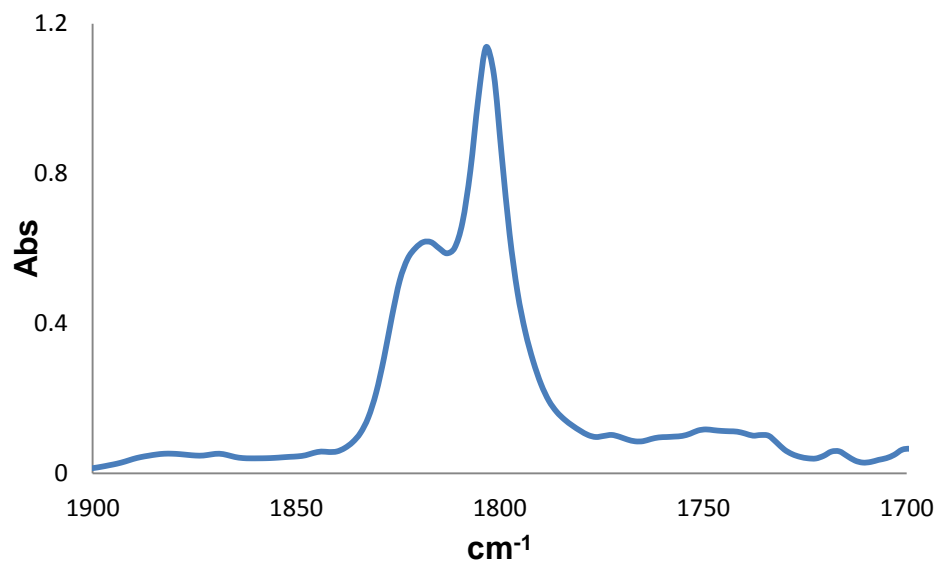
Figure 15. Infrared spectrum in $\nu(C=O)$ region of cyclohexene carbonate in CH_2Cl_2.
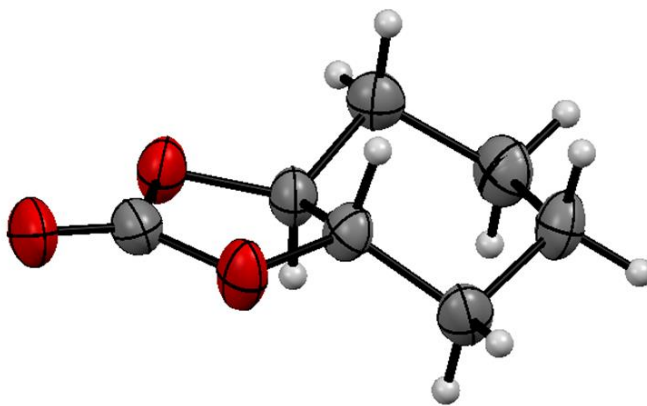
Figure 16. Thermal ellipsoid representation of cyclohexene carbonate.

Scheme 13 depicts the depolymerization reaction pathways of poly(cyclohexene carbonate) leading to cyclohexene carbonate either while the copolymer chain is metal bound or free anion in solution. Since the *trans* cyclic carbonate is observed during the

unzipping of the copolymer only routes **A** and **C** can be operative. However, because the depolymerization was seen only in the presence of the metal catalyst, pathway **A** must be the dominant route to cyclohexene carbonate. As would be anticipated from the depressed rates of *trans*-cyclic carbonate production from poly(cyclohexene carbonate) in the presence of (salen)CrCl, high energy barriers for its formation have been reported in the literature. That is, E_a values of 133.0, 127.2, and 137.5 kJ/mol have been determined for several different metal catalysts.[36] Nevertheless, production of the *cis* isomer of cyclohexene carbonate *via* route **D** has been observed in other catalytic processes.[28]

Scheme 13. Possible reaction pathways for the depolymerization of poly(cyclohexene carbonate) to *trans*-cyclohexene carbonate.

[P]〜〜 = Polymer chain   [M] = Metal complex
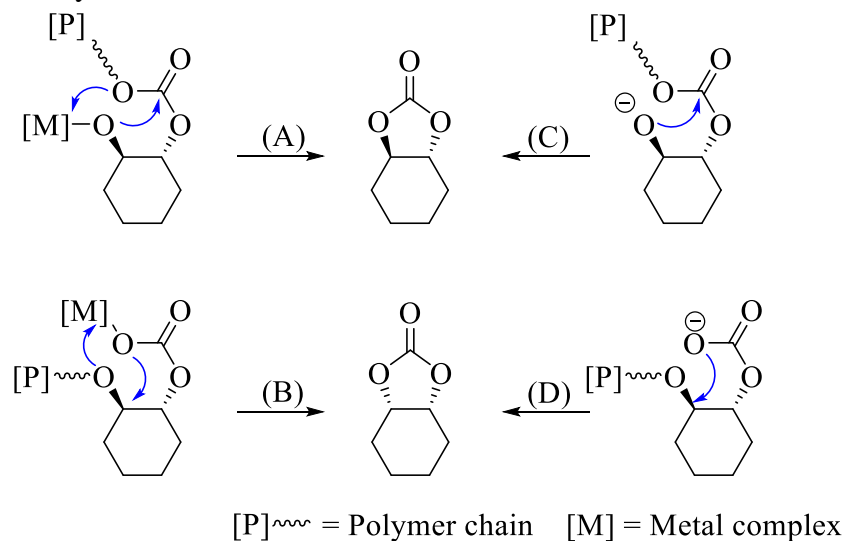
Energy of activation barriers derived from kinetic studies of the

depolymerization reactions. The kinetic parameters for the depolymerization of

poly(styrene carbonate), poly(CO_2-*alt*-epichlorohydrin), and poly(propylene carbonate)

to the corresponding cyclic carbonates were determined in the presence of azide ions in

toluene solution. These processes were carried out under identical reaction conditions at

several temperatures, and were monitored by *in situ* infrared spectroscopy. **Figure 17**

depicts a typical three-dimensional plot of the depolymerization of poly(styrene

carbonate) (ν_{CO_2} @ 1760 cm^{-1}) with concomitant formation of styrene carbonate (ν_{CO_2} @

1830 cm^{-1}). From the two-dimensional profiles of peak absorbance *vs* time, the initial

rates of depolymerization were measured as a function of temperature and are compiled

in **Table 8**.   The energies of activation for the various polycarbonates were determined

from Arrhenius plots as illustrated in **Figure 18** for the poly(styrene carbonate) sample,

and these values are summarized in **Table 9** for the three copolymers studied. Although

utilizing the azide anion as the deprotonating reagent as in **equation 3** leads to a rate

expression which involves an equilibrium constant as well as a rate constant,

temperature effects on the latter constant are expected to be dominant.
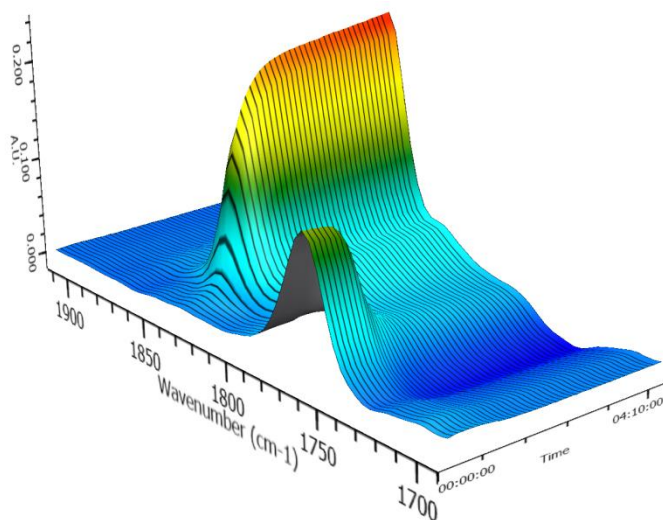
Figure 17. Three-dimensional stack plot of the ν_{CO_2} peaks for the depolymerization of poly(styrene carbonate) to afford styrene carbonate initiated by the anion from n-Bu$_4$NN$_3$ in toluene solution at 90 $^{\circ}$C.

Table 8. Initial reaction rates for anion-assisted polycarbonates depolymerization reactons.

Polycarbonate	Temp (K)	Rate x 10^5 s^{-1}
poly(styrene carbonate)[a]	343	7.23
	353	11.4
	363	16.6
	373	27.5
poly(CO$_2$-*alt*-epichlorohydrin)[b]	343	0.349
	353	0.694
	363	1.45
	373	2.98
poly(propylene carbonate)[b]	343	16.3
	353	42.0
	363	81.5
	373	162

[a]Reaction condition: polycarbonate repeating unit: n-Bu$_4$NN$_3$ = 1000: 1. 0.3M solution in toluene.
[b]Reaction condition: polycarbonate repeating unit: n-Bu$_4$NN$_3$ = 25: 1. 0.3M solution in toluene.
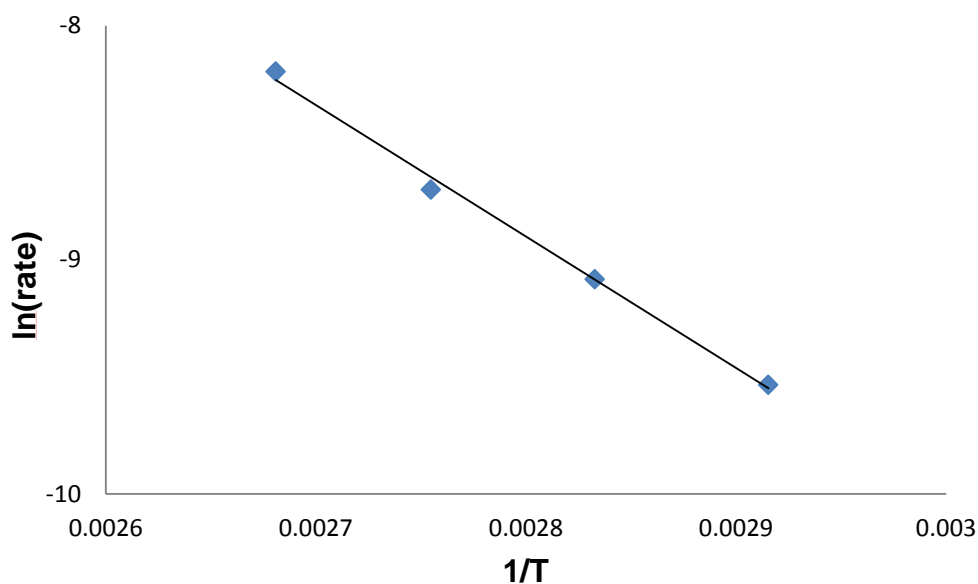
Figure 18. Arrhenius plot of anion-assisted poly(styrene carbonate) depolymerization. $y = -5613x + 6.816$ and $R^2 = 0.9955$.

Table 9. Activation energies for depolymerization processes.

Polycarbonate	E_a (kJ/mol)
poly(styrene carbonate)	46.7 ± 2.2
poly(CO_2-*alt*-epichlorohydrin)	76.2 ± 2.0
poly(propylene carbonate)	80.5 ± 3.6

Hence, these studies reveal the energy of activation barriers to increase in the order: poly(styrene carbonate) < poly(CO_2-*alt*-epichlorohydrin) ≤ poly(propylene carbonate). A similar trend in E_a values has been noted for the formation of cyclic carbonates during the copolymerization of the corresponding epoxides and carbon dioxide catalyzed by (salen)Co(III) catalyst in the presence of initiating anions.[68-69] That is, the E_a value determined for styrene carbonate production was 50.7 kJ/mol, whereas, the respective values for propylene carbonate and (CO_2-epichlorohydrin) carbonate were

found to be 88.0 and 98.5 kJ/mol, respectively. Since these productions represent cyclic carbonate formation *via* composite pathways involving metal bound and free anionic polymer chain backbiting mechanisms, the E_a values observed herein strongly suggest production of cyclic carbonates during copolymerization reactions originate primarily from the free anionic polymer chains.

Further support for this conclusion is seen in the energy of activation barrier we have determined for styrene carbonate production from poly(styrene carbonate) initiated by *n*-Bu$_4$NN$_3$ in the presence of (salen)CrCl. Again, the process was measured by *in situ* infrared spectroscopy with initial rates being determined as previously described. Rate data along with the E_a values determined in this instance are displayed in **Table 10**, with the Arrhenius plot shown in **Figure 19**. The energy of activation, E_a, was found to be significantly higher than in the absence of metal catalyst, being 141.2 kJ/mol. This observation clearly quantifies our earlier assessment that the depolymerization reactions are generally greatly suppressed in the presence of the (salen)CrCl species.

Table 10. Initial reaction rates for poly(styrene carbonate) depolymerization in the presence of metal complex.[a]

Temp (K)	Rate (abs/s) x 10^6	E_a (kJ/mol)
343	5.91	--
353	21.3	141.2
363	105	--
373	290	--

[a]Reaction conditions. Poly(styrene carbonate) repeating unit : (salen)CrCl : *n*-Bu$_4$NN$_3$ = 50:1:2. 0.3 M solution in toluene.
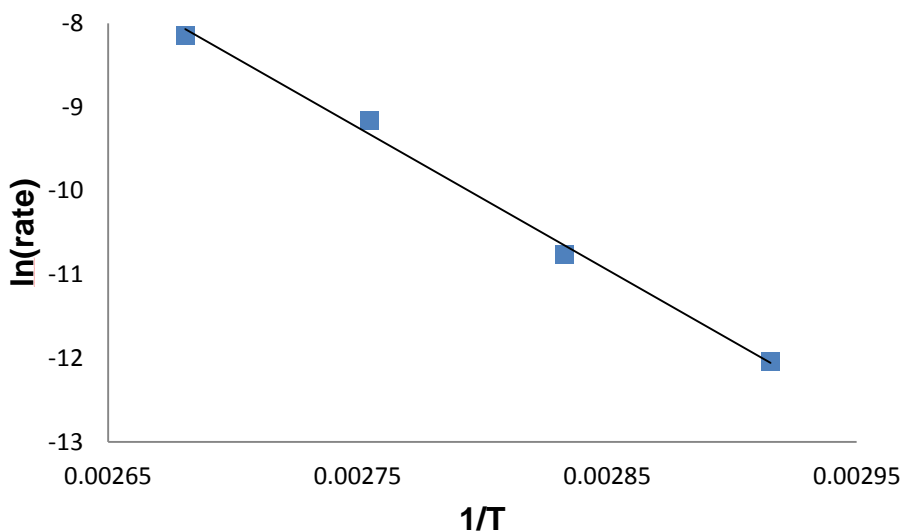
Figure 19. Arrhenius plot of poly(styrene carbonate) depolymerization to styrene carbonate in the presence of (salen)CrCl/n-Bu$_4$NN$_3$. y = -16,990x + 37.5 and R^2 = 0.9950.

Concluding remarks

Herein, we have shown that aliphatic polycarbonates derived from the completely alternating copolymerization of epoxides and carbon dioxide under anaerobic conditions quantitatively depolymerize to the corresponding cyclic carbonates in the presence of anionic initiators. Furthermore, these reactions were demonstrated to proceed *via* an unzipping of the free anionic copolymer chains as opposed to a random disruption, as revealed by a steady decrease in molecular weight with concomitant narrow distribution of the copolymer chain during the depolymerization process. The energy of activation barriers were found to increase for the selected polycarbonates in the order: poly(styrene carbonate) (46.7 kJ/mol) < poly(CO$_2$-*alt*-epichlorohydrin) (76.2

70

kJ/mol) $\leq$ poly(propylene carbonate) (80.5 kJ/mol). Since this trend and magnitude in E_a values agree well with those observed during the copolymerization reactions, it can be assumed that both processes are occurring *via* similar pathways. On the other hand, in the presence of the metal catalyst, (salen)CrCl, and the azide anion, the depolymerization reaction is greatly suppressed presumably due to the anionic copolymer chain binding to the coordinatively unsaturated metal center. That is, in the absence of excessive quantities of epoxide as in the copolymerization process, the anionic copolymer chain binds to the metal center and retards its decomposition to cyclic carbonate. By comparison, the alicyclic polycarbonate, poly(cyclohexene carbonate), was found to undergo the backbiting reaction to cyclohexene carbonate by way of a metal-assisted pathway with a high activation barrier.

These observations point to the necessity of maintaining a close connectivity between the anionic copolymer chain and either the metal center or a proton. In the latter instance, the OH terminated copolymer can *via* a rapid chain transfer process reenter the copolymerization process as has been shown by Nozaki and coworkers.[37] Alternatively, this is best done by appending the onium salt to the salen ligand of the metal catalyst, thereby allowing the anionic copolymer chain to be electrostatically attracted to the metal catalyst.[38, 39b, 40, 80] In addition, we have preliminary data on the depolymerization reaction of the recently prepared poly(indene carbonate) copolymer which reveal the presence of radical intermediates during the depolymerization reactions.[34, 81]

CHAPTER IV

DEPOLYMERIZATION OF POLY(INDENE CARBONATE). A UNIQUE

DEGRADATION PATHWAY[*]

Introduction

  Because of their vast utility, the synthesis of polymers has become key targets of green or sustainable chemistry in the new millennium.[82] In particular, the synthesis of polycarbonates by greener technologies is receiving much current attention.   These include the polycondensation of the BPA derived polymer by replacement of phosgene with diphenylcarbonate (**equation 4**),[5] and the preparation of polycarbonates by the copolymerization of epoxides with carbon dioxide (**equation 5**).[15, 49, 66, 83]   The latter process represents an environmentally-friendly and potentially less expensive route to these important polymeric materials.
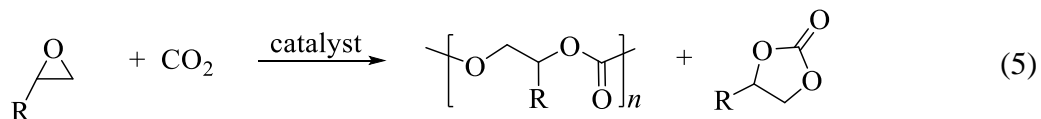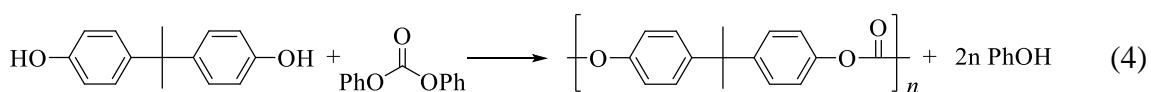
$$(4)$$

$$(5)$$

Poly(indene carbonate) has the highest T_g thus far published from the process of coupling CO_2/epoxides, up to ~140 °C.[34] It is also thermally stable at temperatures of up to nearly 250 °C. Due to its high thermal stability, poly(indene carbonate) may have various applications in the near future. However, the control of the selectivity of poly(indene carbonate) *vs* cyclic indene carbonate during the coupling is still a challenge.[41, 83b, 84] It is commonly accepted that cyclic carbonate byproduct forms *via* one or more of the backbiting processes illustrated in **Scheme 14**. Potential metal-involved and anion-assisted mechanisms both occur concomitantly with alkoxide backbiting and carbonate backbiting to produce cyclic carbonates during initiation, as well as copolymer propagation processes. Thus, studies of cyclic carbonate generation during copolymerization reactions are of significant interest.

Scheme 14.

~ⓟ   growing polymer chain

[M]   metal catalyst

X⁻   anionic initiator
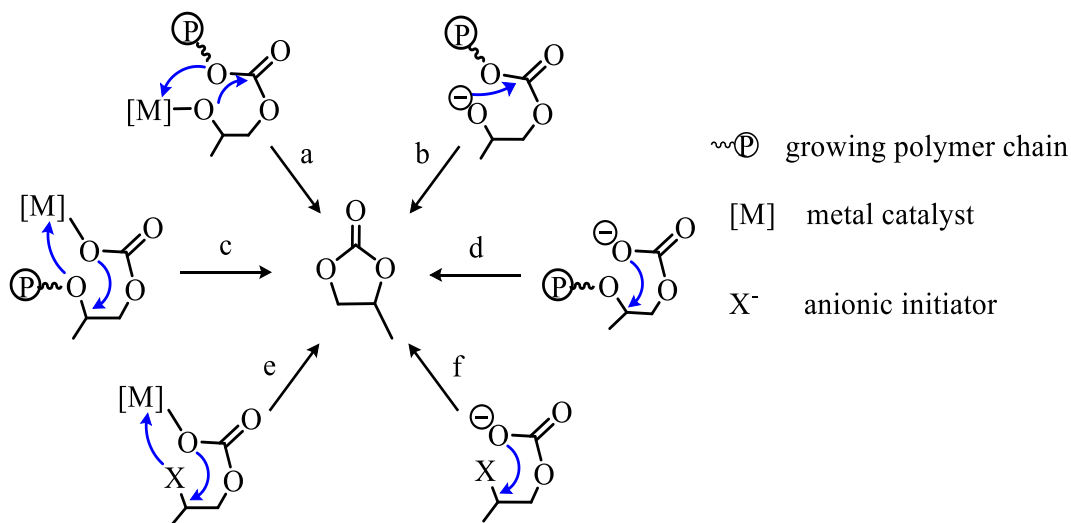
We have previously reported on depolymerization processes of polycarbonates derived from CO_2 and epoxides such as styrene oxide, propylene oxide, and epichlorohydrin.[85] These copolymers were isolated by precipitation from acidic methanol, providing pure polycarbonates with –OH end groups which could be deprotonated by a base. The lowest energy pathways (steps **b** and **d**) for copolymer degradation to cyclic carbonate were shown to proceed in the absence of metal complex. Both experimental and computational studies of the depolymerization process reveal backbiting from an alkoxide chain end to cyclic carbonate (step **b**) is less energetic relative to backbiting from carbonate chain end (step **d**). In some instances, cyclic carbonate production occurs as well following initial epoxide ring-opening and CO_2 addition (step **f**).

Herein, we wish to present results on the depolymerization of poly(indene carbonate). In this instance, because formation of *trans*-indene carbonate by pathway **b** is highly unfavored due to the instability of the fused five-membered rings, *cis*-indene carbonate production can only proceed *via* higher energy pathways **c − f**. In addition, there may be alternative routes to copolymer degradation.

Experimental section

Reagents and methods. Toluene was freshly distilled from sodium/benzophenone. 1,8-diazabicyclo[5.4.0]undec-7-ene (Aldrich) was stirred over CaH_2, vacuum distilled, then stored in the glovebox. (2,2,6,6-Tetramethylpiperidin-1-yl)oxyl (Aldrich), sodium bis(trimethylsilyl)amide (Alfa Aesar), methyl 2-bromo-2-methylpropanoate (Aldrich) were stored in the glovebox. Tetra-*n*-butylammonium azide

(TCI) was stored in the freezer of the glovebox upon arrival. Poly(indene carbonate),[34] poly(styrene carbonate),[77] poly(CO_2-*alt*-epichlorohydrin),[69] and poly(propylene carbonate)[70] were prepared as reported in the literature.

^{1}H NMR spectra were acquired on Unity+ 300 MHz and VXR 300 MHz superconducting NMR spectrometers. *In situ* infrared experiments were performed by using a ReactIR ic10 reaction analysis system with a SiComp ATR crystal (purchased from Mettler Toledo).

Base dependent depolymerization of poly(indene carbonate) monitored by ^{1}H NMR. In an Ar-filled glove box, poly(indene carbonate) (carbonate repeating unit = 0.3mmol), and the appropriate base (0.012mmol) were dissolved in 1mL of *d*-toluene. The solution was prepared in an Ar-filled glove box and transferred into a J-Young tube (0.5mL). The J-Young tube was placed in a 110°C oil bath and the reaction was monitored by ^{1}H NMR. The yield was determined by comparison of the integrals of signals arising from the protons in ^{1}H NMR spectra, including poly(indene carbonate) δ:6.6~6.2 (1H) and 5.7~5.2 (1H) ppm, cyclic indene carbonate δ:4.96 (1H) and 4.28 (1H) ppm, indene oxide δ:3.79 (1H) and 3.57 (1H) ppm, and 2-indanone δ:2.96 (4H) ppm.

Metal-involved depolymerization of poly(indene carbonate) monitored by ^{1}H NMR. In an Ar-filled glove box, poly(indene carbonate) (carbonate repeating unit = 0.3mmol), (R,R')-(N,N'-bis-(3,5-di-tert-butylsalicylidene)-1,2-cyclohexenediimine chromium(III) chloride (3.85mg, 0.006mmol, (salen)CrCl), and *n*-Bu$_4$NN$_3$ (3.47mg, 0.012mmol) were dissolved in 1mL of *d*-toluene. The solution was prepared in an Ar-filled glove box and transferred into a J-Young tube (0.5mL). For the high pressure

experiment, the solution was trapped by liquid nitrogen, followed by Ar removal by vacuum and CO_2 addition. The pressurized J-Young tube was then placed in a 110^oC oil bath, and the reaction was followed by ^1H NMR.

Kinetic studies of depolymerization monitored by *in situ* ATR-FTIR spectroscopy. Poly(indene carbonate) (carbonate repeating unit = 1.2mmol) was dissolved in 3 mL of toluene and heated up to the appropriate temperature. *n*-Bu_4NN_3 (23.1mg, 0.08mmol) was dissolved in 1 mL of toluene and transferred into the heated polycarbonate solution. The infrared spectrometer was set to collect one spectrum every 2 minutes over the corresponding reaction time. Profiles of the absorbance at 1750 cm^{-1} (polymer) and at 1825 cm^{-1} (cyclic carbonate) with time were recorded after baseline correction.

Results and discussion

Depolymerization under basic conditions. As evidence by our previous study, degradation of uncapped polycarbonates such as poly(styrene carbonate) are initiated by deprotonation of the hydroxyl end group, followed by backbiting to generate the corresponding cyclic carbonate (**Scheme 15**).[85] As expected, the rate of initiation of depolymerization is dependent upon the strength of the base. Thus, a strong base, sodium bis(trimethylsilyl)amide (NaHMDS), was chosen to initiate the depolymerization of poly(indene carbonate). The reaction was carried out at 110 ^oC, followed by ^1H NMR. Under these conditions, the endwise scission of poly(indene carbonate) proceeded very slowly, with only 15% of cyclic indene carbonate formed after 9 days. In addition to the cyclic indene carbonate, a trace amount of indene oxide (~ 3%) was also generated

over this time period (**Figure 20a**).   Poly(indene carbonate) was also treated with another organic non-nucleophilic base, DBU, in *d*-toluene at 110 °C, but no depolymerization was observed after 10 days (**Figure 20b**).   Further monitoring of the reaction for an additional 30 days provided cyclic indene carbonate as the sole product.

Scheme 15.

Ⓟ〰 = polymer chain
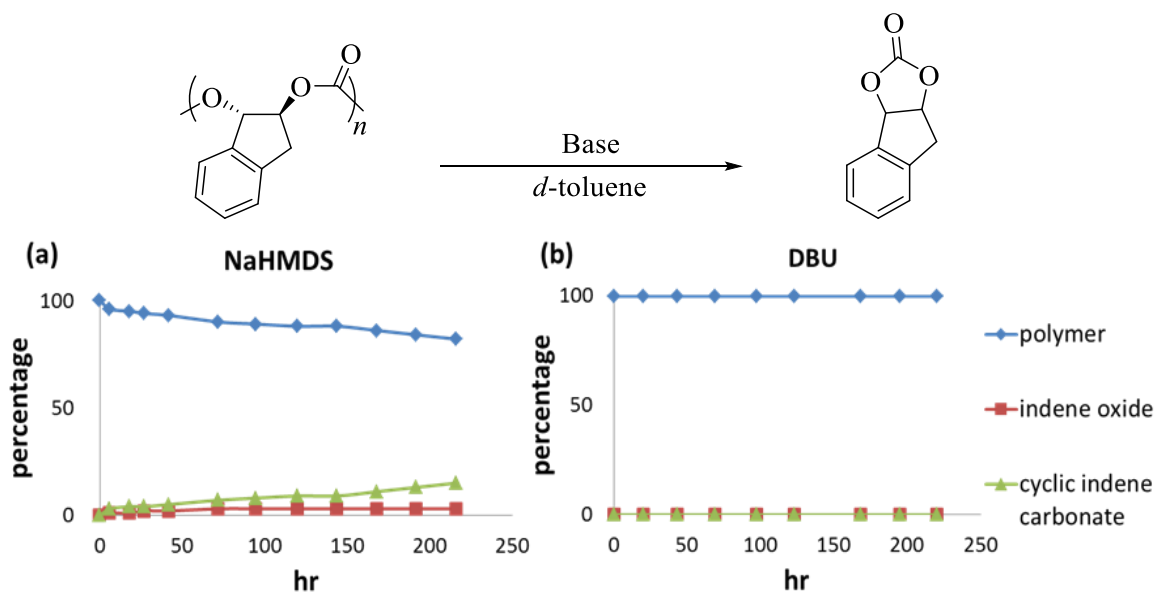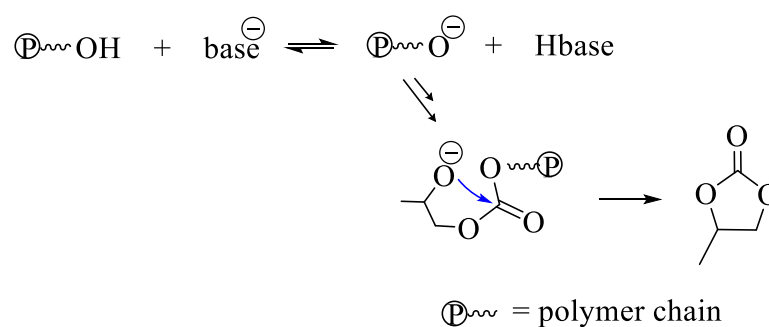
Figure 20. Depolymerization of poly(indene carbonate) at 110 °C initiated by (a) NaHMDS and (b) DBU.

77

In our previous study, azide was used to initiate the decomposition of various polycarbonates.[85] With n-Bu$_4$NN$_3$ as the initiator in the absence of a Cr(III)(salen) complex, degradation of poly(indene carbonate) was minimal at temperatures up to 90 $^{\circ}$C. At 110 $^{\circ}$C, cyclic indene carbonate is observable after one hour as the first depolymerization product. Over time the decarboxylated product, indene oxide, was also observed. After 5 days, the poly(indene carbonate) was completely consumed, converted to 92% cyclic indene carbonate and 8% indene oxide (**Figure 21a**). As azide is a weaker base than NaHMDS or DBU, the decomposition of poly(indene carbonate) by n-Bu$_4$NN$_3$ likely proceeds *via* an alternative pathway, instead of the deprotonation and backbiting process observed for the stronger bases.

Metal-involved pathway. Unlike the aliphatic polycarbonates PSC, PPC, PECC, the depolymerization of poly(indene carbonate) was enhanced in the presence of a metal-based catalyst.[85] In the presence of (salen)CrCl, the decarboxylated monomer, indene oxide, was the first observed product after 1 hour. Indene oxide was subsequently isomerized to form 2-indanone as the minor product. It required ~3 days to complete the degradation process, with 85% of cyclic indene carbonate and 15% of 2-indanone produced (**Figure 21b**). The formation of 2-indanone was not observed in the absence of metal complex. It is therefore likely that the metal complex activates the epoxide for ring opening; but with insufficient CO$_2$ in the system, the epoxide undergoes a Meinwald rearrangement to 2-indanone.[86]
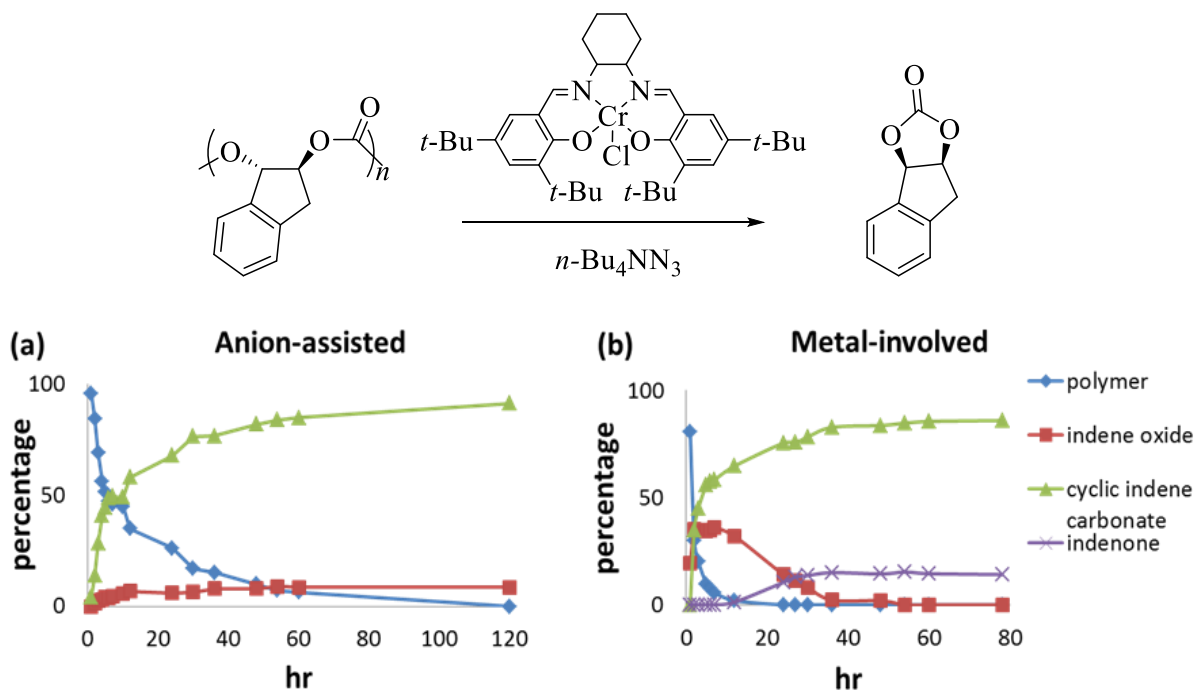
Figure 21. Depolymerization of poly(indene carbonate) *via* (a) anion-assisted and (b) metal-involved pathways.

Influence of high pressure CO_2. As the decarboxylated product, indene oxide, was observed in both the absence and presence of metal complex, analogous experiments involving high pressure CO_2 (100 psi) were carried out to investigate the effect of CO_2 on the depolymerization process. At its height, indene oxide made up only 9% of the reaction mixture, and this intermediate was quickly coupled with CO_2 to form cyclic indene carbonate in the metal-involved decomposition process (**Figure 22**). No 2-indanone formation was observable by ^{1}H NMR and cyclic indene carbonate was the only product in the final reaction mixture. The lower amount of indene oxide observed during the reactions run under high pressure of CO_2 indicates that decarboxylation occurs during degradation process. Additionally, the rate of depolymerization was much

slower under high pressure CO_2 than under 1 atm of argon. The CO_2-hindered depolymerization can be mechanistically explained, as we have previously demonstrated that there is a higher energy barrier of activation for cycloaddition *via* metal carbonate *vs* metal alkoxide anionic end groups.[35] This is not only true for five-membered cyclic carbonates, as polycarbonate degradations to six-membered cyclic carbonates are also inhibited by high pressures of CO_2.[87] These results also support the observation that high pressures of CO_2 suppress cyclic carbonates byproducts formation in CO_2/epoxides copolymerization reactions.
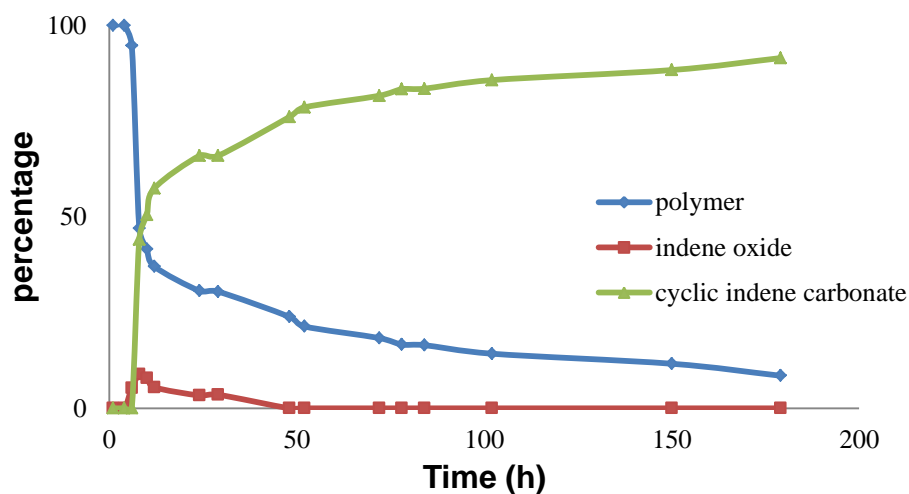
Figure 22. Metal-involved depolymerizations of poly(indene carbonate) under 7 atm CO_2.

High pressure experiments under identical reaction condition in the absence of (salen)CrCl were also investigated (**Figure 23**). Indene oxide was not observed in this instance, indicative of decarboxylation not occuring under these conditions. The

formation of cyclic carbonate was also slower than in the presence of metal catalyst, and appeared to plateau at about 25%.
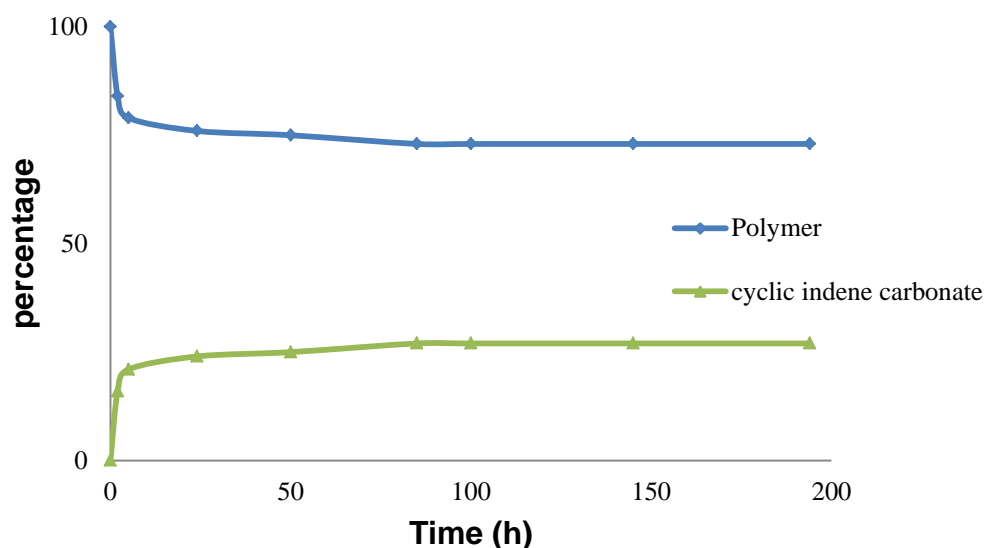
Figure 23. Anion-assisted depolymerization of poly(indene carbonate) under 7 atm CO_2.

Mechanistic investigations. It has become apparent from these initial studies of the degradation of poly(indene carbonate), i.e., the formation of indene oxide and the high rate of reaction in the presence of n-Bu$_4$NN$_3$, that an alternative reaction mechanism is operative. Relevant to this is the previous report that cyclic indene carbonate undergoes decarboxylation in the presence of light to afford both indene oxide and 2-indanone *via* a radical intermediate.[88] In order to confirm whether a radical intermediate was generated during the polymer degradation process, 10% of the radical trap TEMPO (2,2,6,6-tetramethylpiperidin-1-yl)oxyl was added to the reaction matrix. In the presence of TEMPO, no n-Bu$_4$NN$_3$-initiated degradation of poly(indene carbonate)

was observed after 2 days. A control experiment under identical conditions in the absence of TEMPO, provided 32% of indene carbonate and 7% of indene oxide after 3 hours, as revealed by ^{1}H NMR. Following this measurement of product distribution, the NMR tube was brought back into the glovebox, and 10 mol% TEMPO was added. The reaction was equilibrated to 110^oC for several hours, with no further decomposition being observed. This clearly indicates that the N_3-assisted depolymerization process operates by way of a radical intermediate that can be quenched by TEMPO.

On the contrary, TEMPO does not have an effect on the depolymerization process in the presence of the (salen)Cr complex, implying that two different mechanisms are involved in the depolymerization of poly(indene carbonate). In the absence of the (salen)Cr complex, the radical mechanism supports the reaction being retarded at high pressure of CO_2 (**Figure 23**). That is, the intermediate radical can be transferred to CO_2 to form a carbon dioxide based anion-radical, thereby quenching the degradation process. TEMPO displayed no influence on the depolymerization processes involving the previously investigated polycarbonates: poly(styrene carbonate), poly(CO_2-*alt*-epichlorohydrin), and poly(propylene carbonate) (**Table 11**).

Table 11. Depolymerization of polycarbonates in the presence of TEMPO.

Polycarbonate	Cyclic carbonate observed?
poly(indene carbonate)[a]	No
poly(indene carbonate)[b]	Yes
poly(styrene carbonate)[a]	Yes
poly(CO_2-*alt*-epichlorohydrin)[a]	Yes
poly(propylene carbonate)[a]	Yes

[a]Reaction condition: polycarbonate repeating unit: n-Bu$_4$NN$_3$: TEMPO = 50: 2: 5; 0.3 M solution in *d*-toluene, 110 °C. [b]Reaction condition: polycarbonate repeating unit: Cr: n-Bu$_4$NN$_3$: TEMPO = 50: 1: 2: 5; 0.3 M solution in *d*-toluene, 110 °C.

Several additional experiments were carried out to better assess the role of radicals in the degradation of poly(indene carbonate). These are summarized in **Table 12**, where entries **1** and **2** clearly illustrate the influence of added TEMPO. Similarly, entries **3** and **4** demonstrate the use of light to initiate polymer degradation at ambient temperature in the absence of TEMPO. For a degradation reaction performed in the dark with no added TEMPO, the depolymerization process did not occur over a one day period (entry **5**). Entry **6** shows that the radical is not generated by poly(indene carbonate) itself, and that the azide salt is required in order to generate the radical intermediate. Hence, in **Table 12**, the depolymerization of poly(indene carbonate) is shown to proceed *via* a radical pathway involving the azide ion in the presence of light. Furthermore, it was shown that the effective degradation of poly(indene carbonate) occurred over the period of 10 days at 110 °C in the presence of DBU and the radical initiator methyl-2-bromo-2methylpropanoate. The use of AIBN as radical initiator or the utilization of other inorganic or organic bases were much less effective.

Table 12. Anion assisted depolymerization under various reaction conditions.

Entry[a]	Room Light	Temperature (^{o}C)	TEMPO Added?	Product observed?
1	Yes	110	No	Yes
2	Yes	110	Yes	No
3	Yes[b]	25	No	Yes
4	Yes[b]	25	Yes	No
5	No	110	No	No
6[c]	Yes[b]	25	No	No

[a]Reaction condition: poly(indene carbonate) repeating unit: n-Bu$_4$NN$_3$: TEMPO = 50: 2: 5; 0.3 M solution in d-toluene at the listed temperature for 24 hours. [b]Mercury lamp. [c]No n-Bu$_4$NN$_3$ added.

Kinetic studies of the depolymerization reactions. The kinetic parameters for the depolymerization of poly(indene carbonate) to the cyclic indene carbonate were determined in the presence of n-Bu$_4$NN$_3$ in toluene solution in the presence of room light (entry **1** in **Table 12**). These processes were carried out under identical reaction conditions at several temperatures and were monitored by *in situ* infrared spectroscopy. **Figure 24** depicts a typical three-dimensional plot of the depolymerization of poly(indene carbonate) (ν_{CO_2} @ 1750 cm^{-1}) with concomitant formation of indene carbonate (ν_{CO_2} @ 1825 cm^{-1}). The initial rates of cyclic indene carbonate formations were measured as a function of temperature from the two-dimensional profiles of peak absorbance *vs* time (**Table 13**). From the corresponding Arrhenius plot, the energy of activation for the poly(indene carbonate) was determined to be 189 ± 5.8 kJ/mol (**Figure 25**).
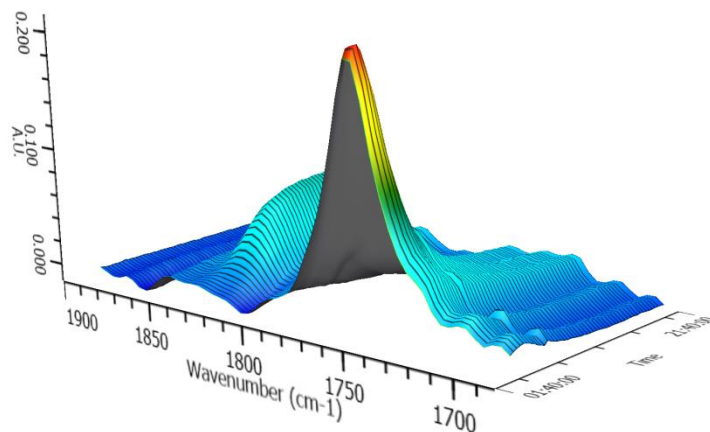
Figure 24. 3-D plot of deploymerization of poly(indene carbonate) in the presence of *n*-Bu$_4$NN$_3$ at 368 K monitored by *in situ* ATR-FTIR.

Table 13. Initial reaction rates for anion-assisted poly(indene carbonate) depolymerization reaction.

Temp (K)	Rate (abs/s) x 10^7	E$_a$ (kJ/mol)
363	9.23	
368	21.0	189 ± 5.8
373	45.4	
378	113	

*Reaction condition: polycarbonate repeating unit: *n*-Bu$_4$NN$_3$ = 15: 1; 0.3 M solution in toluene.
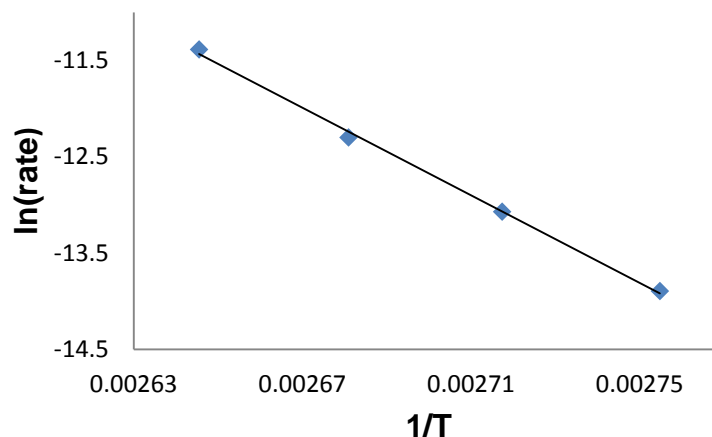
Figure 25. Arrhenius plot of anion-assisted poly(indene carbonate) depolymerization reaction. The R^2 value = 0.998.

Compared with our previous study, the energy of activation barriers for the azide-assisted polycarbonate degradation were found to increase for the selected polycarbonates in the following order: poly(styrene carbonate) (46.7 kJ/mol) < poly(CO_2-alt-epichlorohydrin) (76.2 kJ/mol) < poly(propylene carbonate) (80.5 kJ/mol) < poly(indene carbonate) (189.1 kJ/mol) (**Scheme 16**).[85] It is of note that the pathway involving radical formation required a considerably higher activation barrier.

Scheme 16. The energy of activation barriers for the azide-assisted polycarbonate degradation.

E_a (kJ/mol)   46.7   76.2   80.5   189.1
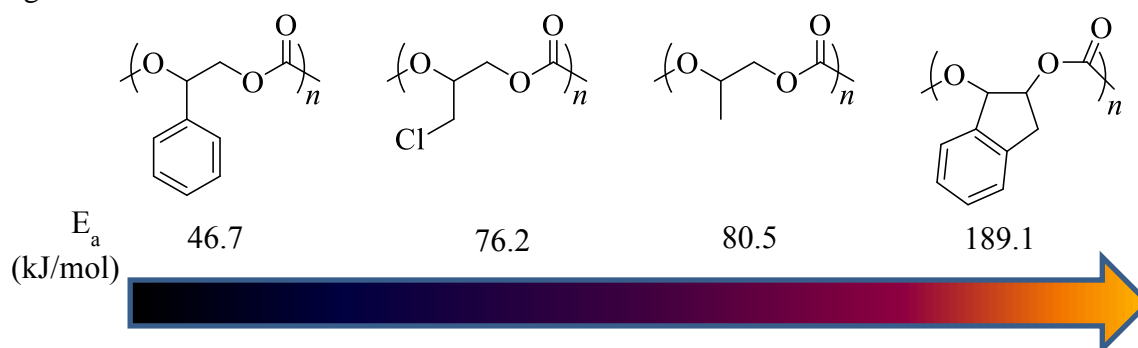
Concluding remarks

Herein, we have demonstrated that the thermal degradation of poly(indene carbonate) to cyclic indene carbonate occurs by a different reaction pathway than other aliphatic polycarbonates examined. Although it is clearly shown that radicals are intimately involved in this process which are generated in the presence of light, the details of this mechanistic route remain poorly understood. The activation barrier for depolymerization was found to be much higher than that observed for other polycarbonates, e.g., some fourfold greater than that of poly(styrene carbonate) at 189.1 kJ•mol^{-1}. A perplexing observation noted during the degradation is illustrated in **Figure 26** where the time dependent traces of the ν_{N_3} vibration at 2015 cm^{-1}, which is blue shifted by 13 cm^{-1} from the free ν_{N_3} mode, and the polycarbonate ν_{CO_3} vibrational mode at 1750 cm^{-1} are intensified in the presence of each other and light. Following the appearance and the decay of these infrared signal with time, at their maxima intensity the onset of the formation of cyclic carbonate occurs (**Figure 26B**). This phenomenon is

87

presently not understood, but will be the subject of continued investigation in our laboratory.

(A)

(B)
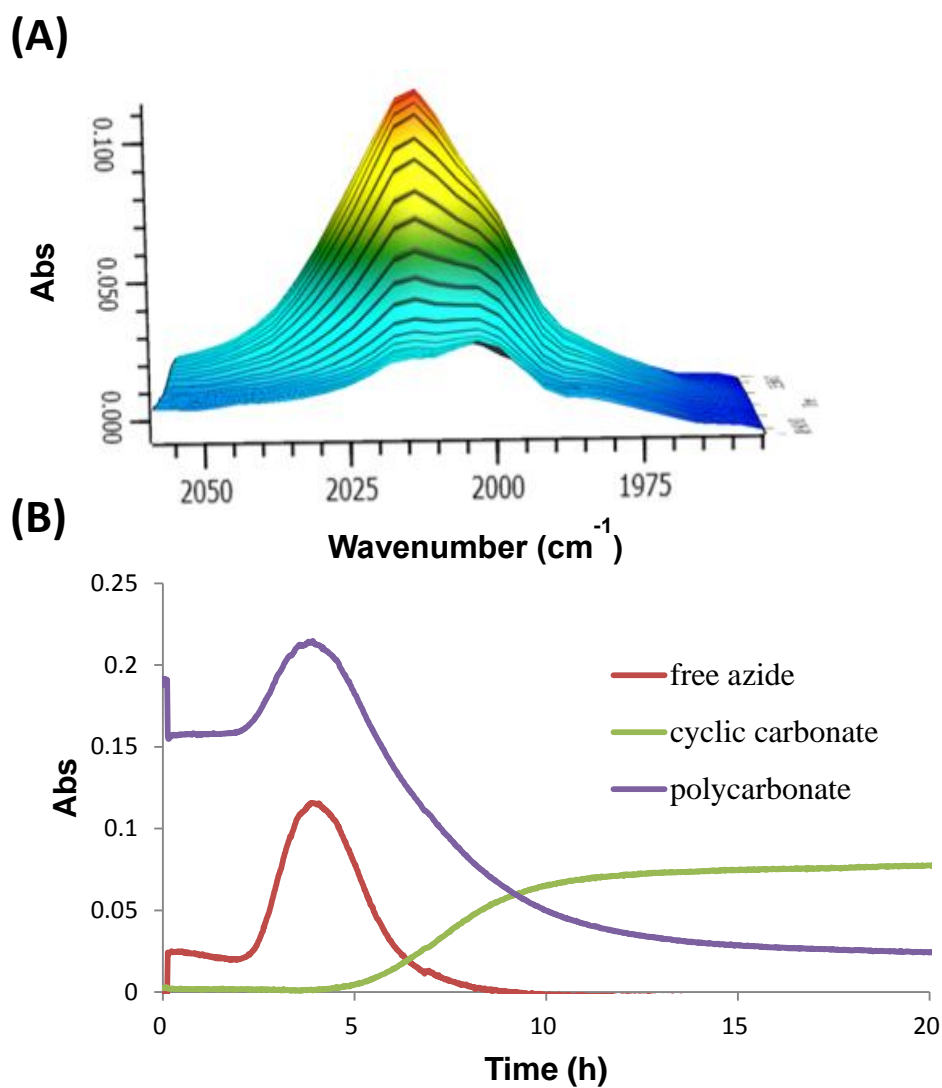
Figure 26. (**A**) Infrared traces in ν_{N_3}-region prior to onset of copolymer degradation to cyclic carbonate. (**B**) Enhancement and decay profiles of azide and polycarbonate infrared absorptions accompanying eventual formation of cyclic carbonate in room light at 368 K.

DEPOLYMERIZATION OF POLY(CYCLOPENTENE CARBONATE) TO

RECOVER CYCLOPENTENE OXIDE STARTING MATERIAL

Introduction

Polycarbonates are a class of engineering thermoplastics with high quality and outstanding properties. They are industrially produced by the condensation reaction between diols and toxic phosgene. Therefore, there is a need to find a safer and more environment friendly synthetic pathway to produce polycarbonates. In 1969, Inoue first demonstrated that polycarbonates can be prepared by the copolymerization of propylene oxide and CO_2.[10] After that, numerous catalyst systems have been developed and work well for the epoxide and CO_2 copolymerization.[15, 49, 66, 83b] Using this method, cyclic carbonate is afforded as a byproduct and some ether linkages are found in the polymer chain (**Scheme 17**). It represents an environmentally-friendly route to make polycarbonates than the current industrial processes.

Scheme 17. Copolymerization of CO_2 and epoxides.
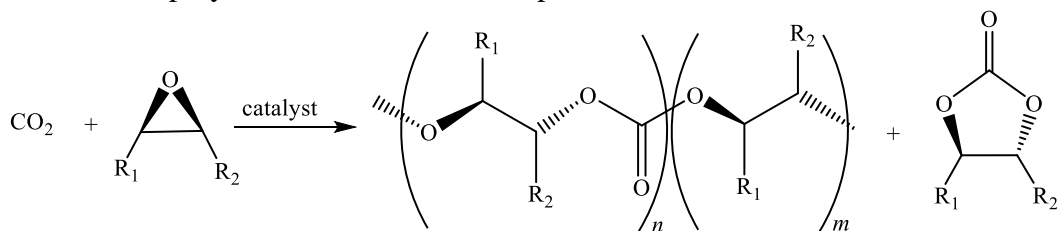
We have previously presented the depolymerization reactions of various polycarbonates and have shown that the polycarbonates can be degraded to corresponding cyclic carbonates *via* backbiting reactions.[85] Five-membered cyclic carbonates are relatively stable, and they cannot be ring-opened to polycarbonates without some loss of CO_2. In contrast, degradation of waste polycarbonate to the monomeric oxide would provide an ideal recycling route: the epoxide product can be converted back to polycarbonate by applying CO_2 and a suitable catalytic system. Being able to be recycled through the monomeric epoxide would cause CO_2/epoxide copolymers to be even greener.

Computational studies of polycarbonates formation from CO_2/epoxides and the kinetics of their metal free degradation have been reported.[89] The enthalpy of polymerization for CO_2/cyclopentene oxide is poorly exothermic because of ring strain and intramolecular steric repulsion. In addition, to form *trans*-cyclopentene carbonate *via* alkoxide backbiting requires an abnormally higher energy barrier. This shows the special nature of poly(cyclopentene carbonate) and implies that a second degradation path might be involved.

Motivated by previous computational studies showing the feasibility of degrading the poly(cyclopentene carbonate) to cyclopentene oxide, we studied the depolymerization of poly(cyclopentene carbonate) in detail. Those results are discussed herein.

Experimental section

Reagents and methods. Toluene and tetrahydrofuran were freshly distilled from sodium/benzophenone. 1,8-Diazabicyclo[5.4.0]undec-7-ene (DBU) (Aldrich) was stirred over CaH_2, vacuum distilled, then stored in the glovebox. Tetra-*n*-butylammonium chloride (Aldrich) was recrystallized from acetone/diethyl ether before use. Sodium bis(trimethylsilyl)amide (NaHMDS) (Alfa Aesar) and (2,2,6,6-tetramethylpiperidin-1-yl)oxyl (TEMPO) (Aldrich) were stored in the glovebox. Tetra-*n*-butylammonium azide (TCI) was stored in the freezer of the glovebox with no further purification.

^{1}H and ^{13}C NMR spectra were acquired on Unity+ 300 MHz and VXR 300 MHz superconducting NMR spectrometers. Infrared spectra were recorded on a Bruker Tensor 27 FTIR spectrometer in CaF_2 solution cells of 0.1 mm pathlength.

Base-initiated depolymerization of poly(cyclopentene carbonate) monitored by ^{1}H NMR. In an Ar-filled glove box, poly(cyclopentene carbonate) (38.5 mg, carbonate repeating unit = 0.3 mmol) and the appropriate base (0.012 mmol) were dissolved in 1mL of *d*-toluene. The solution was then transferred into a J-Young tube (0.4mL). The J-Young tube was placed in a 110 $^{\circ}$C oil bath and the reaction was monitored by ^{1}H NMR. For the high pressure and the reduced pressure experiments, the solution was frozen by liquid nitrogen, and the Ar was removed by vacuum. CO_2 was subsequently added for the high pressure reaction. The J-Young tube was then placed in a 110 $^{\circ}$C oil bath, and the reaction was monitored by ^{1}H NMR. The yields were determined by comparison of the integrals of signals arising from the protons in [1]H

NMR spectra, including poly(cyclopentene carbonate) δ 5.3~5.0 (2H) ppm, *cis*-cyclic cyclopentene carbonate δ 4.08 (2H) ppm, cyclopentene oxide δ 3.06 (2H).

Preparation of acetate end-capped poly(cyclopentene carbonate). Triethylamine (0.3 mL, 2 mmol) and hydroxy-end poly(cyclopentene carbonate) (400 mg) were dissolved in 5 mL of anhydrous THF. Acetyl chloride (0.1 mL, 1.4 mmol) was added dropwise to the stirred THF solution at 0 ^{o}C. The THF solution was allowed to warm to ambient temperature overnight, during which time the Et$_3$NHCl precipitated from the solution. The ammonium salt was removed by filtration through silica gel, and the filtrate was evaporated to remove excess triethylamine. The acetate end-capped poly(cyclopentene carbonate) was precipitated from solution by addition of methanol, isolated by filtration, and dried under reduced pressure.

Depolymerization of acetate end-capped poly(cyclopentene carbonate) monitored by ¹H NMR. Acetate end-capped poly(cyclopentene carbonate) (carbonate repeating unit = 0.3 mmol) and NaHMDS (2.2 mg, 0.012 mmol) were dissolved in 1 mL of *d*-toluene in an Ar-filled glove box and transferred into a J-Young tube (0.4 mL). The J-Young tube was heated to 110 ^{o}C and the reaction was monitored by ¹H NMR.

Metal-involved depolymerization of poly(cyclopentene carbonate) monitored by ¹H NMR. Poly(cyclopentene carbonate) (38.5 mg, carbonate repeating unit = 0.3 mmol), (R,R′)-(*N,N′*-bis-(3,5-di-*tert*-butylsalicylidene)-1,2-cyclohexenediimine chromium(III) chloride (3.85 mg, 0.006 mmol, (salen)CrCl), and *n*-Bu$_4$NN$_3$ (3.47 mg, 0.012 mmol) were dissolved in 1 mL of *d*-toluene. The solution was

prepared in an Ar-filled glove box and transferred into a J-Young tube (0.4 mL). The J-Young tube was placed in a 110 $^{\circ}$C oil bath and the reaction was monitored by ^{1}H NMR.

Results and discussion

Influence of basicity on depolymerization. In our previous studies, tetra-*n*-butylammonium azide (*n*-Bu$_4$NN$_3$) were selected to examine the depolymerization process, since it is common cocatalyst used along with metal salen catalysts in the copolymerization reactions.[85] Tetra-*n*-butylammonium salts were chosen rather than the more commonly used *bis*(triphenylphosphine)iminium salts (PPNX) due to the former salt's better solubility in toluene. The poly(cyclopentene carbonate) sample employed in this study was prepared from cyclopentene oxide and pressurized CO_2, catalyzed by a beta-diiminate Zn complex. It was isolated by precipitation from methanol, providing pure polycarbonate with –OH end groups which could be deprotonated by a base.[90] The depolymerization reactions were carried out in a 0.3 M *d*-toluene solution of copolymer at 110 $^{\circ}$C with a repeating unit : anion molar ratio of 25 : 1. No reaction was found to have occurred after 15 days as monitored by ^{1}H NMR. In addition, a stronger, non-nucleophilic base DBU (1,8-diazabicyclo[5.4.0]undec-7-ene) was employed under the same reaction conditions, and again no degradation products were observed after 15 days. An even stronger base, NaHMDS (sodium bis(trimethylsilyl)amide), was then chosen. Immediately after adding NaHMDS to poly(cyclopentene carbonate), a new peak at 5.26 ppm was observed in the ^{1}H NMR spectrum, even before heat was applied **(Figure 27b)**. Also prior to heating, the infrared spectrum of the reaction mixture was recorded, and the absence of an absorbance band near 1800 cm^{-1} confirmed that no *trans*-cyclopentene

carbonate (the alkoxide back-biting product) had formed. This peak at 5.26 ppm in ^{1}H

NMR was not observed when *n*-Bu$_4$NN$_3$ and DBU were added as basic initiators, so we

attribute this signal to the deprotonated chain end. After tracking for 3 months, the

intensity of broad band at 5.12 ppm was greatly lowered compared with that of the peak

at 5.26 ppm (**Figure 27**). This could be explained by the polymer chain becoming

shorter, so the signals due to the chain end dominate over that of the bulk polymer.
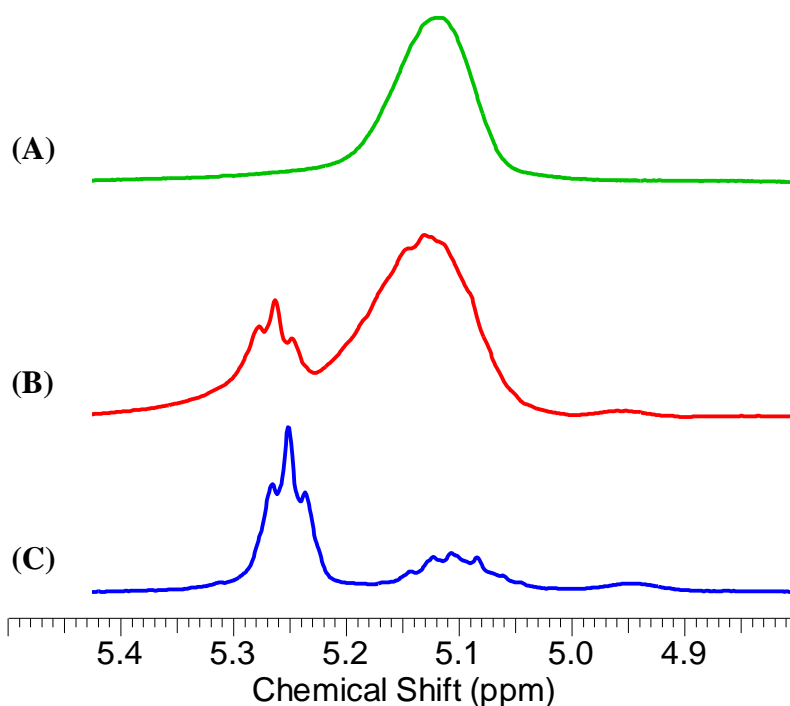
Figure 27. ^{1}H NMR of poly(cyclopentene carbonate) in *d*-toluene. (A) before (B) after
adding NaHMDS (C) after 3 months.

The composition of reaction mixture along with time was shown below (**Table
14**). The first observable decomposition product was cyclopentene oxide; formation of

cis-cyclopentene carbonate, as confirmed by ^{1}H and ^{13}C NMR, took place thereafter. The yields were first calculated from ^{1}H NMR by using *d*-toluene as internal standard. The given numbers were consistent with relative ratio between the integrations of the peaks representing polymer and products. Therefore, the yields shown in this article are obtained from the relative ratios of polymer and products. No *trans*-cyclopentene carbonate was detected along the reaction by NMR. After the *cis*-cyclopentene carbonate started being produced, the ratio between cyclic carbonate and oxide grew at a similar rate. As the reaction proceeded, the rate of cyclic carbonate formation became higher than oxide formation.

Table 14. Base-initiated depolymerization of poly(cyclopentene carbonate).[a]
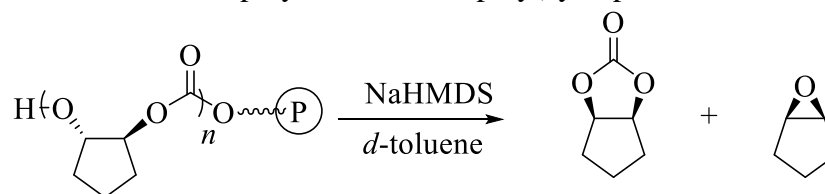
Time (hr)	polymer (%)	cyclic carbonate (%)	oxide (%)
2	98	0	2
4	97	1	2
6	96	2	2
12	91	5	4
48	85	8	7
75	81	10	9
124	78	12	10
170	74	14	12
270	61	20	19
20 days	38	35	27
60 days	24	44	32

[a]Reaction condition: polycarbonate repeating unit: NaHMDS = 25: 1; 0.3 M solution in d-toluene, 110 °C.

The free energy barriers for various polycarbonates to generate the corresponding cyclic carbonates through different pathways have been determined computationally, and poly(cyclopentene carbonate) is a special case. Alkoxide backbiting to form *trans*-cyclopentene carbonate has a high free energy barrier. Furthermore, its formation is endergonic.[89, 91] Therefore, the formation of cyclopentene oxide *via* alkoxide backbiting offered a lower energy pathway, 13.3 kcal/mol *vs.* 19.9 kcal/mol for *trans*-cyclopentene carbonate.[91] This explains why the latter was not observed during the depolymerization process and that cyclopentene oxide was the favored decomposition product.

Combining the experimental observation and computational result, we proposed the reaction pathway as shown in **Scheme 18**. Treatment of poly(cyclopentene carbonate) with NaHMDS causes deprotonation of the hydroxyl end of the polymer chain. The alkoxide proceeds to generate cyclopentene oxide as well as a new polymeric carbonate (Route 2 in **Scheme 18**). However, the formation of *trans*-cyclopentene carbonate is not preferred due to higher energy barrier (Route 1 in **Scheme 18**). After that, backbiting from the carbonate end group occurs to make *cis*-cyclopentene carbonate (Route 3 in **Scheme 18**).
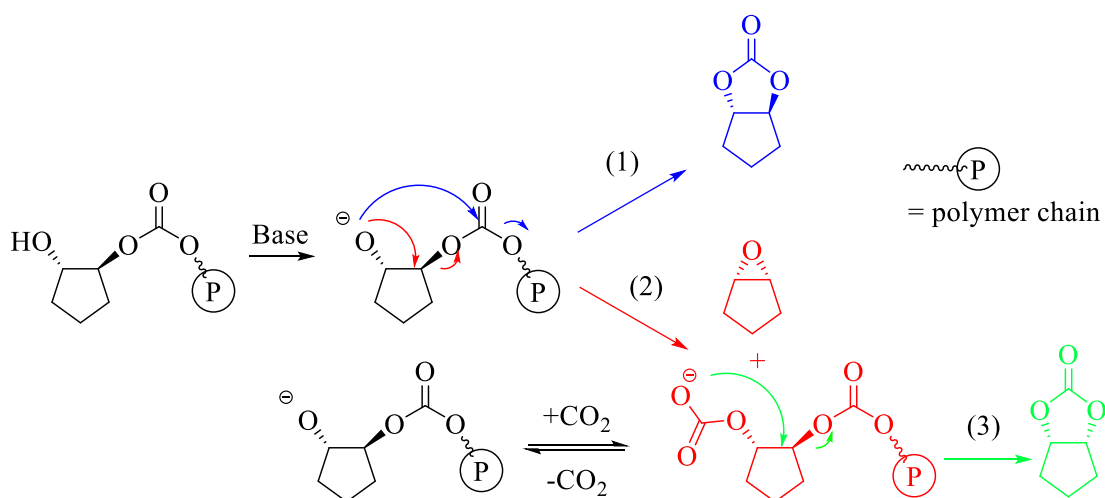
Scheme 18. Possible reaction pathways for base-initiated depolymerization of poly(cyclopentene carbonate).

The rate of cyclic carbonate formation increased as more epoxide was formed (**Table 14**). The carbonate chain end exists in equilibrium with the alkoxide chain end + CO_2. Carbon dioxide was generated along with cyclopentene oxide formation and caused the concentration of CO_2 to increase in the reaction vessel. The accumulated CO_2 favored the carbonate chain end and made *cis*-cyclopentene carbonate the more favorable product *via* carbonate backbiting.

An acetate-capped poly(cyclopentene catbonate) was used to verify base-initiated decomposition pathway. The peak at 5.26 ppm in ^{1}H NMR spectrum is no longer observed, confirming that this signal is only found in the deprotonated chain end. Even when heated to 110 ℃, neither cyclopentene carbonate nor cyclopentene oxide was found by ^{1}H NMR. This proves that the initiation of depolymerization process begins with the deprotonation of the polymer –OH end group. Between n-Bu$_4$NN$_3$, DBU, and

NaHMDS, we found that the degradation rate strongly depends on the basicity of the initiator.

Radical mechanism possibility. The depolymerization study of poly(indene carbonate) by n-Bu$_4$NN$_3$ under room light has been demonstrated to occur *via* a radical pathway.[81] Compared with poly(cyclopentene carbonate), both of them have the unstable fused five-membered ring which might proceed the same reaction pathway during the base-initiated depolymerization process. In order to disprove the existence of a radical process, a radical trap, TEMPO, was employed. The depolymerization of poly(cyclopentene carbonate) was not affected by the presence of TEMPO, and the product mixture had a similar composition to the samples without added TEMPO.

Previously, we found that light is essential to start the depolymerization process in the case of poly(indene carbonate).[81] The effect of light on polymer degradation at 110 °C in the absence of TEMPO was determined for poly(cyclopentene carbonate). Poly(cyclopentene carbonate) was treated with NaHMDS in the J-Young tube covered by aluminum foil, shielding it from light. The degradation in the dark proceeded smoothly. This suggests that, unlike poly(indene carbonate), depolymerization of poly(cyclopentene carbonate) does not involve a radical pathway and does not require the presence of light.

Metal-involved depolymerization. In order to analyze the influence of metal binding of the growing polymer chain on the depolymerization process, depolymerization of poly(cyclopentene carbonate) was examined in the presence of (salen)CrCl/n-Bu$_4$NN$_3$ at a polymer repeating unit:metal:anion ratio of 50:1:2. The

(salen)Co(III) analog was not tested because it is easily reduced to (salen)Co(II) under the reaction conditions. The reaction was monitored by ^{1}H NMR spectroscopy in *d*-toluene at 110 °C under an Ar atmosphere and the results are summarized in Figure 28. This reaction is much faster and generate mostly cyclopentene oxide in the presence of (salen)CrCl/*n*-Bu$_4$NN$_3$ than the base-initiated depolymerization. It took about 30 hours to finish the degradation with the composition of 92% oxide and 8% cyclic carbonate. Compared with base-initiated depolymerization, (salen)CrCl/*n*-Bu$_4$NN$_3$ appears to be a nice catalytic system, providing a lower energy route to convert the poly(cyclopentene carbonate) to its starting material. We emphasize that poly(cyclopentene carbonate) is significantly different to the other studied polycarbonates decomposition reactions which mainly convert polymer to the corresponding cyclic carbonates.[81, 85]
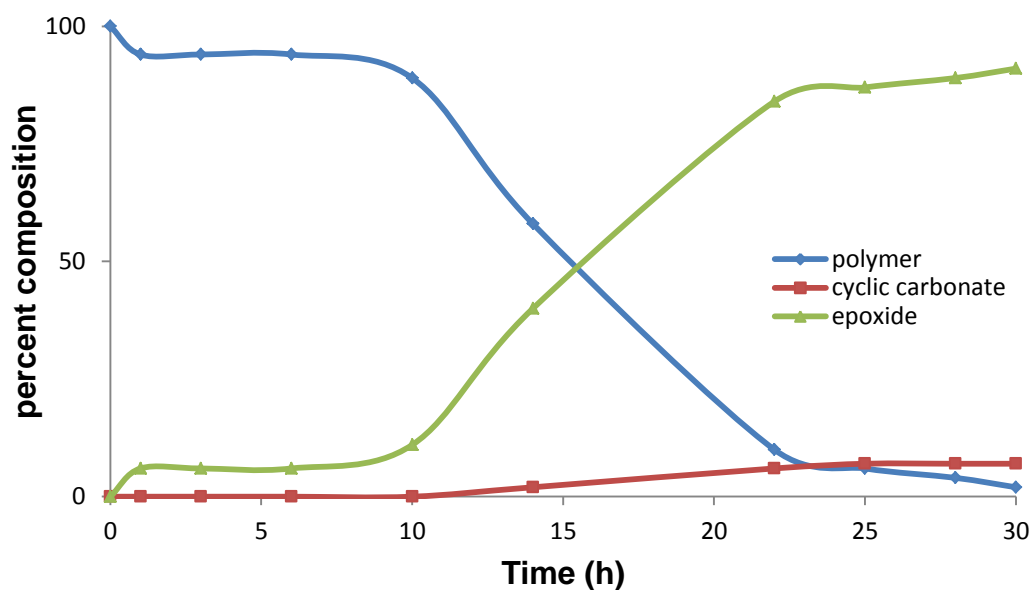
Figure 28. Metal-assisted depolymerization of poly(cyclopentene carbonate).

To judge the importance of N_3^-, a control experiment was performed in which no n-Bu$_4$NN$_3$ was added. In the first five days, some insoluble precipitate was seen inside the reaction mixture, and no decomposition product was observed by ^{1}H NMR (**Table 15**). After another couple days, the reaction seemed homogeneous and some decomposition products were found. This suggests an active catalytic species was formed in the five-day induction period. The detail of the active species is unclear yet, though it is believed that a bimetallic mechanism may be involved.[21, 92]

Table 15. Metal-involved depolymerization of poly(cyclopentene carbonate).[a]
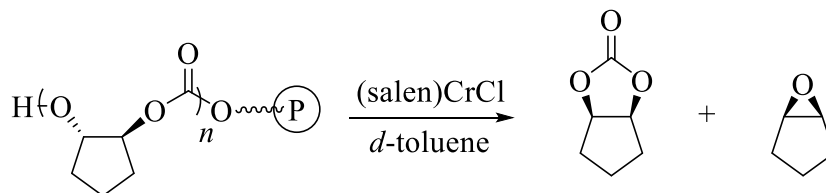
Time (hr)	polymer (%)	cyclic carbonate (%)	oxide (%)
120	100	0	0
169	82	3	15
240	36	5	59
360	14	7	79

[a]Reaction condition: polycarbonate repeating unit: (salen)CrCl = 50: 1; 0.3 M solution in d-toluene, 110 °C.

Influence of high pressure CO$_2$. Since the decarboxylated product, cyclopentene oxide, was observed in the base-degradation of poly(cyclopentene carbonate), analogous experiments involving high pressure CO$_2$ (7 atm) were carried out to investigate the effect of CO$_2$ on the depolymerization process. The compositions of reaction mixture along with time were summarized in **Table 16**. No cyclopentene oxide

formation was observed, and *cis*-cyclopentene carbonate was the only product, indicating that the carbonate backbiting pathway operated. The rates of depolymerization to cyclic monomers were greatly retarded by carbon dioxide comparing with the reaction under 1 atm of Ar. The CO_2-hindered depolymerization can be explained by the higher free energy of activation for cycloaddition *via* carbonate chain end to from *cis*-carbonate (20.3 kcal/mol) *vs.* alkoxide anionic end groups to make oxide (13.3 kcal/mol).[91] This is consistent with the previous studies involving cyclic ethers and CO_2 that show that the carbonate backbiting reaction has a significantly higher free energy of activation compared to the alkoxide backbiting reaction.[35, 87]

Table 16. Base-initiated depolymerization of poly(cyclopentene carbonate) under 7 atm of CO_2.[a]
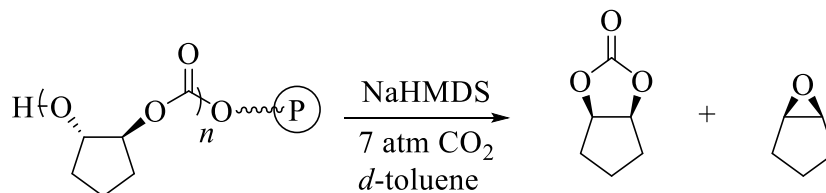
Time (hr)	polymer (%)	cyclic carbonate (%)	oxide (%)
2	100	0	0
6	97	3	0
24	92	8	0
50	91	9	0
100	90	10	0
196	89	11	0
245	88	12	0
360	86	14	0

[a]Reaction condition: polycarbonate repeating unit : NaHMDS = 25 : 1; 0.3 M solution in *d*-toluene, 110 °C, 7 atm CO_2.

A high CO_2 pressure experiment was also carried out in the presence of (salen)CrCl and n-Bu$_4$NN$_3$ catalytic system. As expected, the reaction proceeds slower in a CO_2 atmosphere. On the other hand, an even greater percentage of cyclic carbonate was found in the reaction, although cyclopentene oxide is surprisingly still being the major decomposition product under high pressure condition (**Table 17**). This helps to explain why there have not been reports of poly(cyclopentene carbonate) being successfully produced from cyclopentene oxide and CO_2 with the (salen)CrCl/n-Bu$_4$NN$_3$ catalyst system. Once the polymer chain has formed, it would easily backbite and return into raw material or the cyclic carbonate byproduct.

Table 17. Metal-assisted depolymerization of poly(cyclopentene carbonate) under 7 atm CO_2.[a]
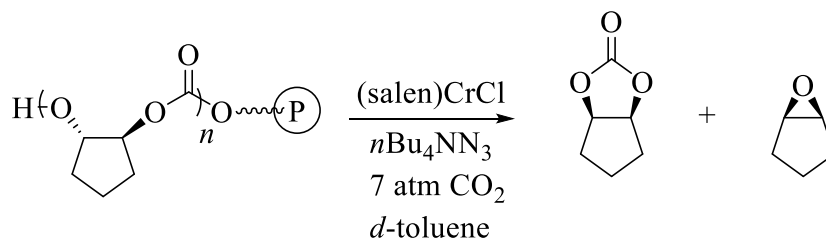
Time (hr)	polymer (%)	cyclic carbonate (%)	oxide (%)
4	100	0	0
24	93	0	7
96	32	16	52
168	23	18	59
243	21	19	60
387	13	20	67
460	12	20	68

[a]Reaction condition: polycarbonate repeating unit: (salen)CrCl: n-Bu$_4$NN$_3$= 50: 1: 2; 0.3 M solution in d-toluene, 110 °C, 7 atm CO_2.

Degradation under reduced pressure. In the reaction pathway we proposed, the CO_2 concentration may control the formation of cyclic carbonate from the generated carbonate chain end backbiting. A base-initiated depolymerization reaction under reduced pressure was tested under identical reaction under reduced pressure (**Table 18**). The Ar atmosphere was removed from the J-Young tube before heating, and a vacuum was reapplied to the J-Young tube everyday to remove the generated CO_2 *via* decarboxylation. Comparing with the result under Ar atmosphere (**Table 14**), the reduced pressure reaction was found to proceed much faster and cyclopentene oxide was strongly favored as the degradation product. This perfectly agreed with the reaction mechanism we proposed for backbiting based on the computational results. In addition, it provides a possibility to regenerate cyclopentene oxide efficiently through the degradation of the polycarbonate in the metal-free system and overcomes producing high fraction of undesired cyclic carbonate otherwise.

Table 18. Base-initiated depolymerization of poly(cyclopentene carbonate) under reduced pressure.[a]
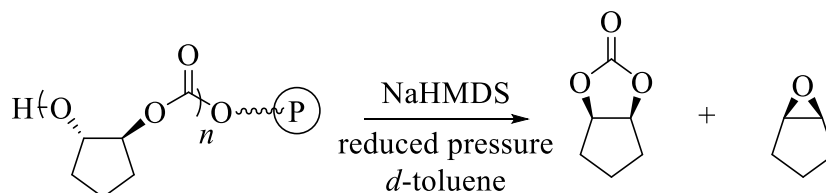
Time (hr)	polymer (%)	cyclic carbonate (%)	oxide (%)
6	85	trace	15
25	64	6	30
48	50	8	42
72	47	8	45

[a]Reaction condition: polycarbonate repeating unit: NaHMDS = 25: 1; 0.3 M solution in *d*-toluene, 110 $^{\circ}$C, vacuum.

Monomer recycling. According to the degradation studies in this article, cyclopentene oxide can be found as major product both in the reduced pressure base-initiation degradation and (salen)Cr-assisted depolymerization. These degradation reactions are ideal examples of monomer recovery from plastic waste. We tried to isolate the cyclopentene oxide product from the reaction mixture by column chromatography, but cyclopentene oxide is easily ring-opened in the presence of silica gel. In addition, the boiling point of cyclopentene oxide is too close to that of the reaction solvent, toluene, to be separated to each other by distillation. 1,2,4-Trichlorobenzene (b.p. 214 $^{\circ}$C) was selected as the alternative reaction solvent. The decomposition was carried out with (salen)CrCl and *n*-Bu$_4$NN$_3$ (repeating unit: metal: N$_3^-$ = 25:1:2) at 110 $^{\circ}$C to see if the same result could be repeated in this high boiling point solvent. After 30 hours, neither polymer nor cyclic carbonate was observed by ^{1}H NMR and the only significant peak was attributed to cyclopentene oxide (**Figure 29**).

Trace amount of cyclic carbonate could only be detected by IR, and no residual polycarbonate was observed. The decomposition of poly(cyclopentene carbonate) can be performed in 1,2,4-trichlorobenzene which provides an opportunity for cyclopentene oxide to be isolated from the reaction mixture by distillation.
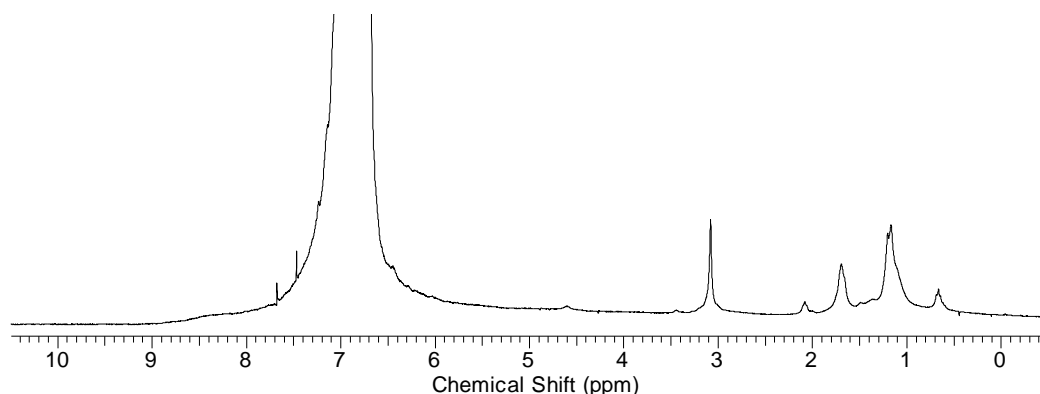
Figure 29. ^{1}H NMR of base-initiated depolymerization of poly(cyclopentene carbonate) in 1,2,4-trichlorobenzene at 110 ^{o}C after 30 hr. Giant peaks at 7 ppm are due to solvent.

To examine the stability of cyclopentene oxide in the presence of (salen)CrCl, *n*-Bu$_4$NN$_3$, and 1,2,4-trichlorobenzene under high temperature, a larger scale mixture was heated to 120 ^{o}C under air for 2 days. Cyclopentene oxide was recovered almost quantitatively by distillation without applying vacuum. Thus, the cyclopentene oxide product would not be ring-opened in the presence of (salen)CrCl and *n*-Bu$_4$NN$_3$. We have thus demonstrated a scalable method to recycle cyclopentene oxide from the degradation of poly(cyclpentene carbonate).

Concluding remarks

We have described the degradation of poly(cyclopentene carbonate) performed under different conditions. In the base-initiated depolymerization, cyclopentene oxide was formed first and then *cis*-cyclopentene carbonate formation started at a higher rate. Degradation experiments were performed for poly(cyclopentene carbonate) under various conditions: in the presence of high pressure CO_2, in the presence of a radical trap, and using acetate end-capped polymers. The experimental and computational results were used to prove that the depolymerization starts with deprotonation of the hydroxyl chain end by strong base, followed by alkoxide backbiting to make cyclopentene oxide. *trans*-Cyclopentene carbonate is not observed due to the high free energy barrier for its formation. After that, carbonate chain ends were generated followed by backbiting to make *cis*-carbonate.

Depolymerization reactions catalyzed by (salen)CrCl were also carried out. Surprisingly, cyclopentene oxide became the major product in the metal-involved experiments, even under 7 atm CO_2. This reaction had a faster reaction rate than the metal free depolymerizations, and the reaction was enhanced by addition of onium salt without long induction period. Although the mechanism remains poorly understood, these observations suggest a relatively low energy barrier for this route.

Further measures can be used to enhance cyclopentene oxide production. For the base-initiated process, application of a mild vacuum helps shift the product ratio in favor of the epoxide; the rate of the reaction is accelerated as well. The metal-involved process can be carried out in high-boiling 1,2,4-trichlorobenzene, and the epoxide

produced can be distilled out of the reaction mixture without being affected by side-reactions. Both pathways are thus viable routes for plastic waste to be recycled *via* the epoxide monomer.

CHAPTER VI

ALIPHATIC POLYCARBONATES PRODUCED FROM THE COUPLING OF

CARBON DIOXIDE AND OXETANES AND THEIR DEPOLYMERIZATION VIA

CYCLIC CARBONATE FORMATION[*]

Introduction

Four-membered cyclic ethers, oxetanes, have been underutilized because of their commercial inaccessibility and laborious synthesis. Nevertheless, these small molecules are currently receiving much attention in medicinal chemistry and drug delivery studies.[93] Our interest in these cyclic ethers is their ability to react with carbon dioxide to provide polycarbonates.[94] These studies were inspired by the numerous successful catalytic systems investigated for the coupling of oxiranes and CO_2 to yield an array of polycarbonate materials.[15, 49, 66a, 95] **Equations 6** and **7** illustrate these processes which are generally carried out at modest pressures of carbon dioxide, i.e., < 3.0 MPa.
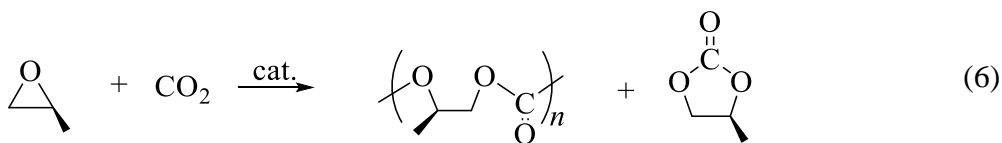
$$\text{(6)}$$

$$\text{(7)}$$
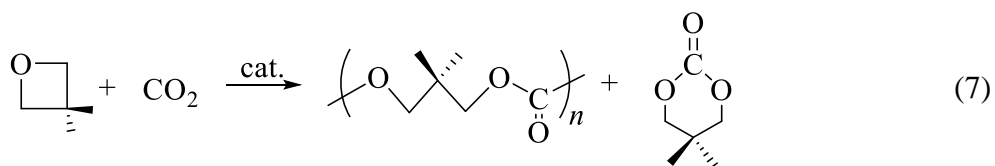
Although the five-membered cyclic carbonates formed from epoxides and CO_2 are thermodynamically more stable than the corresponding polycarbonate, ring-opening polymerization (ROP) of six-membered cyclic carbonates readily occurs to provide its polycarbonate counterpart with complete retention of carbon dioxide.[96]   In previous studies, we have addressed this issue by examining the copolymerization of oxetane with carbon dioxide to determine the origin of the polycarbonate, i.e., whether it is afforded by alternating enchainment of the comonomers CO_2/oxetane or the ROP of initially formed trimethylene carbonate (**Scheme 19**).[24]

Scheme 19.
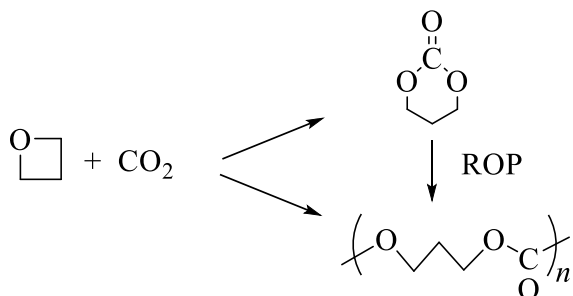
For catalyst systems comprised of (salen)CrCl complexes in the presence of onium salt initiators, the reaction can be tuned to proceed selectively *via* the route involving the ROP of preformed trimethylene carbonate.   This was achieved by the

judicious choice of onium salt and reaction conditions of temperature and pressure. In this manner, polycarbonates are afforded which contain only trace quantities of ether linkages in the copolymer backbone. As indicated in **equation 7** in most instances the copolymerization of oxetane and CO_2 provides small quantities of trimethylene carbonate (TMC) as a coproduct. This observation suggests that the free energy change associated with the ROP of TMC to poly(TMC), although negative, is not very large in magnitude. Hence, it should in principle be able to depolymerize these polycarbonates into their monomer units, six-membered cyclic carbonate, under suitable reaction conditions (**equation 8**).[97]

$$\text{(structure)} \quad \overset{\text{cat.}}{\rightleftharpoons} \quad \text{(structure)} \qquad (8)$$
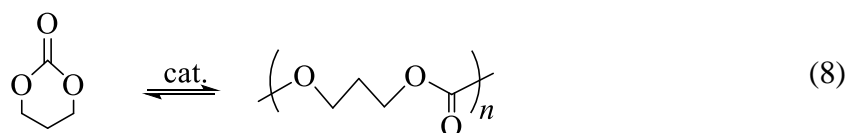
Herein we wish to explore other four-membered cyclic ether monomers for the synthesis of copolymer from carbon dioxide, thereby generating other polycarbonates with different properties.

Experimental section

Reagents and methods. Unless otherwise specified, all syntheses and manipulations were carried out on a double-manifold Schlenk vacuum line under an atmosphere of argon or in an argon filled glove box. Toluene and tetrahydrofuran were freshly distilled from sodium/benzophenone. Ethanol and methanol were freshly

distilled from Mg/I$_2$. Diethyl ether, dichloromethane, and hexanes were purified by an MBraun Manual Solvent Purification System packed with Alcoa F200 activated alumina desiccant. 1,1,2,2-tetrachloroethane (TCE) (TCI) was freshly distilled over CaH$_2$. 3-methyl-3-oxetanemethanol (Alfa Aesar) was used as received. Triethylamine was freshly distilled over CaH$_2$ before use. Ethyl chloroformate (Aldrich), diethyl methylmalonate (Alfa Aesar), *n*-butyllithium (Aldrich), lithium aluminum hydride (Alfa Aesar), chloromethyl methyl ether (Aldrich), sodium hydride (60% in mineral oil) (Alfa Aesar), dimethyl sulfate (Alfa Aesar), potassium hydroxide (EMD), ethylenediamine (Aldrich), 1,2-phenylenediamine (ACROS), chromium(II) chloride (Alfa Aesar), sodium hydroxide (EMD), sodium sulfate (EMD), and magnesium sulfate (EMD) , alkyl-1,3-propandiols were used as received. Tetra-*n*-butylammonium azide was stored in the freezer of the glove box upon arrival. Bone-dry carbon dioxide supplied in a high-pressure cylinder and equipped with a liquid dip tube was purchased from Scott Specialty Gases. The corresponding salen ligands and chromium complexes were synthesized as described in the literature.[98]

^{1}H NMR spectra were acquired on Unity+ 300 MHz and VXR 300 MHz superconducting NMR spectrometers. Molecular weight determinations (M_n and M_w) were carried out with Viscotek Modular GPC apparatus equipped with ViscoGEL^{TM} I-series columns (H + L), and Model 270 dual detector comprised of RI and Light Scattering detectors. High-pressure reaction measurements were performed using an ASI ReactIR 1000 reaction analysis system with stainless steel Parr autoclave modified

with a permanently mounted ATR crystal (SiComp) at the bottom of the reactor (purchased from Mettler Toledo).

Synthesis of 3-methoxy-methyl-3-methyloxetane. This derivative of oxetane was prepared according to the procedure reported by McAlees with some modifications.[99] A solution of 3-methyl -3-oxetanemethanol (50 g, 0.489 mol) in THF (~ 100 mL) was added *via* syringe to a suspension of sodium hydride (23.5 g, 60% in mineral oil) in THF (1 L)) that was previously cooled to 0 ^{o}C using an ice/water bath. After warming the reaction mixture to room temperature the solution was stirred for 24 h. Dimethyl sulfate (86.4 g, 0.685 mol) was added dropwise (exothermic reaction) *via* syringe to the reaction solution that was previusly cooled to 0 ^{o}C using an ice/water bath. After warming the solution to room temperature, the mixture was stirred for 24 h at ambient temperature. A solution of sodium hydroxide (30 g in 50 mL of water) was then added, and most of the THF was removed by distillation. The residue was extracted with diethyl ether, and the ether extract was dried over Na_2SO_4 and vacuum distilled to give 3-methoxy-methyl-3-methyloxetane (MMO) (36 g, 63.3%). ^{1}H NMR (300 MHz, CDCl$_3$): δ 4.45 (d, 2H, OCH_2), 4.30 (d, 2H, OCH_2), 3.40 (s, 2H, CH_2), 3.35 (s, 3H, OCH_3), 1.26 (s, 3H, CH_3).

Synthesis of 3-benzyloxy-methyl-3-methyloxetane. A benzene solution (50 mL) of 3-methyl-3-oxetanemethanol (20 g, 0.20 mol) and benzyl bromide (33.5 g, 0.20 mol) was stirred with 50% sodium hydroxide aqueous solution (80 mL) and tetra-*n*-butylammonium bromide (9.5 g 0.03 mol). After stirring for two days at room temperature, the organic layer was collected and the organic solvent was removed. The

desired product was afforded as a colorless liquid in 70% yield (27.1 g) after distillation under reduced pressure. ^{1}H NMR(300 MHz, CDCl$_3$) : δ7.37~7.24 (m, 5H,-Ar), 4.58 (s, 2H, -CH_2-Ar), 4.54 (d, 2H, -OCH_2), 4.37 (d, 2H, -OCH_2), 3.53 (s, 2H, CH_2), 1.34 (s, 3H, CH_3).

Synthesis of 2-methoxy-methyl-2-methyl malonic acid diethyl ester. This compound was prepared according to the procedure reported by Doherty.[100] A tetrahydrofuran solution (40 mL) of diethyl methylmalonate (5 g, 0.0287 mol) was cooled to -78 °C and treated with a 1.64 M solution of n-butyllithium in hexanes (17.5 mL, 0.0287 mol). The resulting mixture was stirred rapidly and after warming to room temperature, was transferred dropwise *via* cannula a tetrahydrofuran solution (30 mL) of chloromethyl methyl ether (2.9 g, 0.0287 mol). After stirring the reaction solution overnight the solvent was removed under vacuum and the residue extracted into diethyl ether (2 × 30 mL), washed with water (2 × 30 mL), dried over MgSO$_4$, filtered, and the solvent was removed to afford the desired ester as a pale yellow/colorless oil in 80% yield (5.02 g). ^{1}H NMR (300 MHz, CDCl$_3$): δ 4.13 (quart, 4H, J = 7.0 Hz, CH_2CH$_3$), 3.66 (s, 2H, CH_2), 3.28 (s, 3H, OCH_3), 1.42 (s, 3H, CH_3), 1.19 (t, 6H, J = 7.1 Hz, CH$_2$CH_3).

Synthesis of 2-benzyloxy-methyl-2-methyl malonic acid diethyl ester. In a similar manner to that above, a tetrahydrofuran solution (40 mL) of diethyl methylmalonate (5g, 0.0287 mol) was cooled to -78 °C and treated with a 2.5 M solution of n-butyllithium in hexanes (11.5 mL, 0.0287 mol). The mixture is stirred and after warming to room temperature, was transferred dropwise *via* cannula a tetrahydrofuran

solution (35 mL) of chloromethoxymethyl-benzene (4.50 g, 0.0287 mol). After stirring overnight the solution was removed over vacuum and the residue extracted into diethyl ether (2 x 30 mL), washed with water (2 x 30 mL), dried over MgSO$_4$, and filtered. The solvent was removed to afford the product as a colorless oil in 96% yield (8.14 g). ^{1}H NMR(300 MHz, CDCl$_3$) : δ7.37~7.24 (m, 5H,-Ar), 4.54 (s, 2H, -C*H$_2$*-Ar), 4.18 (q, 4H, -C*H$_2$*CH$_3$), 3.81 (s, 2H, C*H$_2$*), 1.53 (s, 3H, C*H$_3$*), 1.23 (t, 6H, -CH$_2$C*H$_3$*).

Synthesis of 2-methoxy-methyl-2-methyl-1,3-propanediol. This compound was prepared according to the procedure reported by Doherty.[100] A solution of 2-methoxy-methyl-2-methyl malonic acid diethyl ester (5 g, 0.0229 mol) in tetrahydrofuran (20 mL) was added dropwise *via* cannula to a stirred suspension of LiAlH$_4$ (4.36 g, 0.115 mol) in tetrahydrofuran (80 mL), at 0 ^{o}C. The reaction mixture was allowed to warm to room temperature and stirred for an additional 4 h. After cooling to 0 ^{o}C, the resulting suspension was diluted with diethyl ether (100 mL) and quenched by addition of water (10 mL), followed by KOH (2.8 g in 10 mL of water), and finally water (10 mL), and stirred for 1 h. After hydrolysis was complete, the resulting mixture was filtered and the solids were washed with diethyl ether (2 × 25 mL). The organic fractions were combined, and dried over MgSO$_4$, and the solvent was removed to afford 2-methoxy-methyl-2-methyl-1,3-propanediol as a colorless oil in 90% yield. ^{1}H NMR (300 MHz, CDCl$_3$): δ 3.65 (d, 2H, $J = 10.7$ Hz, OC*H$_2$*), 3.54 (d, 2H, $J = 10.7$ Hz, OC*H$_2$*), 3.37 (s, 2H, C*H$_2$*), 3.33 (s, 3H, OC*H$_3$*), 0.79 (s, 3H, C*H$_3$*).

Synthesis of 2-benzyloxy-methyl-2-methyl-1,3-propanediol. A tetrahydrofuran solution (30 mL) of 2-benzyloxy-methyl-2-methyl-malonic acid diethyl

ester (8.14 g, 0.0277 mol) was added dropwise *via* cannula to a stirred suspension of LiAlH$_4$ (5.25 g, 0.138 mol) in tetrahydrofuran (100 mL) at 0 $^{\text{o}}$C. The reaction mixture was allowed to warm to room temperature and stirred for overnight. After cooling to 0 $^{\text{o}}$C, the resulting suspension was diluted with diethyl ether (100mL) and quenched by addition of water(10mL), followed by KOH (3 g in 1 0mL of water), and finally water (10 mL), and stirred for a further 1 hr. After the hydrolysis was complete, the resulting mixture was filtered and the solids were washed with diethyl ether (2 x 25mL). The organic fractions were combined, and dried over MgSO$_4$. The solvent was removed to afford 2-benzyloxymethyl-2-methyl-1,3-propanediol as a white solid in 87% yield (5.06 g). ^{1}H NMR(300 MHz, CDCl$_3$) : δ 7.40~7.28 (m, 5H,-Ar), 4.52 (s, 2H, -CH_2Ar), 3.70 (d, 2H, -OCH_2), 3.61 (d, 2H, -OCH_2), 3.47 (s, 2H, CH_2), 2.39 (m, 2H, OH), 0.83 (s, 3H, CH_3).

Synthesis of 5-methoxy-methyl-5-methyl-1,3-dioxan-2-one. This compound was synthesized according to the procedure reported by Endo for the synthesis of trimethylene carbonate with a slight modification.[101] Triethylamine (21.4 g, 0.211 mol) was added dropwise *via* syringe to a solution of 2-methoxy-methyl-2-methyl-1,3-propanediol (13.5 g, 0.100 mol) and ethyl chloroformate (21.7 g, 0.201 mol) in 700 mL of THF at 0°C over a period of 30 min. The reaction mixture was stirred overnight at room temperature. The precipitated triethylamine hydrochloride salt was isolated by filtration, and the filtrate was concentrated under vacuum. The oily residue was vacuum distilled to afford 5-methoxy-methyl-5-methyl-1,3-dioxan-2-one as colorless oil. After a period of several months colorless crystals grew and were successfully analyzed by X-

115

ray crystallography. ^{1}H NMR (300 MHz, CDCl$_3$): δ 4.27 (d, 2H, OCH_2), 4.02 (d, 2H, OCH_2), 3.31 (s, 3H, OCH_3), 3.28 (s, 2H, CH_2), 1.03 (s, 3H, CH_3).

Synthesis of 5-benzyloxy-methyl-5-methyl-1,3-dioxan-2-one. Triethylamine (5.11 g, 0.05 mol) was added dropwise *via* syringe to a solution of 2-benzyloxymethyl-2-methyl-1,3-propanediol (5.06 g, 0.0241 mol) and ethyl chloroformate (5.25 g, 0.0483 mol) in 50 mL of tetrahydrofuran at 0 ^{o}C over a period of 30 min. The reaction mixture was stirred overnight at ambient temperature. The precipitated triethylamine hydrochloride salt was removed by filtration, and the filtrate was concentrated under vacuum. Colorless oil 5-benzyloxymethyl-5-methyl-1,3-dioxan-2-one (3.85g, 70%) was afforded after chromatography purification (EA: hexane = 1:1, Rf~0.45). ^{1}H NMR(300 MHz, CDCl$_3$) : δ7.42~7.26 (m, 5H,-Ar), 4.53 (s, 2H, CH_2-Ar), 4.36 (d, 2H, -OCH_2), 4.07 (d, 2H, -OCH_2), 3.41 (s, 2H, CH_2), 1.11 (s, 3H, CH_3). ^{13}C NMR(300 MHz, CDCl$_3$) : δ148.17, 137.38, 128.34, 127.86, 127.49, 73.86, 73.48, 71.01, 32.92, 17.32. Anal. Calcd for C$_{13}$H$_{16}$O$_4$: C, 66.09; H, 6.83. Found C, 66.14; H, 7.04.

General procedure for synthesis of alkyl subsituded-1,3-dioxan-2-one from 1,3-propandiol derivatives . Triethylamine (5.11 g, 0.05 mol) was added dropwise *via* syringe to a solution of alkyl subsituded-1,3-propanediol (0.0241 mol) and ethyl chloroformate (5.25 g, 0.0483 mol) in 50 mL of tetrahydrofuran at 0 ℃ over a period of 30 min. The reaction mixture was stirred overnight at ambient temperature. The precipitated triethylamine hydrochloride salt was removed by filtration, and the filtrate was concentrated under vacuum. Corresponding alkyl subsituded-1,3-dioxan-2-one was afforded after chromatography purification or recrystallization.

Substrate binding and ring-opening step examined by infrared spectroscopy.
3-methoxy-methyl-3-methyloxetane binding and ring-opening step studies were examined by solution infrared spectroscopy. The catalytic system used in these studies was a (salen)Cr(III)Cl (50 mg) complex (*N,N'*-bis(3,5-di-*tert*-butylsalicylidene)-1,2-ethylenediimine chromium(III) chloride) in the presence of *n*-Bu$_4$NN$_3$ as cocatalyst and using TCE as the solvent (4 mL).

X-ray structural studies. For these structures, a Bausch and Lomb 10× microscope was used to identify suitable crystals. Each crystal was coated in paratone, affixed to a nylon loop, and placed under streaming nitrogen (110K) in a Bruker-D8 Adv GADDS X-ray diffractometer. Space group determinations were made on the basis of systematic absences and intensity statistics. All crystal structures were solved by direct methods and were refined by full-matrix least-squares on F^2. All hydrogen atoms were placed in idealized positions and refined with fixed isotropic displacements parameters equal to 1.2 (1.5 for methyl protons), times the equivalent isotropic displacements parameters of the atoms to which they were attached. All non-hydrogen atoms were refined with anisotropic displacement parameters.

The following are the programs that were used: data collection and cell refinements; FRAMBO Version 4.1.05 (GADDS),[102] data reductions; SAINTPLUS Version 6.63,[73] absorption correction; SADABS,[74] structural solutions; SHELXS-97,[75] structural refinement; SHELXL-97;[76] molecular graphics and preparation of material for publication; SHELXTL, version 6.14,[103] and X-Seed, version 1.5.[104]

117

General procedure for copolymerization reactions of 3-methoxy-methyl-3-methyloxetane and CO₂. In a typical experiment, the appropiate amount of catalyst, cocatalyst (*n*-Bu₄NN₃), and 4 g of MMO were delivered *via* the injection port into a 300-mL stainless steel Parr autoclave reactor that was previously dried in vacuo overnight at 80 °C. The autoclave was then pressurized with 3.5 MPa of CO_2 and the temperature was increased to 110 °C. The monomer:catalyst:cocatalyst ratio was maintained at 275:1:2, and the reaction was run for the corresponding reaction time. After the reaction was stopped, the autoclave was put into ice, cooled down to 10 °C, and vented in a fume hood. The percent conversion to products was determined based on the amount of oxetane monomer left in the reaction solution as ascertained by ^{1}H NMR in $CDCl_3$: MMO: δ 4.45 (d, 2H, OCH_2), 4.30 (d, 2H, OCH_2), 3.40 (s, 2H, CH_2), 3.35 (s, 3H, OCH_3), 1.26 (s, 3H, CH_3). Furthermore, the quantities of 5-methoxy-methyl-5-methyl-1,3-dioxan-2one, polycarbonate, and ether linkages in the copolymer were determined by integrating the peak area of the corresponding resonances in $CDCl_3$: Polycarbonate: δ 4.07 (s, 4H, OCH_2), 3.31 (s, 3H, OCH_3), 3.26 (s, 2H, CH_2), 1.0 (s, 3H, CH_3), cyclic carbonate: δ 4.27 (d, 2H, OCH_2), 4.02 (d, 2H, OCH_2), 3.31 (s, 3H, OCH_3), 3.28 (s, 2H, CH_2), 1.03 (s, 3H, CH_3), and ether linkages: δ 0.9 (s, 3H, CH_3), with other resonances being obscured by the intense polymer signals.

Copolymerization reaction monitored by *in situ* IR spectroscopy. In a typical experiment, the appropiate amount of complex **8**, cocatalyst, (*n*-Bu₄NN₃), and oxetane monomer (8 g) were dissolved in 6 mL of toluene and delivered via the injection port into a 300-mL stainless steel Parr autoclave reactor that was previously dried in vacuo

overnight at 80 °C. The monomer:catalyst:cocatalyst ratio was maintained at 150:1:2. The autoclave is modified with a 30 bounce SiComp window to allow for the use of an ASI ReactIR 1000 system equipped with a MCT detector. In this manner a 128-scan background spectrum was collected after the reaction mixture was heated to 110 °C. The autoclave was pressurized with 3.5 MPa of CO_2, and the infrared spectrometer was set to collect one spectrum every 3 min over a 48 h period. Profiles of the absorbance at 1750 cm^{-1} (polymer) and at 1770 cm^{-1} (cyclic carbonate) with time were recorded after base line correction. After the reaction was stopped, the autoclave was cooled down to room temperature and vented in a fume hood. The reaction solution was analyzed by ^{1}H NMR spectroscopy in the same manner as above, to determine the percent conversion to products, and the percentages of polycarbonate, cyclic carbonate and ether linkages.

Depolymerization of poly(3-benzyloxy-methyl-3-methyl-oxetane carbonate). Poly(3-benzyloxy-methyl-3-methyl-oxetane carbonate) (60mg, 0.25mmol), (*N,N'-bis*-(3,5-*di-tert*-butylsalicylidene)-1,2-ethylenediimine chromium(III) chloride (3 mg, 0.005 mmol), and *n*-Bu$_4$NN$_3$ (2.8 mg, 0.01 mmol) were dissolved in 2.4 mL of *d*-toluene in the glove box and transferred into a J. Young NMR tube (1.2 mL). The tube was evacuated at liquid nitrogen temperature and refilled with argon or CO_2. The tube was placed in a 110°C oil bath and the reaction was monitored by ^{1}H NMR spectroscopy.

General procedure for polymerization of poly(subsituded-oxetane carbonate) from subsituded-1,3-dioxan-2-one. Subsituded-1,3-dioxan-2-one (0.25 mmol), (*N,N'-bis*-(3,5-*di-tert*-butylsalicylidene)-1,2-ethylenediimine chromium(III) chloride(3 mg, 0.005 mmol), and *n*-Bu$_4$NN$_3$ (2.8 mg, 0.01 mmol) were dissolved in 2.4 mL of *d*-toluene

in the glove box and transferred into a J. Young NMR tube (1.2 mL). The tube was placed in a 110℃ oil bath and the reaction was monitored by ^{1}H NMR spectroscopy.

Statistical deconvolution of FTIR spectra. FTIR spectra were deconvoluted using Peakfit, version 4.12 (Peakfit for Windows, v. 4.12; SYSTAT Software Inc., San Jose, CA, 2003). Statistical treatment was a residuals method utilizing a combination Gaussian-Lorentzian summation of amplitudes with a linear baseline and Savitsky-Golay smoothing.

Results and discussion

The oxetane, 3-methyl-3-oxetane methanol (**4**), is commercially available and can be readily converted to the corresponding methoxy or O-benzyl derivatives. Derivatization of **4** prior to copolymerization with CO_2 is required in order to avoid rapid chain transfer reactions between the growing polymer chain and the alcoholic monomer, thereby prohibiting polymer formation. For example, depronation of **4** with NaH in mineral oil followed by the treatment with dimethyl sulfate generated 3-methoxy-methyl-3-methyl oxetane (MMO) (**5**) in 63% yield (**equation 9**).[99] In subsequent postsynthetic modification of these copolymers *via* deprotection of the –OH function it is possible to prepare hydrophilic polycarbonates (**equation 10**).[105]

$$\text{4} \xrightarrow[\text{Me}_2\text{SO}_4]{\text{NaH}} \text{5} \qquad (9)$$

$$\text{R = Me (5)} \quad \text{R = benzyl (6)} \quad + \text{ CO}_2 \xrightarrow{\text{cat.}} \text{[polymer]}_n \xrightarrow[\text{deprotection}]{\text{postsynthetic}} \text{hydrophilic polycarbonate}_n \qquad (10)$$
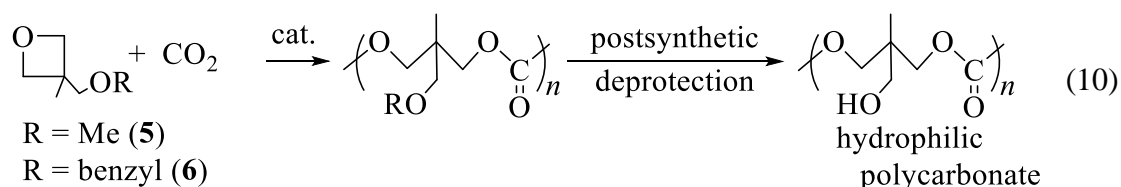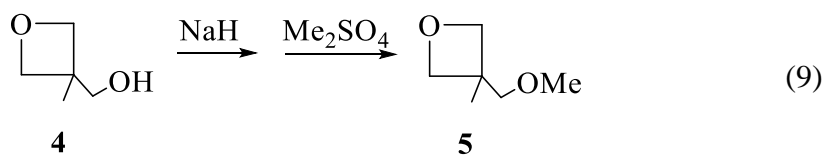
The corresponding six-membered cyclic carbonates can be prepared from the respective 1,3-propanediol with ethylchloroformate in the presence of stoichiometric quantities of triethylamine.[101] For example, 5-methoxy-methyl-5-methyl-1,3-dioxan-1-one (**7**), was prepared from methoxy-methyl-5-methyl-1,3-propanediol and its structure was confirmed by X-ray crystallography. **Figure 30** contains a thermal ellipsoid drawing of **7** with a list of selected bond distances and bond angles provided in **Table 19**.

As illustrated in **Figure 31** the oxetane monomer and products from the coupling reactions of monomer **5** with carbon dioxide are easily accounted for using ^1H NMR spectroscopy. In this instance the relative quantities of copolymer along with any accompanying ether linkages and cyclic carbonate can be assessed by integrating the areas under the peaks of the corresponding resonances at 1.00, 0.90, and 1.03 ppm, respectively. *In situ* infrared monitoring of the reaction's progress can be achieved by

observing the growth of the carbonyl vibrations of the copolymer and cyclic carbonate in

a mixture of toluene and oxetane monomer at 1750 and 1770 cm^{-1}, respectively.
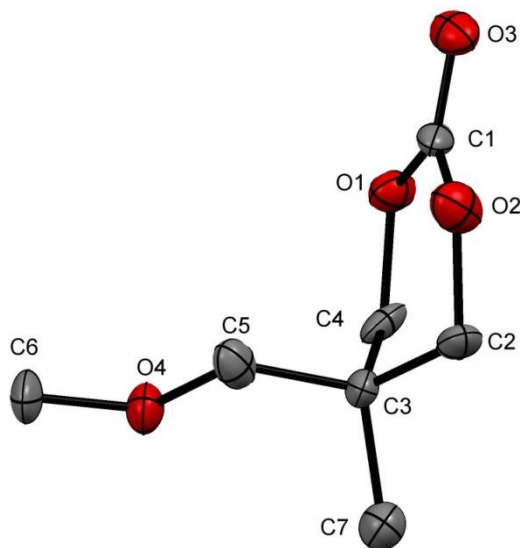
Figure 30. Thermal ellipsoid plot of 5-methoxy-methyl-5-methyl-1,3-dioxan-2-one. H atoms are omitted for clarity.

Table 19. Selected bond distances and angles for 5-methoxy-methyl-5-methyl-1,3-dioxan-2-one.[a]

O(1)-C(1)	1.357(12)
O(3)-C(1)	1.187(12)
O(1)-C(4)	1.460(12)
O(4)-C(6)	1.418(13)
O(3)-C(1)-O(1)	118.3(10)
O(2)-C(1)-O(1)	119.7(9)
C(2)-C(3)-C(4)	105.6(8)
C(5)-O(4)-C(6)	111.4(8)

[a]Units of bond angles and bond distances are (°) and (Å), respectively.
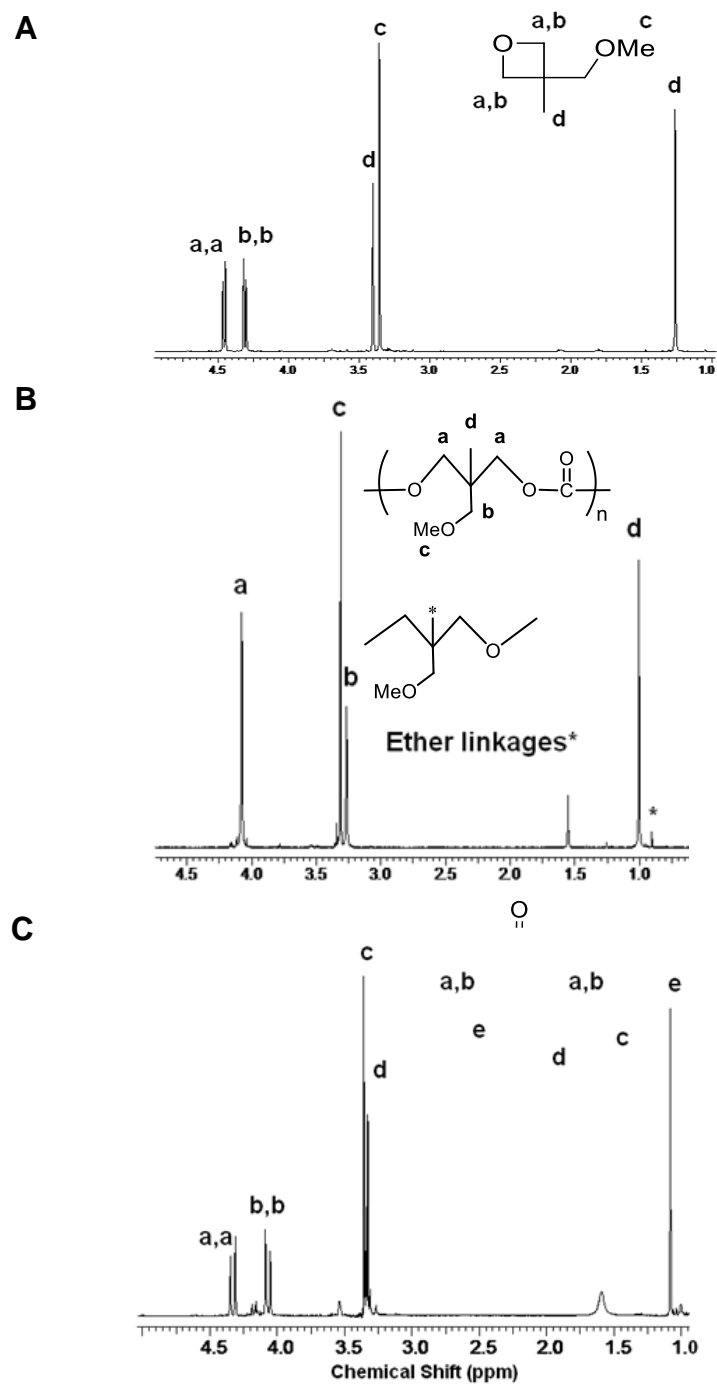
Figure 31. ^{1}H NMR in CDCl$_3$ of (A) MMO, (B) Polycarbonate obtained from MMO and CO$_2$, and (C) Cyclic carbonate.

We present here copolymerization studies of oxetane derivatives and CO_2 employing the (salen)CrCl/onium salt catalyst system utilized in our previous investigations. Initially complex **8** (**Figure 32**) in the presence of n-Bu$_4$NN$_3$ was used to examine the selectivity and catalytic activity for copolymer formation from the coupling of monomer **5** and carbon dioxide. The copolymerization reactions were performed under identical reaction conditions, i.e., 110 $^\circ$C, 3.5 MPa CO_2 pressure, and the monomer:catalyst:cocatalyst ratio was maintained at 275:1:2. The results of this study are summarized in **Table 20**. The product mixtures were analyzed by ^{1}H NMR spectroscopy, with quantities of copolymer, cyclic carbonate and ether linkages in the copolymer determined by integrating the proton resonances at 1.00, 1.03, and 0.90 ppm, respectively. As is readily evident from **Table 20**, the yield of copolymer greatly exceeds the cyclic carbonate in all instances. It should also be pointed out that the reaction occurs on a much slower time scale than the oxetane/CO_2 process and results in a much greater amount of cyclic carbonate product at high conversion.[24, 94] 100% CO_2 content corresponds to a *completely alternating* copolymer with *no* ether linkages, i.e., it represents the maximum allowable CO_2 content in the copolymer. Some researchers prefer to define a completely alternating copolymer with a CO_2 content of 50%.

8
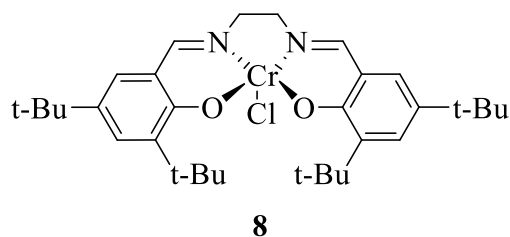
Figure 32. *N,N'*-bis(3,5-di-*tert*-butylsalicylidene)-1,2-ethylenediimine chromium(III) chloride.

Table 20. Copolymerization of 3-methoxy-methyl-3-methyloxetane (MMO) and CO_2 catalyzed by complex **8** in the presence of *n*-Bu$_4$NN$_3$ at various reaction times.[a]

Time (days)	% Poly- carbonate	% Cyclic carbonate	% CO$_2$ content	% Conversion
1	77.6	22.4	75.4	23.3
2	85.4	14.5	73.6	52.7
3	85.7	14.2	87.6	76.7

[a]Copolymerization conditions: Catalyst loading = 0.012 mol %, 4 g of MMO, 2 equiv. of *n*-Bu$_4$NN$_3$, M/I = 275, 3.5 MPa of CO_2, at 110℃. Percent conversion to products, product distributions, and % of CO_2 content were determined by ^{1}H NMR spectroscopy.

Substrate binding and ring-opening studies. Since oxetane monomers containing substituents in the 3-position are sterically more encumbering than oxetane, a comparative study of the binding of monomer **5** with that of the parent oxetane to the Cr(III) center in (salen)CrCl was conducted employing infrared spectroscopy.[94c] For this investigation complex **8** in the presence of two equivalents of *n*-Bu$_4$NN$_3$ was utilized, where the ν_{N_3} stretching vibrations provide accessible probes for both binding and ring-opening steps. The results of this study are depicted in **Scheme 20** and **Figure 33**.

Scheme 20. Ring-Opening Step of MMO Catalyzed by (salen)Cr(N$_3$)$_2^-$.
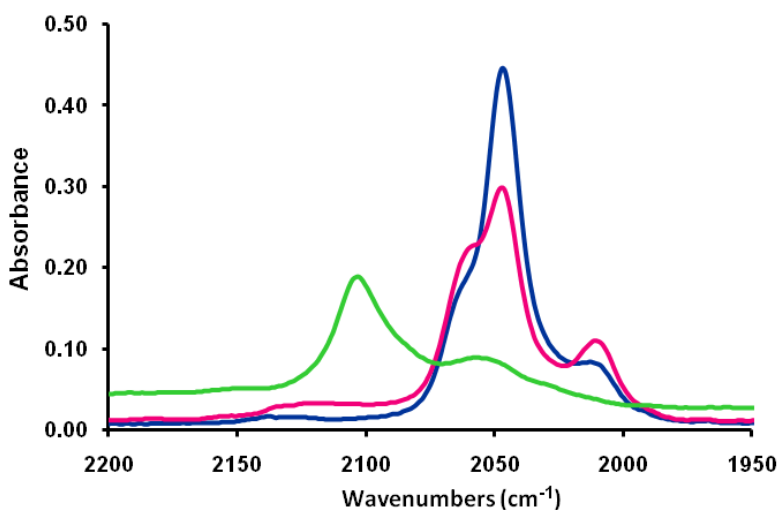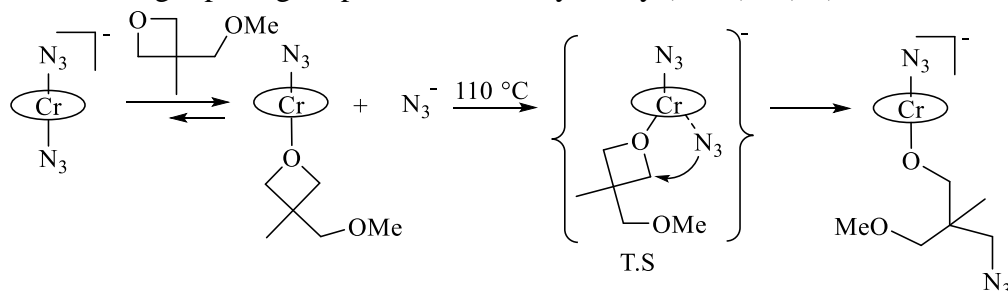
Figure 33. Spectra of TCE solutions of chromium salen chloride complex with 2 equivalents of n-Bu$_4$NN$_3$ (blue line), after addition of 100 equivalents of MMO at ambient temperature and stirred for 3 hr (pink line), and after stirring the reaction solution at 110°C for 24 hr (green line).

As indicated in **Scheme 20**, upon addition of two equivalents of n-Bu$_4$NN$_3$ to (salen)CrCl in weakly coordinating tetrachloroethane solvent, the anionic six-coordinate *bis*-azide species (salen)Cr(N$_3$)$_2^-$ readily forms at ambient temperature. This is apparent in the ν_{N_3} stretching region with the appearance of an infrared band at 2047 cm^{-1} with a shoulder at 2057 cm^{-1} (blue line, **Figure 33**). It should be noted here that the n-Bu$_4$N$^+$

salt of (salen)Cr(N$_3$)$_2$$^-$ anion has been fully characterized by X-ray crystallography.[94c, 106] Upon stirring the reaction mixture with the addition of 100-fold excess of 3-methoxy-methyl-3-methyloxetane to the *bis*-azide complex displaces some of the azide anion for 24 hr at ambient temperature no significant changes in the infrared spectrum resulted, indicative of the ring-opening process of MMO requiring higher temperatures (pink line, **Figure 33**). Indeed, heating the reaction mixture at 110 ^{o}C led to oxetane ring-opening by azide as indicated by the organic azide band at 2100 cm^{-1}. After heating the reaction solution for 24 hr at 110 ^{o}C, the main infrared stretching band observed was that of organic azide (green line, **Figure 33**). It should be noted that an analogous experiment employing oxetane as monomer, led to oxetane ring-opening by azide at 110 ^{o}C after only 3 hr.[94c] Hence, these results indicate that the ring-opening of monomer **5** by azide is much slower than that of the parent oxetane. This is consistent with 3-methoxy-methyl-3-methyloxetane being more sterically hindered than oxetane. Additionally, the presence of electron donating substituents on the 3-position of trimethylene oxide electronically retards the ring-opening step.

Copolymerization of 5 and carbon dioxide monitored by *in situ* IR spectroscopy. **Figure 34** shows the reaction profiles of both copolymer and cyclic carbonate formation for the copolymerization reaction of MMO and CO$_2$ carried out at 110 ^{o}C and 3.5 MPa in the presence of complex **8** along with 2 equivalents of *n*-Bu$_4$NN$_3$. It is clearly observed under these reaction conditions that the formation of MTC is enhanced over the formation of copolymer during the early stages of the coupling reaction, followed by a slow decrease in cyclic carbonate concentration over time.

Concomitantly, the formation of poly(MTC) is initially inhibited, followed by rapid copolymer production over the remaining course of the reaction. These results are consistent with formation of copolymer at least in part *via* ring-opening of the preformed cyclic carbonate and the presence of an equilibrium between the cyclic carbonate and the copolymer products which only slightly favors the copolymer product at equilibrium. Importantly, the percentage of copolymer in the product mixture is about 80% at 110 $^{\circ}$C based on the assumption that the extinction coefficients for the $\nu_{c=o}$ vibrations in the two products are similar. This observation in turn is consistent with more definitive quantification of the product distribution based on ^{1}H NMR experiments as presented in **Table 20**. It is also to be noted here that the product apportionment is much more in favor of the copolymer (> 95%) for the reaction involving CO_2 and the parent oxetane monomer.[94]

Figure 34. (**A**) Three-dimensional stack plot of IR spectra collected every 3 min during the copolymerization reaction of MMO and CO_2. (**B**) Reaction profiles obtained after deconvolution of selected IR spectra, indicating copolymer and cyclic carbonate formation with time.

On the other hand, the coupling reaction of CO_2 with the sterically more bulky oxetane, 3-benzyloxy-methyl-3-methyloxetane (**6**), afforded an equilibrium distribution of copolymer to cyclic carbonate of about 60% at 110 $^{\circ}$C. The reaction profiles for the production of copolymer and cyclic carbonate from the coupling of monomer **6** and CO_2 are illustrated in **Figure 35**. These observations strongly suggest that the steric requirements of the substituents on the 3-position of oxetane govern the relative stabilities of the cyclic carbonate and polycarbonate afforded from CO_2 and oxetanes.

129

Consistent with these qualitative observations is the data reported in **Figure 36** for the reaction between 3,3-dimethyloxetane and carbon dioxide carried out under similar catalytic conditions as those in **Figure 34**. In this instance the equilibrium product distribution was observed to be 88% in favor of copolymer. Hence, the equilibrium distribution of copolymer to cyclic carbonate produced from the coupling of oxetanes and CO_2 was found to decrease in the order: oxetane > 3,3-dimethyloxetane > 3-methoxy-methyl-3-methyloxetane > 3-benzyloxy-methyl-3-methyloxetane.

The equilibra between cyclic carbonates with different substituents on their 5-positions and their corresponding polycarbonates were also examined, as shown in **Table 21**. The six-membered cyclic carbonate was dissolved in d-toluene in the presence of (salen)CrCl and n-Bu$_4$NN$_3$, and the reaction solution was transferred into the argon filled J. Young NMR tube. The reaction was carried out in the bath of 110 ^{o}C and monitored by ^{1}H NMR. Comparing entries 1 and 2, the additional methyl group lowers the polycarbonate portion dropping from 77% to 54% after equilibrium was reached. As the substituents become bigger, the cyclic carbonates become more highly favored (entries 1-5). There is no polycarbonate found when both substituents are ethyl groups. This observation was also confirmed by IR (entry 5). Furthermore, several cyclic carbonates with substituents in the 4- and 6-position were synthesized (**9a-9c, Figure 37**). However, no ring-opening polymerization was observed in any of these cases under the same reaction conditions in **Table 21**.

Figure 35. **(A)** Three-dimensional stack plot of IR spectra collected every 3 min during the copolymerization reaction of 3-benzyloxy-methyl-3-methyloxetane and CO_2. **(B)** Reaction profiles obtained after deconvolution of selected IR spectra, indicating copolymer and cyclic carbonate formation with time. Reaction carried out at 110°C in toluene, at 3.5 MPa of CO_2 pressure, in the presence of complex **8** and 2 equiv. of *n*-Bu_4NN_3.

Figure 36. (**A**) Three-dimensional stack plot of IR spectra collected every 3 min during the copolymerization reaction of 3,3-dimethyloxetane and CO_2. (**B**) Reaction profiles obtained after deconvolution of selected IR spectra, indicating copolymer and cyclic carbonate formation with time. Reaction carried out at 110°C in toluene, at 3.5 MPa of CO_2 pressure, in the presence of complex **8** and 2 equiv. of n-Bu$_4$NN$_3$.

Table 21. Equilibria between polycarbonates and corresponding cyclic carbonates.[a]

Entry	R_1	R_2	Polymer (%)[b]	Cyclic carbonate (%)[b]
1	H	H	77	23
2	Me	H	54	46
3	Me	Me	41	59
4	Et	Me	15	85
5	Et	Et	0	100

[a]Reaction conditions: cyclic carbonate (0.125 mmol), n-Bu$_4$NN$_3$ (0.005 mmol), (N,N'-*bis*-(3,5-*di-tert*-butylsalicylidene)-1,2-ethylenediimine chromium(III) chloride(0.0025 mmol), d-toluene (1.2 mL), 110℃.
[b] determined by ^{1}H NMR spectroscopy.

9a: R_1 = Me; R_2 = H ; R_3 = H
9b: R_1 = Me; R_2 = Me ; R_3 = H
9c: R_1 = Me; R_2 = Me ; R_3 = Me

Figure 37. 4,6-substituted-cyclic carbonates.

A similar observation was reported by Endo and coworkers when examining the ring-opening polymerization of a series of six-membered cyclic carbonates.[97]   In the study by Endo and coworkers the order of percent conversion of cyclic carbonate to polycarbonate was:

We have initiated an investigation of the equilibrium process in **equation 11** as

$$\text{(11)}$$

catalyzed in toluene by complex **8** in the presence of two equivalents of n-Bu$_4$NN$_3$. It is

noteworthy that computational studies have shown that conformational isomerization

between the two conformers of closely related six-membered cyclic carbonates occurs

with a low activation barrier and with little thermodynamic difference between the

equatorial *vs* axial conformers.[107] It is of interest to note here that the crystals isolated

for 5-methoxy-methyl-5-methyl-1,3-dioxan-2-one (**equation 12**) were of the axial

conformer.

$$\text{(12)}$$
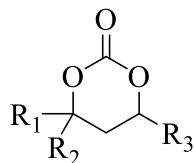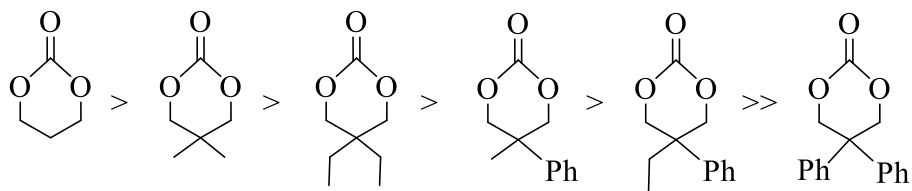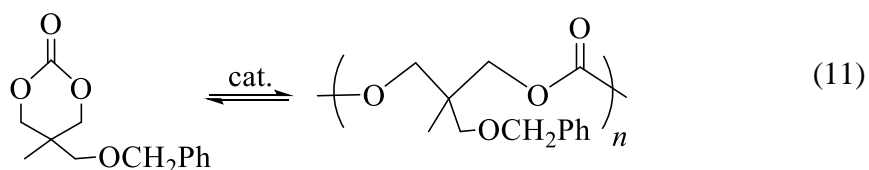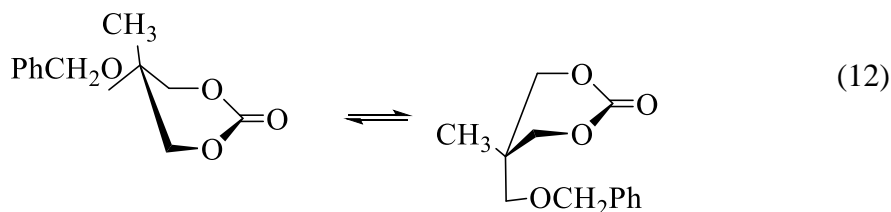
Figure 38 depicts the rates of depolymerization of poly(5-methyl-5-benzyloxy-methyl-1,3-dioxan-2-one) and the concomitant formation of the corresponding cyclic carbonate for reactions carried out in toluene at 110 ^{o}C in both argon and CO_2 atmospheres. The polycarbonate used in this study was made from monomer 3 and CO_2 catalyzed by complex 5 in the presence of 2 equiv of n-Bu$_4$NN$_3$ at 3.5 MPa of CO_2 at 110 °C. The purified copolymer isolated had 12% ether linkages (88% CO_2 content) and exhibited an M$_n$ value of 4326, PDI = 1.32, and a T$_g$ of −2.16 °C. As is evident in Figure 38 the rate of depolymerization to cyclic monomer is greatly retarded by carbon dioxide.   This is consistent with views based on cycloaddition studies involving epoxides and CO_2, where the process proceeding *via* the carbonate species has a significantly higher energy of activation compared to that occurring by way of an alkoxy species (**Scheme 21**).[35, 67]   On the other hand, the forward reaction in **equation 11** to provide copolymer from the cyclic carbonate proceeds at 110 ^{o}C at a faster rate than the reverse process.   This fits with our observation of the oxetane/CO_2 coupling process, where the reaction appears to be proceeding by initial formation of cyclic carbonate prior to ring opening polymerization to copolymer since these reactions were performed at elevated pressures of CO_2.
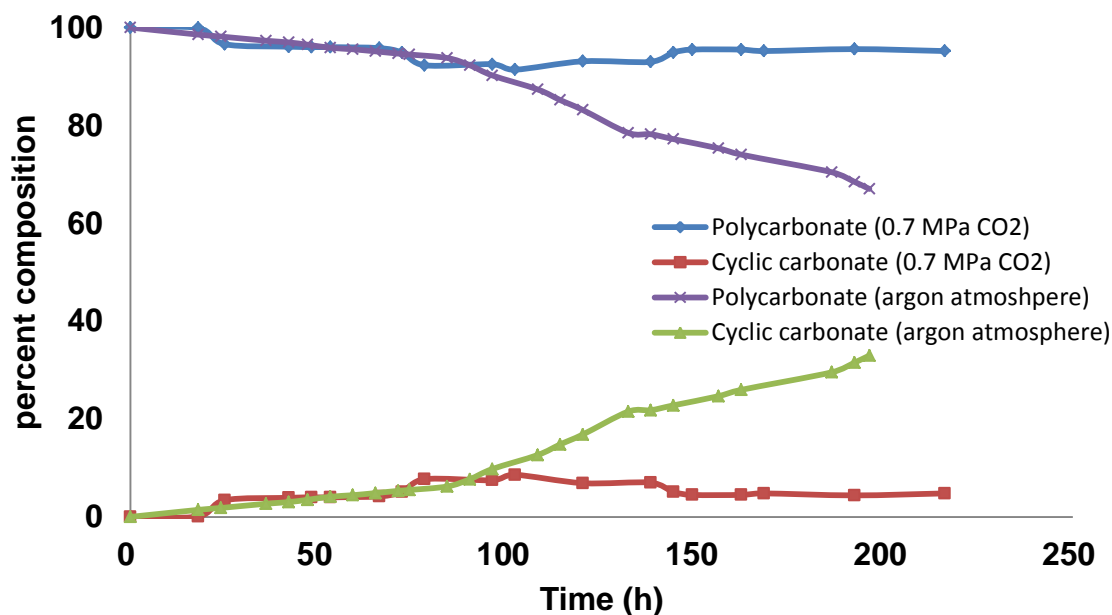
Figure 38. Depolymerization of poly(5-benzyloxy-methyl-5-methyl-1,3-dioxan-2-one) to the corresponding cyclic carbonate in toluene at 110 $^{\circ}$C as catalyzed by complex **8** in the presence of 2 equivalents of *n*-Bu$_4$NN$_3$.

Scheme 21.
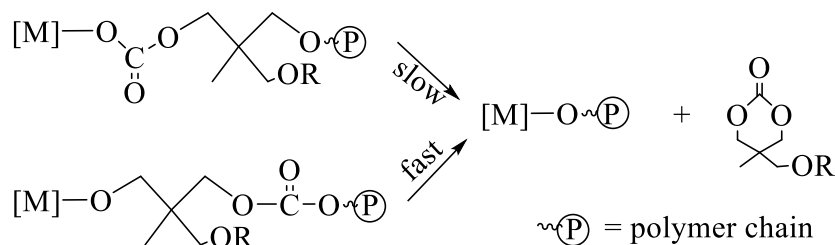
In addition, crystal structures of some of the cyclic carbonates were obtained. Their thermal ellipsoid plots are shown in **Figure 39**. The relationship between the structures of cyclic carbonates and their equilibrium distributions is still under investigation in our laboratory.
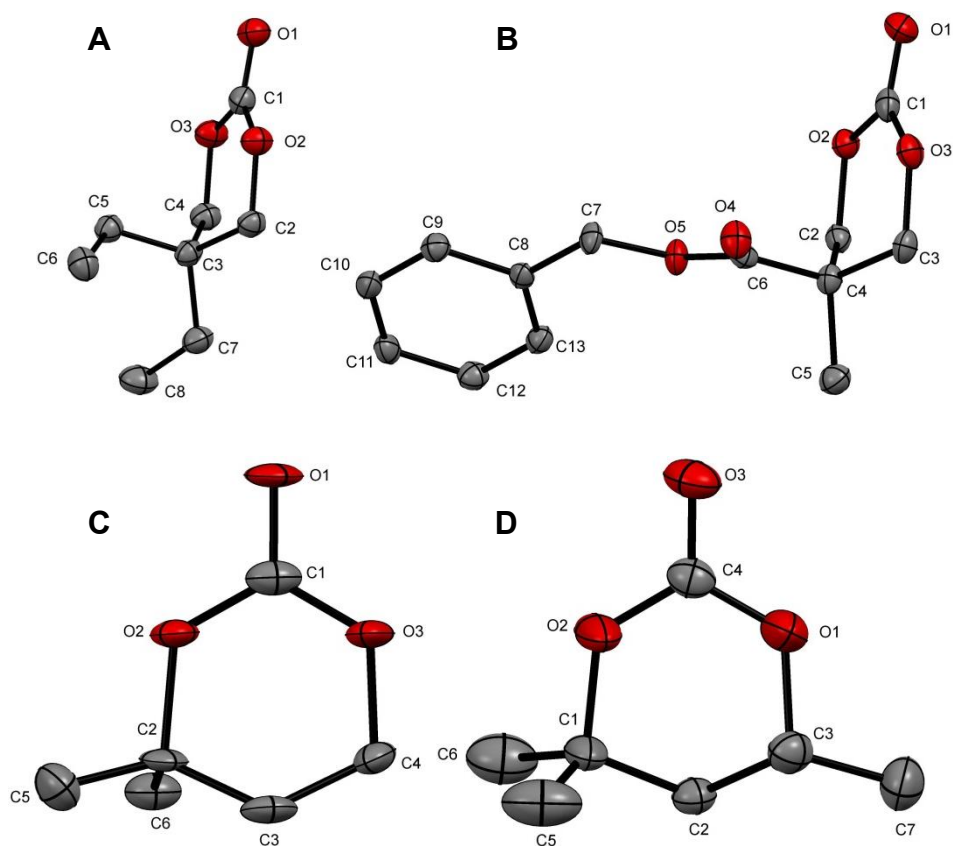
Figure 39. Thermal ellipsoid representations of **(A)** 5,5-diethyl-1,3-dioxan-2-one **(B)** benzyl 5-methyl-2-oxo-1,3-dioxane-5-carboxylate **(C)** 4,4-dimethyl-1,3-dioxan-2-one (**9b**) **(D)** 4,4,6-trimethyl-1,3-dioxan-2-one (**9c**). H atoms are omitted for clarity.

Concluding remarks

Herein we have extended our studies of the coupling reaction of CO_2 with oxetanes, focusing on oxetanes that are doubly substituted at the 3-position with substituents of varying steric requirements. Presented in these investigations were 3-methyloxetanes further substituted at the 3-position with methyl, $-CH_2OMe$, and $-CH_2OCH_2Ph$. Formation of the copolymer was found to proceed *via* preformed six-membered cyclic carbonate to a greater extent as the steric bulk of the substituents in the

137

3-position increased. That is, the degree of copolymer formation from oxetane and CO_2 by way of ring-opening polymerization of the first formed cyclic carbonate increased in the order listed below at 110 ^{o}C. Furthermore, the rate of the CO_2/oxetane coupling process was found to decrease in this order.
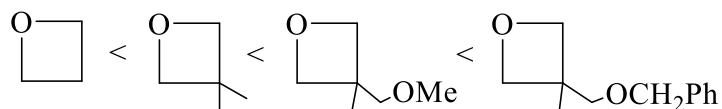
The thermal stability of the six-membered cyclic carbonate *vs* copolymer increased as well with an increase in the steric requirements of the substituents in the 3-position of the oxetane monomer. For example, only a trace of trimethylene carbonate is seen upon copolymerizing oxetane and CO_2, whereas, the coupling of 3-benzyloxy-methyl-3-methyloxetane and CO_2 afforded an equilibrium product distribution of copolymer to cyclic carbonate of 60 % at 110 ^{o}C. A noteworthy observation was that the rate of the isolated purified polycarbonate of polycarbonate and cyclic carbonate was greatly retarded by the presence of carbon dioxide. An ongoing effort in our laboratory is to develop an effective postsynthetic hydrogenation process for converting the benzyloxy-methyl copolymer to the hydrophilic polycarbonate containing pendant hydroxyl groups.

CHAPTER VII

CONCLUSIONS

Because of the numerous applications of polycarbonates, it is important that their manufacturing processes become more environmentally benign. However, the industrial production methods are mainly using toxic phosgene as starting material. Therefore, several modifications have been developed to reduce the use of phosgene. One of such improvements that received a lot of attention is the synthesis of polycarbonate from CO_2 and epoxide in the presence of Zn-based catalyst system discovered by Inoue in 1969. Inspired by Inoue and other outstanding researchers, our research group has been making polycarbonates in a variety of systems involving salen metal complexes as catalysts.

The synthesis of polycarbonates made from CO_2 and epoxides with electron-withdrawing substituents is challenging due to the enhancement of cyclic carbonate production in these instances. In chapter II, the polycarbonates made from CO_2 and epoxides such as styrene oxide and epichlorohydrin were successfully produced in the presence of (salen)Co(III) catalytic systems. The poly(styrene carbonate) afforded from the living polymerization gives perfectly alternative copolymer with less than 1% ether linkages and a glass-transition temperature of 80 ^{o}C. The polymer selectivity over cyclic carbonate can be enhanced through employing bifunctional catalysts. Poly(CO_2-*alt*-epichlorohydrin) is also obtained from CO_2 and epichlorohydrin using (salen)Co catalysts. The bifunctional catalysts bearing an appended TBD or quaternary ammonium salt on the ligands have shown higher selectivities and activities than regular

binary catalytic system for the CO_2/epichlorohydrin copolymerization. More than 99% carbonate linkages are found in the produced polycarbonate.

Furthermore, the activation energy barriers of polycarbonate and cyclic carbonate in the coupling reaction of CO_2 and epichlorohydrin were determined to be 53.1 and 98.5 kJ/mol. During the epichlorohydrin/CO_2 coupling process, cyclic carbonate formation is entropically favored. The difference in activation energy barriers for cyclic carbonate *vs* copolymer formation for the epichlorohydrin process is less than that of propylene oxide: 45.4 *vs* 53.5 kJ/mol. Similarities, the activation barriers for styrene oxide/CO_2 coupling to afford the two products have been measured, 40.4 and 50.7 kJ/mol. In particular for the propylene oxide/CO_2 reaction, cycloaddition occurs with significantly higher activation energy over that for copolymer formation.

From chapter II, we found that the cyclic carbonate formation *via* backbiting from polycarbonate plays an important role in controlling the selectivity of polycarbonate in CO_2/epoxide copolymerizations, especially for epoxide with an electron-withdrawing substituent. The investigation on depolymerization of polycarbonate *via* backbiting process has been done. In chapter III, we have shown the depolymerizations of aliphatic polycarbonates derived from copolymerization of epoxides and carbon dioxide to afford the corresponding cyclic carbonates in the presence of anionic initiators. This process is a highly ordered degradation of a free anionic chain initiated by an appropriate base. It is proven by a steady decrease in molecular weight with concomitant narrow distribution of the copolymer chain during the depolymerization process. Reaction rates depend on the basicity of the anionic

initiator, with $N_3^- > Cl^- >> Br^-$. The energy of activation barriers were found to increase for the selected polycarbonates in the order: poly(styrene carbonate) (46.7 kJ/mol) < poly(CO_2-*alt*-epichlorohydrin) (76.2 kJ/mol) ≤ poly(propylene carbonate) (80.5 kJ/mol). On the other hand, the depolymerization was highly suppressed in the presence of (salen)CrCl. This is due to the anionic polymer chain binding to the unsaturated metal center. This action stabilizes the free anionic chain, preventing from backbiting process to make corresponding cyclic carbonate. In contrast, poly(cyclohexene carbonate) was found to undergo the backbiting reaction to *trans*-cyclohexene carbonate by way of a metal-assisted pathway with a high activation barrier. The anion-assisted pathway was not observed.

In chapter IV, a unique degradation pathway was found in the anion-assisted depolymerization of poly(indene carbonate), the polycarbonate with highest glass-transition temperature reported from CO_2/epoxide copolymerization. The depolymerization initiated by azide is much faster than those initiated by stronger base, ie. NaHMDS and DBU. This suggests that the thermal degradation of poly(indene carbonate) to monomeric materials proceeds *via* an alternative pathway instead of the deprotonation and backbiting process that is observed for aliphatic polycarbonates. Pressurized CO_2 experiments were carried out to prove that decarboxylation occurs in the decomposition process. The presence of a radical intermediate was discovered and confirmed by quenching the degradation with the addition of TEMPO, a common radical trap. The radical initiators are generated in the presence of light; however the detailed mechanism is still poorly understood. The activation barrier of the azide-initiated

decomposition of poly(indene carbonate) was found to be at 189.1 kJ/mol, much higher than the other studied polycarbonates.

Next we focused on the depolymerization of poly(cyclopentene carbonate), which has a similar five-membered ring structure to poly(indene carbonate). The base-initiated depolymerization of poly(cyclopentene carbonate) only occurs in the presence of a strong base, e.g. NaHMDS. Cyclopentene oxide and *cis*-cyclic cyclopentene carbonate are both found as decomposition products. Computational results perfectly explain the experimental observations and their possible reaction pathways. The depolymerization starts from a deprotonation of the hydroxyl group on the chain end, then the backbiting occurs via the generated alkoxide end to form cyclopentene oxide instead of cyclic carbonate. This is due to the lower energy barrier, and it is unique to poly(cyclopentene carbonate). After that, a new carbonate chain end is formed and can be (1) converted to an alkoxide chain end by releasing a CO_2 or (2) can undergo a backbiting to form *cis*-cyclic carbonate. Compared to base-initiated depolymerization, cyclopentene oxide becomes the major product (more than 90%) in the metal-involved degradation of poly(cyclopentene carbonate), even under 100 psi of CO_2 pressure that has been added to suppress the decarboxylation. For recycling proposes, reduced pressure has been successfully applied to shorten the reaction time and to increase the yield of cyclopentene oxide. The generated cyclopentene oxide can then be isolated by distillation from a high boiling solvent in the metal-involved depolymerization of poly(cyclopentene carbonate). That is, the starting material of making polycarbonate can

be recovered and then be reused. This method demonstrates an ideal model for plastic recycling process.

Distinct from five-membered cyclic carbonates, six-membered cyclic carbonates are less stable than their corresponding polycarbonates so that they could undergo ring-opening polymerization to produce polycarbonates. In chapter VI, the copolymerization of CO_2 and 3-methoxymethyl-3-methyl oxetane is first studied to examine the effect on substituted at the 3-position with substituents of varying steric requirements comparing with oxetane/CO_2 copolymerization by *in situ* IR. The coupling reaction of CO_2 with the sterically more bulky oxetane, 3-benzyloxy-methyl-3-methyloxetane, to afford the equilibrium between polycarbonate and cyclic carbonate was also investigated. The equilibrium distribution of copolymer to cyclic carbonate produced from the coupling of oxetanes and CO_2 is found to decrease in the order: oxetane > 3,3-dimethyloxetane > 3-methoxy-methyl-3-methyloxetane > 3-benzyloxy-methyl-3-methyloxetane. Several alkyl-substituted trimethylene carbonates were synthesized and ring-opened to confirm the effect of steric hindrance on equilibrium distributions. Their crystal structures are obtained for further study on the relationship between equilibrium distributions. Moreover, the depolymerization of poly(5-methyl-5-benzyloxy-methyl-1,3-dioxan-2-one) was also carried out in the presence of (salen)CrCl and azide. When CO_2 pressure was applied, longer reaction time was required to reach equilibrium because backbiting *via* the carbonate species has a higher energy barrier than by the pathway of an alkoxide unit. The postsynthetic hydrogenation process for converting the benzyloxy-methyl copolymer to the hydrophilic polycarbonate is still under investigation in our laboratory.

143

To conclude, it is with hope that the studies in this dissertation have demonstrated that the investigated models of the backbiting process of polycarbonates mimics the cyclic carbonate byproduct formation during the coupling of cyclic ethers and CO_2. During the copolymerization process, the selectivity of polymer over cyclic carbonate can be controlled by applying appropriate catalysts even for substrates bearing electron-withdrawing substituents. Polycarbonates can be degraded to monomeric materials *via* different reaction pathways, and the generated materials may be useful for further applications. *In situ* IR has proven to be a very useful technique for kinetic and mechanistic studies of both copolymerization and depolymerization. It is my firm belief that exploring suitable depolymerization methods would continue to expand the scale of research and open up new opportunities in this area in both industry and academia.

REFERENCES

1. Allcock, H. R.; Lampe, F. W.; Mark, J. E. *Contemporary polymer chemistry*. 3rd ed.; Prentice Hall: New Jersey, 2003.

2. Walley, S. M.; Field, J. E.; Blair, P. W.; Milford, A. J. *International Journal of Impact Engineering* **2004,** *30*, 1, 31-53.

3. Serini, V., Polycarbonates. In *Ullmann's Encyclopedia of Industrial Chemistry*, Wiley-VCH Verlag GmbH & Co. KGaA: 2000.

4. Kim, W. B.; Joshi, U. A.; Lee, J. S. *Ind. Eng. Chem. Res.* **2004,** *43*, 9, 1897-1914.

5. Fukuoka, S.; Tojo, M.; Hachiya, H.; Aminaka, M.; Hasegawa, K. *Polym. J* **2007,** *39*, 2, 91-114.

6. Komiya, K.; Fukuoka, S.; Aminaka, M.; Hasegawa, K.; Hachiya, H.; Okamoto, H.; Watanabe, T.; Yoneda, H.; Fukawa, I.; Dozono, T., In *Green Chemistry: Designing Chemistry for the Environment*, Anastas, P. T.; Williamson, T. C., Eds. American Chemical Society: Washington, DC, 1996; pp 20-32.

7. (a) Inoue, S.; Kitamura, K.; Tsuruta, T. *Makromol. Chem.* **1969,** *126*, 1, 250-265; (b) Takeda, N.; Inoue, S. *Makromol. Chem.* **1978,** *179*, 5, 1377-1381.

8. (a) Hara, T.; Okamoto, S. *Jpn. J. Appl. Phys.* **1964,** *3*, 499-500; (b) Matsuoka, S.; Ishida, Y. *J. polym. sci., C Polym. symp.* **1966,** *14*, 1, 247-259.

9. Hughes, C.; vom Saal, F. S. *Environ. Health Perspect.* **2005,** *113*, 8, 926.

10. Inoue, S.; Koinuma, H.; Tsuruta, T. *J. Polym. Sci. B Polym. Lett.* **1969,** *7*, 4, 287-292.

11. Takeda, N.; Inoue, S. *Bull. Chem. Soc. Jpn.* **1978,** *51*, 12, 3564-3567.

12. (a) Darensbourg, D. J.; Holtcamp, M. W. *Macromolecules* **1995,** *28*, 22, 7577-7579; (b) Darensbourg, D. J.; Holtcamp, M. W.; Struck, G. E.; Zimmer, M. S.; Niezgoda, S. A.; Rainey, P.; Robertson, J. B.; Draper, J. D.; Reibenspies, J. H. *J. Am. Chem. Soc.* **1998,** *121*, 1, 107-116.

13. (a) Super, M.; Berluche, E.; Costello, C.; Beckman, E. *Macromolecules* **1997,** *30*, 3, 368-372; (b) Super, M.; Beckman, E. J. *Macromol. Symp.* **1998,** *127*, 1, 89-108.

14. Cheng, M.; Lobkovsky, E. B.; Coates, G. W. *J. Am. Chem. Soc.* **1998,** *120*, 42, 11018-11019.

15. Coates, G. W.; Moore, D. R. *Angew. Chem. Int. Ed.* **2004,** *43*, 48, 6618-6639.

16. (a) Chisholm, M. H.; Huffman, J. C.; Phomphrai, K. *Journal of the Chemical Society, Dalton Transactions* **2001,** *0*, 3, 222-224; (b) Chisholm, M. H.; Gallucci, J.; Phomphrai, K. *Inorg. Chem.* **2002,** *41*, 10, 2785-2794.

17. (a) Cheng, M.; Attygalle, A. B.; Lobkovsky, E. B.; Coates, G. W. *J. Am. Chem. Soc.* **1999,** *121*, 49, 11583-11584; (b) Chamberlain, B. M.; Cheng, M.; Moore, D. R.; Ovitt, T. M.; Lobkovsky, E. B.; Coates, G. W. *J. Am. Chem. Soc.* **2001,** *123*, 14, 3229-3238.

18. Rieth, L. R.; Moore, D. R.; Lobkovsky, E. B.; Coates, G. W. *J. Am. Chem. Soc.* **2002,** *124*, 51, 15239-15248.

19. Mang, S.; Cooper, A. I.; Colclough, M. E.; Chauhan, N.; Holmes, A. B. *Macromolecules* **2000,** *33*, 2, 303-308.

20. Darensbourg, D. J.; Yarbrough, J. C. *J. Am. Chem. Soc.* **2002,** *124*, 22, 6335-6342.

21. Hansen, K. B.; Leighton, J. L.; Jacobsen, E. N. *J. Am. Chem. Soc.* **1996,** *118*, 44, 10924-10925.

22. Darensbourg, D. J. *Inorg. Chem.* **2010,** *49*, 23, 10765-10780.

23. Darensbourg, D. J.; Fitch, S. B. *Inorg. Chem.* **2009,** *48*, 18, 8668-8677.

24. Darensbourg, D. J.; Moncada, A. I. *Macromolecules* **2010,** *43*, 14, 5996-6003.

25. Cohen, C. T.; Chu, T.; Coates, G. W. *J. Am. Chem. Soc.* **2005,** *127*, 31, 10869-10878.

26. (a) Kember, M. R.; Knight, P. D.; Reung, P. T. R.; Williams, C. K. *Angew. Chem. Int. Ed.* **2009,** *48*, 5, 931-933; (b) Kember, M. R.; White, A. J. P.; Williams, C. K. *Inorg. Chem.* **2009,** *48*, 19, 9535-9542.

27. Kember, M. R.; White, A. J. P.; Williams, C. K. *Macromolecules* **2010,** *43*, 5, 2291-2298.

28. Buchard, A.; Kember, M. R.; Sandeman, K. G.; Williams, C. K. *Chem. Commun.* **2011,** *47*, 1, 212-214.

29. Kember, M. R.; Williams, C. K. *J. Am. Chem. Soc.* **2012,** *134*, 38, 15676-15679.

30. (a) Qin, Y.; Wang, X.; Zhang, S.; Zhao, X.; Wang, F. *J. Polym. Sci. A Polym. Chem.* **2008,** *46*, 17, 5959-5967; (b) Ren, W.-M.; Liu, Y.; Wu, G.-P.; Liu, J.; Lu, X.-B. *J. Polym. Sci. A Polym. Chem.* **2011,** *49*, 22, 4894-4901.

31. Nakano, K.; Hashimoto, S.; Nakamura, M.; Kamada, T.; Nozaki, K. *Angew. Chem. Int. Ed.* **2011,** *50*, 21, 4868-4871.

32. Wu, G.-P.; Ren, W.-M.; Luo, Y.; Li, B.; Zhang, W.-Z.; Lu, X.-B. *J. Am. Chem. Soc.* **2012,** *134*, 12, 5682-5688.

33. Wu, G.-P.; Xu, P.-X.; Lu, X.-B.; Zu, Y.-P.; Wei, S.-H.; Ren, W.-M.; Darensbourg, D. J. *Macromolecules* **2013,** *46*, 6, 2128-2133.

34. Darensbourg, D. J.; Wilson, S. J. *J. Am. Chem. Soc.* **2011,** *133*, 46, 18610-18613.

35. Darensbourg, D. J.; Bottarelli, P.; Andreatta, J. R. *Macromolecules* **2007,** *40*, 21, 7727-7729.

36. (a) Darensbourg, D. J.; Yarbrough, J. C.; Ortiz, C.; Fang, C. C. *J. Am. Chem. Soc.* **2003,** *125*, 25, 7586-7591; (b) Xiao, Y.; Wang, Z.; Ding, K. *Macromolecules* **2006,** *39*, 1, 128-137; (c) Jutz, F.; Buchard, A.; Kember, M. R.; Fredriksen, S. B.; Williams, C. K. *J. Am. Chem. Soc.* **2011,** *133*, 43, 17395-17405.

37. Nakano, K.; Kamada, T.; Nozaki, K. *Angew. Chem. Int. Ed.* **2006,** *45*, 43, 7274-7277.

38. Noh, E. K.; Na, S. J.; S, S.; Kim, S.-W.; Lee, B. Y. *J. Am. Chem. Soc.* **2007,** *129*, 26, 8082-8083.

39. (a) S, S.; Min, J. K.; Seong, J. E.; Na, S. J.; Lee, B. Y. *Angew. Chem. Int. Ed.* **2008,** *47*, 38, 7306-7309; (b) Na, S. J.; S, S.; Cyriac, A.; Kim, B. E.; Yoo, J.; Kang, Y. K.; Han, S. J.; Lee, C.; Lee, B. Y. *Inorg. Chem.* **2009,** *48*, 21, 10455-10465; (c) Yoo, J.; Na, S. J.; Park, H. C.; Cyriac, A.; Lee, B. Y. *Dalton Trans.* **2010,** *39*, 10, 2622-2630.

40. Ren, W.-M.; Liu, Z.-W.; Wen, Y.-Q.; Zhang, R.; Lu, X.-B. *J. Am. Chem. Soc.* **2009,** *131*, 32, 11509-11518.

41. Darensbourg, D. J.; Wilson, S. J., unpublished result.

42.   Shah, S. H.; Khan, Z. M.; Raja, I. A.; Mahmood, Q.; Bhatti, Z. A.; Khan, J.; Farooq, A.; Rashid, N.; Wu, D. *J. Hazard. Mater.* **2010,** *179*, 1–3, 15-20.

43.   SPI Resin Identification Code - Guide to Correct Use. http://www.plasticsindustry.org/AboutPlastics/content.cfm?ItemNumber=823&navItemNumber=2144 (accessed April 2nd.).

44.   Plastic Packaging Resins. http://plastics.americanchemistry.com/Education-Resources/Plastics-101/Plastics-Resin-Codes-PDF.pdf (accessed April 2nd.).

45.   Manrich, S.; Santos, A. l. S. F. *Plastic recycling*. Nova Science Publishers New York, 2009.

46.   Al-Salem, S. M.; Lettieri, P.; Baeyens, J. *Waste Manage.* **2009,** *29*, 10, 2625-2643.

47.   Saikia, N.; de Brito, J. *Constr. Build. Mater.* **2012,** *34*, 0, 385-401.

48.   Sasse, F.; Emig, G. *Chem. Eng. Technol.* **1998,** *21*, 10, 777-789.

49.   (a) Darensbourg, D. J. *Chem. Rev.* **2007,** *107*, 6, 2388-2410; (b) Darensbourg, D. J.; Mackiewicz, R. M.; Phelps, A. L.; Billodeaux, D. R. *Acc. Chem. Res.* **2004,** *37*, 11, 836-844; (c) Chisholm, M. H.; Zhou, Z. *J. Mater. Chem.* **2004,** *14*, 21, 3081-3092; (d) Sugimoto, H.; Inoue, S. *J. Polym. Sci. A Polym. Chem.* **2004,** *42*, 22, 5561-5573.

50.   (a) Moore, D. R.; Cheng, M.; Lobkovsky, E. B.; Coates, G. W. *Angew. Chem. Int. Ed.* **2002,** *41*, 14, 2599-2602; (b) Nakano, K.; Nozaki, K.; Hiyama, T. *J. Am. Chem. Soc.* **2003,** *125*, 18, 5501-5510; (c) Lee, B. Y.; Kwon, H. Y.; Lee, S. Y.; Na, S. J.; Han, S.-i.; Yun, H.; Lee, H.; Park, Y.-W. *J. Am. Chem. Soc.* **2005,** *127*, 9, 3031-3037.

51. (a) Chen, X.; Shen, Z.; Zhang, Y. *Macromolecules* **1991,** *24*, 19, 5305-5308; (b) Tan, C.-S.; Hsu, T.-J. *Macromolecules* **1997,** *30*, 11, 3147-3150; (c) Liu, B.; Zhao, X.; Wang, X.; Wang, F. *J. Polym. Sci. A Polym. Chem.* **2001,** *39*, 16, 2751-2754; (d) Cui, D.; Nishiura, M.; Hou, Z. *Macromolecules* **2005,** *38*, 10, 4089-4095.

52. (a) Aida, T.; Inoue, S. *J. Am. Chem. Soc.* **1983,** *105*, 5, 1304-1309; (b) Chisholm, M. H.; Zhou, Z. *J. Am. Chem. Soc.* **2004,** *126*, 35, 11030-11039; (c) Darensbourg, D. J.; Billodeaux, D. R. *Inorg. Chem.* **2005,** *44*, 5, 1433-1442.

53. (a) Eberhardt, R.; Allmendinger, M.; Rieger, B. *Macromol. Rapid Commun.* **2003,** *24*, 2, 194-196; (b) Li, B.; Wu, G.-P.; Ren, W.-M.; Wang, Y.-M.; Rao, D.-Y.; Lu, X.-B. *J. Polym. Sci. A Polym. Chem.* **2008,** *46*, 18, 6102-6113; (c) Nakano, K.; Nakamura, M.; Nozaki, K. *Macromolecules* **2009,** *42*, 18, 6972-6980.

54. Qin, Z.; Thomas, C. M.; Lee, S.; Coates, G. W. *Angew. Chem. Int. Ed.* **2003,** *42*, 44, 5484-5487.

55. (a) Lu, X.-B.; Wang, Y. *Angew. Chem. Int. Ed.* **2004,** *43*, 27, 3574-3577; (b) Paddock, R. L.; Nguyen, S. T. *Macromolecules* **2005,** *38*, 15, 6251-6253; (c) Lu, X.-B.; Shi, L.; Wang, Y.-M.; Zhang, R.; Zhang, Y.-J.; Peng, X.-J.; Zhang, Z.-C.; Li, B. *J. Am. Chem. Soc.* **2006,** *128*, 5, 1664-1674.

56. (a) Stevens, H. C. P. P. G. C. U.S. Patent No. 3,248,415, 1966; (b) Inoue, S.; Koinuma, H.; Tsuruta, T. *Makromol. Chem.* **1969,** *130*, 1, 210-220; (c) Lee, Y. B.; Shin, E. J.; Yoo, J. Y. *J. Korean Int. Eng. Chem* **2008,** *19*, 133-136; (d) Allen, S. D.; Byrne, C. M.; Coates, G. W., Carbon dioxide as a renewable C1 feedstock: Synthesis and characterization of polycarbonates from the alternating

copolymerization of epoxides and CO2. In *Feedstocks for the Future: Renewables for the Production of Chemicals and Materials*, Bozell, J. P., M., Ed. American Chemical Society: Washington, DC, 2006; Vol. , pp 116-128; (e) Darensbourg, D. J.; Fitch, S. B. *Inorg. Chem.* **2008,** *47*, 24, 11868-11878; (f) Shen, Z.; Chen, X.; Zhang, Y. *Macromol. Chem. Phys.* **1994,** *195*, 6, 2003-2011.

57. Zou, Z.-Q.; Ji, W.-D.; Luo, J.-X.; Zhang, M.; Chen, L.-B. *Polym. Mater. Sci. Eng.* **2010,** *26*, 1-4.

58. Lin, B.; Whalen, D. L. *J. Org. Chem.* **1994,** *59*, 7, 1638-1641.

59. Watson, J. M.; Young, B. L. *J. Org. Chem.* **1974,** *39*, 1, 116-117.

60. Baggett, J. M.; Pruitt, M. E. U.S. Patent No. 2,871,219, 1959.

61. Kuran, W.; Niestochowski, A. *Polym. Bull. (Berlin)* **1980,** *2*, 6, 411-416.

62. Schaus, S. E.; Brandes, B. D.; Larrow, J. F.; Tokunaga, M.; Hansen, K. B.; Gould, A. E.; Furrow, M. E.; Jacobsen, E. N. *J. Am. Chem. Soc.* **2002,** *124*, 7, 1307-1315.

63. Darensbourg, D. J.; Rodgers, J. L.; Mackiewicz, R. M.; Phelps, A. L. *Catal. Today* **2004,** *98*, 4, 485-492.

64. Hirahata, W.; Thomas, R. M.; Lobkovsky, E. B.; Coates, G. W. *J. Am. Chem. Soc.* **2008,** *130*, 52, 17658-17659.

65. Hirano, T.; Inoue, S.; Tsuruta, T. *Makromol. Chem.* **1975,** *176*, 7, 1913-1917.

66. (a) Kember, M. R.; Buchard, A.; Williams, C. K. *Chem. Commun.* **2011,** *47*, 1, 141-163; (b) Klaus, S.; Lehenmeier, M. W.; Anderson, C. E.; Rieger, B. *Coord. Chem. Rev.* **2011,** *255*, 13–14, 1460-1479; (c) Lu, X.-B.; Darensbourg, D. J. *Chem. Soc. Rev.* **2012,** *41*, 4, 1462-1484.

67. Luinstra, G. A.; Haas, G. R.; Molnar, F.; Bernhart, V.; Eberhardt, R.; Rieger, B. *Chem. Eur. J.* **2005,** *11*, 21, 6298-6314.

68. Wu, G.-P.; Wei, S.-H.; Ren, W.-M.; Lu, X.-B.; Li, B.; Zu, Y.-P.; Darensbourg, D. J. *Energy Environ. Sci.* **2011,** *4*, 12, 5084-5092.

69. Wu, G.-P.; Wei, S.-H.; Ren, W.-M.; Lu, X.-B.; Xu, T.-Q.; Darensbourg, D. J. *J. Am. Chem. Soc.* **2011,** *133*, 38, 15191-15199.

70. Darensbourg, D. J.; Phelps, A. L. *Inorg. Chem.* **2005,** *44*, 13, 4622-4629.

71. Darensbourg, D. J.; Mackiewicz, R. M.; Billodeaux, D. R. *Organometallics* **2005,** *24*, 1, 144-148.

72. *APEX2, version 2009.7–0*, Bruker AXS Inc.: Madison, WI, 2007.

73. *SAINTPLUS: Program for Reduction of Area Detector Data, version 6.63*, Bruker AXS Inc.: Madison, WI, 2007.

74. Sheldrick, G. M. *SADABS: Program for Absorption Correction of Area Detector Frames*, Bruker AXS Inc.: Madison, WI, 2001.

75. Sheldrick, G. M. *SHELXS-97: Program for Crystal Structure Solution*, Universität Göttingen: Göttingen, Germany, 1997.

76. Sheldrick, G. M. *SHELXL-97: Program for Crystal Structure Refinement*, Universität Göttingen: Göttingen, Germany, 1997.

77. Wu, G.-P.; Wei, S.-H.; Lu, X.-B.; Ren, W.-M.; Darensbourg, D. J. *Macromolecules* **2010,** *43*, 21, 9202-9204.

78. (a) Inoue, S. *J. Polym. Sci. A Polym. Chem.* **2000,** *38*, 16, 2861-2871; (b) Sugimoto, H.; Ohtsuka, H.; Inoue, S. *J. Polym. Sci. A Polym. Chem.* **2005,** *43*, 18, 4172-4186.

79. Darensbourg, D. J.; Lewis, S. J.; Rodgers, J. L.; Yarbrough, J. C. *Inorg. Chem.* **2003,** *42*, 2, 581-589.

80. S, S.; Min, J. K.; Seong, J. E.; Na, S. J.; Lee, B. Y. *Angew. Chem.* **2008,** *120*, 38, 7416-7419.

81. Darensbourg, D. J.; Wei, S.-H.; Wilson, S. J. *Macromolecules* **2013**, ASAP.

82. Coates, G. W.; Hillmyer, M. A. *Macromolecules* **2009,** *42*, 21, 7987-7989.

83. (a) Darensbourg, D. J.; Holtcamp, M. W. *Coord. Chem. Rev.* **1996,** *153*, 0, 155-174; (b) Darensbourg, D. J.; Wilson, S. J. *Green Chem.* **2012,** *14*, 10, 2665-2671; (c) Lu, X.-B.; Ren, W.-M.; Wu, G.-P. *Acc. Chem. Res.* **2012,** *45*, 10, 1721-1735.

84. Liu, J.; Ren, W.-M.; Liu, Y.; Lu, X.-B. *Macromolecules* **2013,** *46*, 4, 1343-1349.

85. Darensbourg, D. J.; Wei, S.-H. *Macromolecules* **2012,** *45*, 15, 5916-5922.

86. Uchida, T.; Irie, R.; Katsuki, T. *Synlett* **1999,** *1999*, 07, 1163-1165.

87. Darensbourg, D. J.; Moncada, A. I.; Wei, S.-H. *Macromolecules* **2011,** *44*, 8, 2568-2576.

88. White, R. C.; Drew, P.; Moorman, R. *J. Heterocycl. Chem.* **1988,** *25*, 6, 1781-1783.

89. Darensbourg, D. J.; Yeung, A. D. *Macromolecules* **2013,** *46*, 1, 83-95.

90. (a) Ellis, W. C.; Coates, G. W. **2013**, manuscript in preparation; (b) Ellis, W. C.; Coates, G. W., Catalyst design for isotactic polycarbonates from CO2and cyclic epoxides In *244th ACS National Meeting & Exposition*, Philadelphia, PA, United States,, 2012; p INOR20.

91. Darensbourg, D. J.; Yeung, A. D.; Wei, S.-H. *Green Chem.* **2013**, ASAP.

92. Konsler, R. G.; Karl, J.; Jacobsen, E. N. *J. Am. Chem. Soc.* **1998,** *120*, 41, 10780-10781.

93. (a) Loy, R. N.; Jacobsen, E. N. *J. Am. Chem. Soc.* **2009,** *131*, 8, 2786-2787; (b) Wuitschik, G.; Carreira, E. M.; Wagner, B. r.; Fischer, H.; Parrilla, I.; Schuler, F.; Rogers-Evans, M.; Müller, K. *J. Med. Chem.* **2010,** *53*, 8, 3227-3246.

94. (a) Darensbourg, D. J.; Ganguly, P.; Choi, W. *Inorg. Chem.* **2006,** *45*, 10, 3831-3833; (b) Darensbourg, D. J.; Moncada, A. I.; Choi, W.; Reibenspies, J. H. *J. Am. Chem. Soc.* **2008,** *130*, 20, 6523-6533; (c) Darensbourg, D. J.; Moncada, A. I. *Inorg. Chem.* **2008,** *47*, 21, 10000-10008.

95. (a) Ochiai, B.; Endo, T. *Prog. Polym. Sci.* **2005,** *30*, 2, 183-215; (b) Nakano, K.; Kosaka, N.; Hiyama, T.; Nozaki, K. *Dalton Trans.* **2003,** *0*, 21, 4039-4050; (c) Darensbourg, D. J.; Andreatta, J. R.; Moncada, A. I., Polymers from Carbon Dioxide: Polycarbonates, Polythiocarbonates, and Polyurethanes. In *Carbon Dioxide as Chemical Feedstock*, Aresta, M., Ed. Wiley-VCH: Weinheim, Germany, 2010; pp 213-248; (d) Darensbourg, D., Salen Metal Complexes as Catalysts for the Synthesis of Polycarbonates from Cyclic Ethers and Carbon Dioxide. In *Synthetic Biodegradable Polymers*, Rieger, B.; Künkel, A.; Coates, G. W.; Reichardt, R.; Dinjus, E.; Zevaco, T. A., Eds. Springer Berlin Heidelberg: 2012; Vol. 245, pp 1-27.

96. Clements, J. H. *Ind. Eng. Chem. Res.* **2003,** *42*, 4, 663-674.

97. Matsuo, J.; Aoki, K.; Sanda, F.; Endo, T. *Macromolecules* **1998,** *31*, 14, 4432-4438.

98. Darensbourg, D. J.; Mackiewicz, R. M.; Rodgers, J. L.; Fang, C. C.; Billodeaux, D. R.; Reibenspies, J. H. *Inorg. Chem.* **2004,** *43*, 19, 6024-6034.

99. McAlees, A. J.; McCrindle, R.; Woon-Fat, A. R. *Inorg. Chem.* **1976,** *15*, 5, 1065-1074.

100. Doherty, S.; Robins, E. G.; Nieuwenhuyzen, M.; Champkin, P. A.; Clegg, W. *Organometallics* **2002,** *21*, 20, 4147-4158.

101. Ariga, T.; Takata, T.; Endo, T. *Macromolecules* **1997,** *30*, 4, 737-744.

102. *FRAMBO:FRAME Buffer Operation*, v.4.1.05; Bruker AXS Inc.: Madison, WI.

103. Sheldrick, G. M. *SHELXTL*, v. 6.14; Bruker-Nonius Inc.: Madison, WI, 2000.

104. Barbour, L. J. *J. Supramol. Chem.* **2001,** *1*, 4–6, 189-191.

105. (a) Ray, W. C.; Grinstaff, M. W. *Macromolecules* **2003,** *36*, 10, 3557-3562; (b) Westwood, G.; Horton, T. N.; Wilker, J. J. *Macromolecules* **2007,** *40*, 11, 3960-3964.

106. Darensbourg, D. J.; Mackiewicz, R. M. *J. Am. Chem. Soc.* **2005,** *127*, 40, 14026-14038.

107. Kuramshina, A. E.; Bochkor, S. A.; Kuznetsov, V. V. *Russ. J. Gen. Chem.* **2009,** *79*, 4, 787-790.

APPENDIX A

COPYRIGHT INFORMATION

Copyright Clearance Center   **RightsLink®**

Home   Account Info   Help

ACS Publications
High quality. High impact.

Title: Highly Selective Synthesis of CO2 Copolymer from Styrene Oxide

Author: Guang-Peng Wu, Sheng-Hsuan Wei, Xiao-Bing Lu, Wei-Min Ren, and Donald J. Darensbourg

Publication: Macromolecules

Publisher: American Chemical Society

Date: Nov 1, 2010

Copyright © 2010, American Chemical Society

Logged in as:
Sheng-Hsuan Wei
Account #:
3000632883

LOGOUT

BACK   CLOSE WINDOW

RightsLink®

ACS Publications
High quality. High impact.

Title: Perfectly Alternating Copolymerization of CO2 and Epichlorohydrin Using Cobalt(III)-Based Catalyst Systems

Author: Guang-Peng Wu, Sheng-Hsuan Wei, Wei-Min Ren, Xiao-Bing Lu, Tie-Qi Xu, and Donald J. Darensbourg

Publication: Journal of the American Chemical Society

Publisher: American Chemical Society

Date: Sep 1, 2011

Copyright © 2011, American Chemical Society

Logged in as:
Sheng-Hsuan Wei
Account #:
3000632883

LOGOUT

PERMISSION/LICENSE IS GRANTED FOR YOUR ORDER AT NO CHARGE

This type of permission/license, instead of the standard Terms & Conditions, is sent to you because no fee is being charged for your order. Please note the following:

- Permission is granted for your request in both print and electronic formats, and translations.
- If figures and/or tables were requested, they may be adapted or used in part.
- Please print this page for your records and send a copy of it to your publisher/graduate school.
- Appropriate credit for the requested material should be given as follows: "Reprinted (adapted) with permission from (COMPLETE REFERENCE CITATION). Copyright (YEAR) American Chemical Society." Insert appropriate information in place of the capitalized words.
- One-time permission is granted only for the use specified in your request. No additional uses are granted (such as derivative works or other editions). For any other uses, please submit a new request.

BACK   CLOSE WINDOW

157

Automatic reply: copyright reuse request- Energy Environ. Sci., 2011,4, 5084-5092

CONTRACTS-COPYRIGHT (shared) <Contracts-Copyright@rsc.org>   2013年5月16日上午4:16
收件者： Sheng-Hsuan Wei <shwei0624@gmail.com>

Dear Sheng-Hsuan

Permission is not needed to reproduce your article in your thesis.

Best wishes

Gill

Gill Cockhead (Mrs), Publishing Contracts & Copyright Executive

Royal Society of Chemistry, Thomas Graham House

Science Park, Milton Road, Cambridge CB4 0WF, UK

Tel +44 (0) 1223 432134, Fax +44 (0) 1223 423623

http://www.rsc.org

Copyright
Clearance
Center

RightsLink®

Home   Account Info   Help

ACS Publications
High quality. High impact.

Title: Depolymerization of Polycarbonates Derived from Carbon Dioxide and Epoxides to Provide Cyclic Carbonates. A Kinetic Study

Author: Donald J. Darensbourg and Sheng-Hsuan Wei

Publication: Macromolecules

Publisher: American Chemical Society

Date: Aug 1, 2012

Copyright © 2012, American Chemical Society

Logged in as:
Sheng-Hsuan Wei
Account #:
3000632883

LOGOUT

PERMISSION/LICENSE IS GRANTED FOR YOUR ORDER AT NO CHARGE

This type of permission/license, instead of the standard Terms & Conditions, is sent to you because no fee is being charged for your order. Please note the following:

- Permission is granted for your request in both print and electronic formats, and translations.
- If figures and/or tables were requested, they may be adapted or used in part.
- Please print this page for your records and send a copy of it to your publisher/graduate school.
- Appropriate credit for the requested material should be given as follows: "Reprinted (adapted) with permission from (COMPLETE REFERENCE CITATION). Copyright (YEAR) American Chemical Society." Insert appropriate information in place of the capitalized words.
- One-time permission is granted only for the use specified in your request. No additional uses are granted (such as derivative works or other editions). For any other uses, please submit a new request.

BACK   CLOSE WINDOW

RightsLink®

ACS Publications
High quality. High impact.

Title: Depolymerization of Poly(indene carbonate). A Unique Degradation Pathway

Author: Donald J. Darensbourg, Sheng-Hsuan Wei, and Stephanie J. Wilson

Publication: Macromolecules

Publisher: American Chemical Society

Date: May 1, 2013

Copyright © 2013, American Chemical Society

Logged in as:
Sheng-Hsuan Wei
Account #:
3000632883

LOGOUT

PERMISSION/LICENSE IS GRANTED FOR YOUR ORDER AT NO CHARGE

This type of permission/license, instead of the standard Terms & Conditions, is sent to you because no fee is being charged for your order. Please note the following:

- Permission is granted for your request in both print and electronic formats, and translations.
- If figures and/or tables were requested, they may be adapted or used in part.
- Please print this page for your records and send a copy of it to your publisher/graduate school.
- Appropriate credit for the requested material should be given as follows: "Reprinted (adapted) with permission from (COMPLETE REFERENCE CITATION). Copyright (YEAR) American Chemical Society." Insert appropriate information in place of the capitalized words.
- One-time permission is granted only for the use specified in your request. No additional uses are granted (such as derivative works or other editions). For any other uses, please submit a new request.

BACK   CLOSE WINDOW

Copyright
Clearance
Center

RightsLink®

Home   Account Info   Help

ACS Publications
High quality. High impact.

Title: Aliphatic Polycarbonates Produced from the Coupling of Carbon Dioxide and Oxetanes and Their Depolymerization via Cyclic Carbonate Formation

Author: Donald J. Darensbourg, Adriana I. Moncada, and Sheng-Hsuan Wei

Publication: Macromolecules

Publisher: American Chemical Society

Date: Apr 1, 2011

Copyright © 2011, American Chemical Society

Logged in as:
Sheng-Hsuan Wei
Account #:
3000632883

LOGOUT

PERMISSION/LICENSE IS GRANTED FOR YOUR ORDER AT NO CHARGE

This type of permission/license, instead of the standard Terms & Conditions, is sent to you because no fee is being charged for your order. Please note the following:

- Permission is granted for your request in both print and electronic formats, and translations.
- If figures and/or tables were requested, they may be adapted or used in part.
- Please print this page for your records and send a copy of it to your publisher/graduate school.
- Appropriate credit for the requested material should be given as follows: "Reprinted (adapted) with permission from (COMPLETE REFERENCE CITATION). Copyright (YEAR) American Chemical Society." Insert appropriate information in place of the capitalized words.
- One-time permission is granted only for the use specified in your request. No additional uses are granted (such as derivative works or other editions). For any other uses, please submit a new request.

BACK   CLOSE WINDOW

161

^{1}H NMR SPECTRA IN CHAPTER III
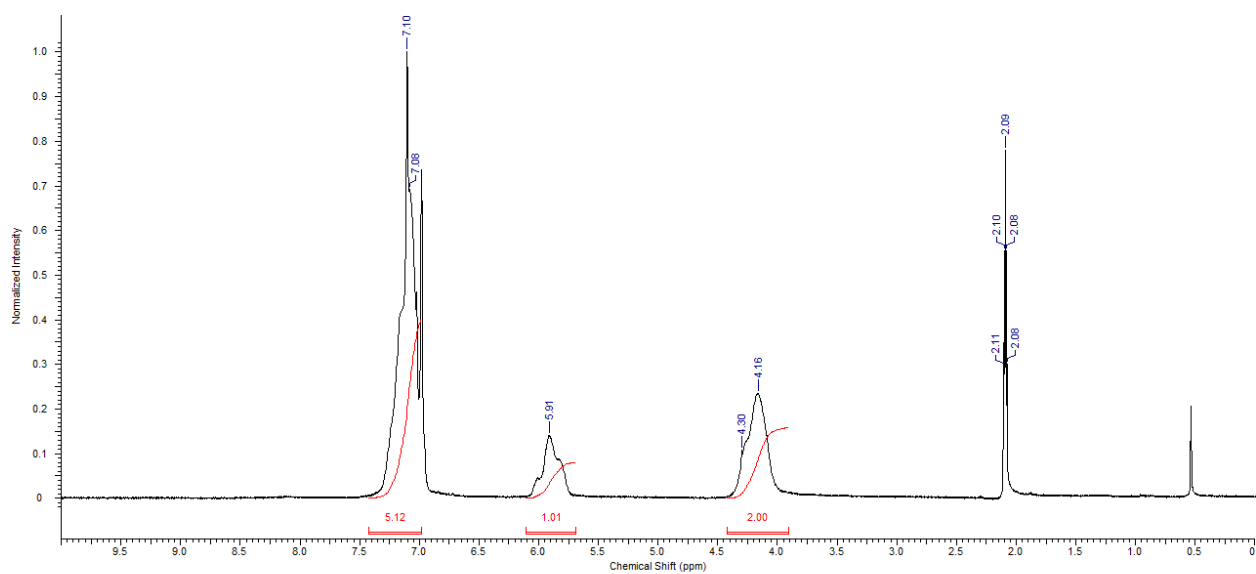
Figure B-1. Poly(styrene carbonate) in *d*-toluene.
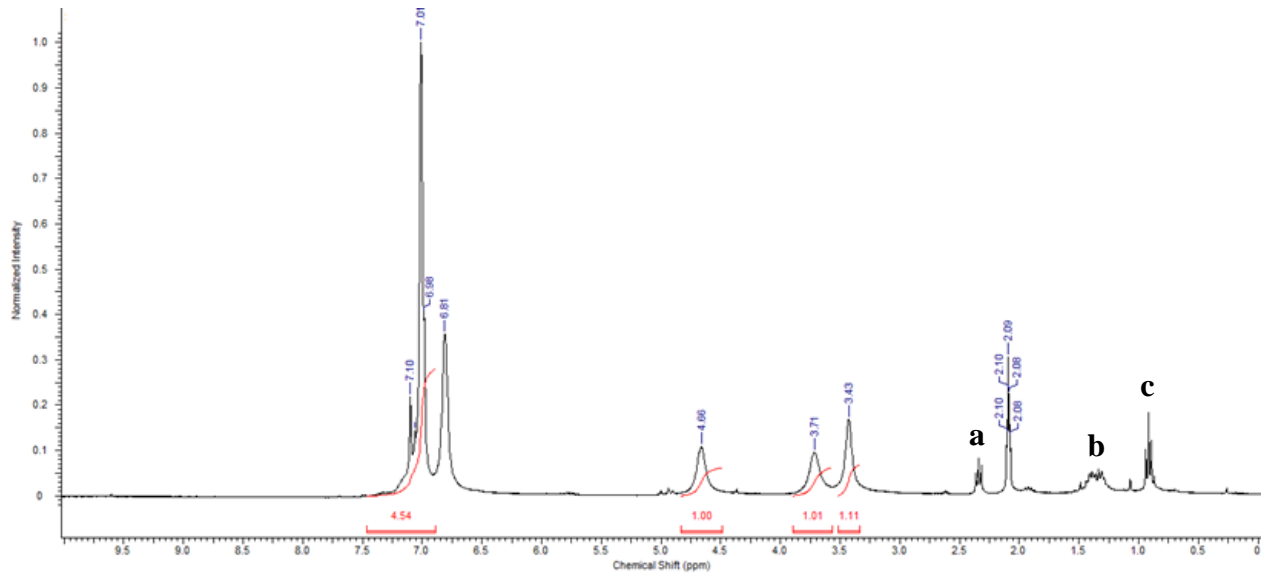
Figure B-2. Quantitative depolymerization of poly(styrene carbonate) in *d*-toluene. (**Table 6**). Peaks at **a**, **b**, and **c** are due to *n*-Bu$_4$N$^+$.

SUPPORTING CRYSTALLOGRAPHIC DATA FOR CHAPTER III
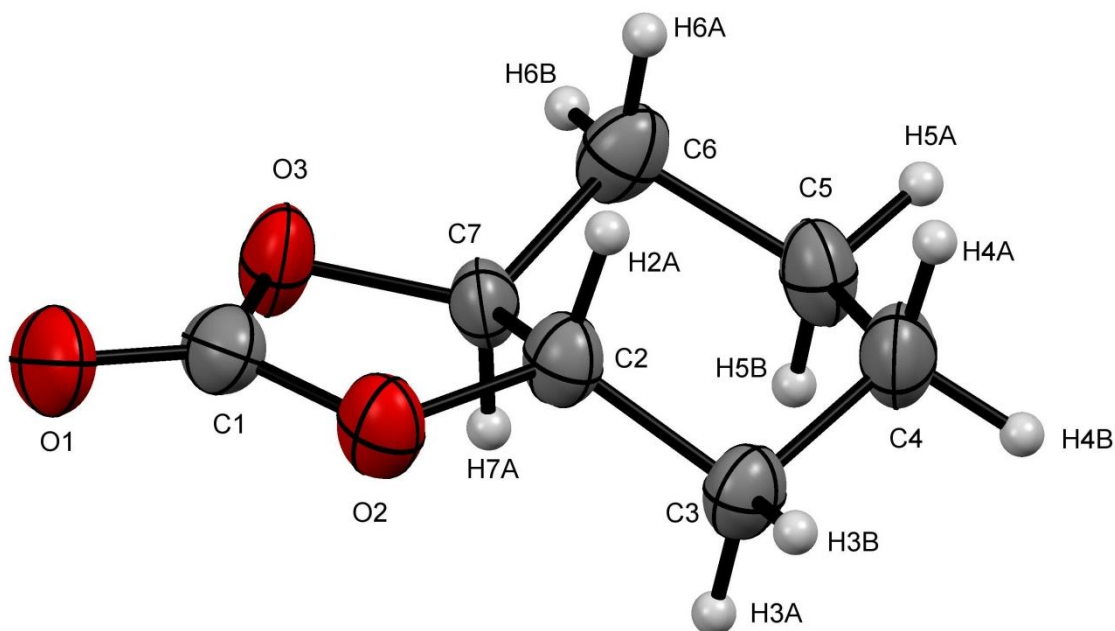
Table C-1. Crystal data and structure refinement for OP212121.

Identification code	op212121	
Empirical formula	C7 H10 O3	
Formula weight	142.15	
Temperature	110(2) K	
Wavelength	0.71073 Å	
Crystal system	Orthorhombic	
Space group	P2(1)2(1)2(1)	
Unit cell dimensions	a = 6.393(2) Å	a= 90°.
	b = 9.267(3) Å	b= 90°.
	c = 11.825(4) Å	g = 90°.
Volume	700.5(4) Å ^{3}	

Z	4
Density (calculated)	1.348 Mg/m^3
Absorption coefficient	0.105 mm^{-1}
F(000)	304
Crystal size	0.20 x 0.20 x 0.20 mm^3
Theta range for data collection	2.79 to 25.98°.
Index ranges	-7<=h<=7, -11<=k<=11, -14<=l<=14
Reflections collected	7222
Independent reflections	1374 [R(int) = 0.0350]
Completeness to theta = 25.98°	100.0 %
Absorption correction	Semi-empirical from equivalents
Max. and min. transmission	0.9793 and 0.9793
Refinement method	Full-matrix least-squares on F^2
Data / restraints / parameters	1374 / 193 / 122
Goodness-of-fit on F^2	0.479
Final R indices [I>2sigma(I)]	R1 = 0.0330, wR2 = 0.0799
R indices (all data)	R1 = 0.0389, wR2 = 0.0891
Absolute structure parameter	-1.1(14)
Largest diff. peak and hole	0.123 and -0.146 e.Å^{-3}

Table C-2. Atomic coordinates (x 10^4) and equivalent isotropic displacement parameters (Å ^{2}x 10^3) for OP212121. U(eq) is defined as one third of the trace of the orthogonalized U^{ij} tensor.

	x	y	z	U(eq)
C(1)	3721(3)	6839(2)	1209(1)	38(1)
C(2)	2183(18)	9013(13)	1489(10)	36(1)
C(3)	1693(10)	10173(6)	2337(6)	37(2)
C(4)	1820(30)	11584(16)	1630(20)	44(1)
C(5)	3937(17)	11777(11)	1021(8)	41(1)
C(6)	4416(15)	10483(8)	240(7)	42(2)
C(7)	4331(13)	9196(10)	1031(7)	33(1)
C(2A)	2608(6)	9023(5)	1734(3)	36(1)
C(3A)	798(5)	10050(3)	1715(3)	42(1)
C(4A)	1815(16)	11571(7)	1664(10)	44(1)
C(5A)	3399(6)	11725(4)	698(3)	41(1)
C(6A)	5094(5)	10536(3)	684(4)	39(1)
C(7A)	3874(5)	9159(4)	689(3)	33(1)
O(1)	3988(2)	5557(1)	1187(1)	52(1)
O(2)	2190(2)	7490(1)	1784(1)	43(1)
O(3)	4947(2)	7790(1)	666(1)	45(1)

Table C-3. Bond lengths [Å] and angles [°] for OP212121.

C(1)-O(1)	1.200(2)
C(1)-O(2)	1.336(2)
C(1)-O(3)	1.342(2)
C(2)-O(2)	1.454(13)
C(2)-C(7)	1.486(12)
C(2)-C(3)	1.502(10)
C(3)-C(4)	1.553(14)
C(4)-C(5)	1.547(13)
C(5)-C(6)	1.544(10)
C(6)-C(7)	1.517(10)
C(7)-O(3)	1.428(10)
C(2A)-O(2)	1.447(5)
C(2A)-C(7A)	1.483(5)
C(2A)-C(3A)	1.498(5)
C(3A)-C(4A)	1.553(8)
C(4A)-C(5A)	1.533(6)
C(5A)-C(6A)	1.546(4)
C(6A)-C(7A)	1.496(4)
C(7A)-O(3)	1.443(4)
O(1)-C(1)-O(2)	124.16(16)
O(1)-C(1)-O(3)	123.84(16)
O(2)-C(1)-O(3)	111.99(13)
O(2)-C(2)-C(7)	101.2(8)
O(2)-C(2)-C(3)	122.4(9)
C(7)-C(2)-C(3)	110.8(9)
C(2)-C(3)-C(4)	103.5(10)
C(5)-C(4)-C(3)	113.1(12)
C(6)-C(5)-C(4)	111.3(11)
C(7)-C(6)-C(5)	103.6(7)
O(3)-C(7)-C(2)	105.1(7)
O(3)-C(7)-C(6)	121.4(7)

C(2)-C(7)-C(6)	110.3(9)
O(2)-C(2A)-C(7A)	102.6(3)
O(2)-C(2A)-C(3A)	118.8(3)
C(7A)-C(2A)-C(3A)	110.8(4)
C(2A)-C(3A)-C(4A)	104.7(4)
C(5A)-C(4A)-C(3A)	112.9(6)
C(4A)-C(5A)-C(6A)	113.9(4)
C(7A)-C(6A)-C(5A)	104.0(3)
O(3)-C(7A)-C(2A)	101.6(3)
O(3)-C(7A)-C(6A)	120.1(3)
C(2A)-C(7A)-C(6A)	111.1(4)
C(1)-O(2)-C(2A)	106.71(19)
C(1)-O(2)-C(2)	108.6(4)
C(2A)-O(2)-C(2)	15.7(5)
C(1)-O(3)-C(7)	107.1(4)
C(1)-O(3)-C(7A)	106.92(18)
C(7)-O(3)-C(7A)	20.1(3)

Symmetry transformations used to generate equivalent atoms:

Table C-4. Anisotropic displacement parameters $(\text{Å}^2 \text{x } 10^3)$ for OP212121. The anisotropic displacement factor exponent takes the form: $-2p^2[\ h^2\ a^{*2}U^{11} + ... + 2\ h\ k\ a^*\ b^*\ U^{12}\ ]$

	U^{11}	U^{22}	U^{33}	U^{23}	U^{13}	U^{12}
C(1)	46(1)	31(1)	38(1)	-3(1)	-3(1)	-1(1)
C(2)	39(2)	26(1)	41(2)	0(1)	3(2)	-2(1)
C(3)	36(3)	37(3)	40(3)	-3(2)	8(3)	3(2)
C(4)	48(1)	33(1)	51(1)	-1(1)	7(1)	11(1)
C(5)	42(2)	28(1)	54(2)	6(2)	6(2)	4(1)
C(6)	45(5)	38(3)	42(4)	-4(3)	14(3)	-5(3)
C(7)	35(2)	26(1)	38(2)	2(1)	3(1)	8(1)
C(2A)	39(2)	26(1)	41(2)	0(1)	3(2)	-2(1)
C(3A)	34(1)	42(1)	50(2)	0(1)	8(1)	5(1)
C(4A)	48(1)	33(1)	51(1)	-1(1)	7(1)	11(1)
C(5A)	42(2)	28(1)	54(2)	6(2)	6(2)	4(1)
C(6A)	37(2)	28(1)	53(2)	-2(2)	8(2)	-1(1)
C(7A)	35(2)	26(1)	38(2)	2(1)	3(1)	8(1)
O(1)	74(1)	25(1)	57(1)	-3(1)	-3(1)	0(1)
O(2)	49(1)	30(1)	50(1)	4(1)	10(1)	-4(1)
O(3)	52(1)	26(1)	56(1)	-3(1)	17(1)	5(1)

Table C-5. Hydrogen coordinates (x 10^4) and isotropic displacement parameters ($Å^2$x 10^3) for OP212121.

	x	y	z	U(eq)
H(2A)	1189	9136	843	43
H(3A)	2731	10179	2958	45
H(3B)	278	10039	2660	45
H(4A)	681	11581	1062	53
H(4B)	1583	12419	2140	53
H(5A)	3904	12674	566	49
H(5B)	5065	11873	1589	49
H(6A)	3355	10397	-366	50
H(6B)	5817	10578	-109	50
H(7A)	5245	9441	1690	40
H(2AA)	3519	9280	2391	43
H(3AA)	-66	9944	2405	50
H(3AB)	-94	9879	1044	50
H(4AA)	702	12304	1568	53
H(4AB)	2529	11767	2391	53
H(5AA)	4092	12677	762	49
H(5AB)	2637	11705	-30	49
H(6AA)	5973	10609	-3	47
H(6AB)	6003	10604	1360	47
H(7AA)	2889	9185	32	40

APPENDIX D

SUPPORTING CRYSTALLOGRAPHIC DATA FOR CHAPTER VI
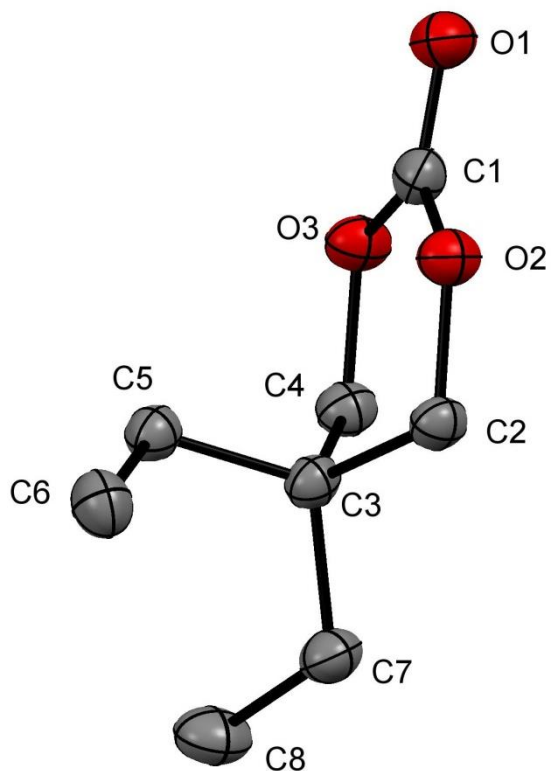
Table D-1. Crystal data and structure refinement for mp21c.

Identification code	mp21c	
Empirical formula	C8 H14 O3	
Formula weight	158.19	
Temperature	110(2) K	
Wavelength	0.71073 Å	
Crystal system	Monoclinic	
Space group	P2(1)/c	
Unit cell dimensions	a = 7.034(9) Å	a= 90°.
	b = 5.695(8) Å	b= 97.506(15)°.
	c = 21.42(3) Å	g = 90°.
Volume	850.6(19) Å^3	

Z	4
Density (calculated)	1.235 Mg/m^3
Absorption coefficient	0.093 mm^{-1}
F(000)	344
Crystal size	0.40 x 0.20 x 0.10 mm^3
Theta range for data collection	1.92 to 28.43°.
Index ranges	-9<=h<=9, -7<=k<=7, -28<=l<=28
Reflections collected	9466
Independent reflections	2100 [R(int) = 0.0486]
Completeness to theta = 28.43°	97.9 %
Absorption correction	Semi-empirical from equivalents
Max. and min. transmission	0.9907 and 0.9637
Refinement method	Full-matrix least-squares on F^2
Data / restraints / parameters	2100 / 0 / 102
Goodness-of-fit on F^2	1.067
Final R indices [I>2sigma(I)]	R1 = 0.0450, wR2 = 0.1242
R indices (all data)	R1 = 0.0648, wR2 = 0.1400
Largest diff. peak and hole	0.219 and -0.271 e.Å^{-3}

Table D-2. Atomic coordinates (x 10^4) and equivalent isotropic displacement parameters (Å ^{2}x 10^3) for mp21c. U(eq) is defined as one third of the trace of the orthogonalized U^{ij} tensor.

	x	y	z	U(eq)
C(1)	2069(2)	2433(2)	2313(1)	27(1)
C(2)	3205(2)	-140(2)	3197(1)	26(1)
C(3)	2764(2)	1815(2)	3645(1)	24(1)
C(4)	897(2)	2906(2)	3332(1)	27(1)
C(5)	4376(2)	3681(2)	3728(1)	27(1)
C(6)	6317(2)	2840(3)	4064(1)	35(1)
C(7)	2420(2)	649(2)	4271(1)	30(1)
C(8)	1980(2)	2347(3)	4787(1)	40(1)
O(1)	1988(2)	2944(2)	1761(1)	35(1)
O(2)	3230(1)	710(2)	2554(1)	29(1)
O(3)	1046(1)	3654(2)	2688(1)	29(1)

Table D-3. Bond lengths [Å] and angles [°] for mp21c.

_____

C(1)-O(1)	1.212(2)
C(1)-O(2)	1.337(2)
C(1)-O(3)	1.3410(19)
C(2)-O(2)	1.462(2)
C(2)-C(3)	1.528(2)
C(3)-C(4)	1.526(2)
C(3)-C(7)	1.544(2)
C(3)-C(5)	1.547(2)
C(4)-O(3)	1.462(2)
C(5)-C(6)	1.534(2)
C(7)-C(8)	1.531(2)
O(1)-C(1)-O(2)	120.15(13)
O(1)-C(1)-O(3)	119.95(14)
O(2)-C(1)-O(3)	119.85(14)
O(2)-C(2)-C(3)	112.25(13)
C(4)-C(3)-C(2)	104.78(12)
C(4)-C(3)-C(7)	109.44(12)
C(2)-C(3)-C(7)	107.44(14)
C(4)-C(3)-C(5)	110.31(14)
C(2)-C(3)-C(5)	111.52(13)
C(7)-C(3)-C(5)	112.99(12)
O(3)-C(4)-C(3)	111.66(11)
C(6)-C(5)-C(3)	115.73(14)
C(8)-C(7)-C(3)	115.15(14)
C(1)-O(2)-C(2)	121.69(11)
C(1)-O(3)-C(4)	121.66(12)

_____

Symmetry transformations used to generate equivalent atoms:

Table D-4. Anisotropic displacement parameters ($\mathring{A}^2$x 10^3) for mp21c. The anisotropic displacement factor exponent takes the form: $-2p^2[\,h^2\,a*^2U^{11} + ... + 2\,h\,k\,a*\,b*\,U^{12}\,]$

	U^{11}	U^{22}	U^{33}	U^{23}	U^{13}	U^{12}
C(1)	29(1)	23(1)	29(1)	0(1)	4(1)	-3(1)
C(2)	31(1)	21(1)	26(1)	3(1)	5(1)	3(1)
C(3)	27(1)	20(1)	26(1)	1(1)	6(1)	1(1)
C(4)	29(1)	26(1)	27(1)	1(1)	8(1)	3(1)
C(5)	30(1)	23(1)	28(1)	0(1)	7(1)	0(1)
C(6)	32(1)	36(1)	35(1)	-5(1)	3(1)	-2(1)
C(7)	35(1)	27(1)	30(1)	4(1)	9(1)	-1(1)
C(8)	49(1)	44(1)	28(1)	2(1)	13(1)	6(1)
O(1)	43(1)	33(1)	29(1)	4(1)	6(1)	-1(1)
O(2)	35(1)	27(1)	27(1)	2(1)	8(1)	6(1)
O(3)	34(1)	27(1)	27(1)	3(1)	6(1)	7(1)

Table D-5. Hydrogen coordinates (x 10^4) and isotropic displacement parameters (Å ^{2}x 10^3) for mp21c.

	x	y	z	U(eq)
H(2A)	4443	-822	3349	31
H(2B)	2246	-1365	3195	31
H(4A)	-131	1768	3328	32
H(4B)	578	4249	3577	32
H(5A)	4564	4263	3315	32
H(5B)	3947	4990	3963	32
H(6A)	6183	2401	4489	52
H(6B)	7240	4085	4068	52
H(6C)	6744	1509	3845	52
H(7A)	1359	-443	4186	36
H(7B)	3550	-255	4429	36
H(8A)	3057	3368	4898	60
H(8B)	1735	1472	5152	60
H(8C)	871	3267	4636	60
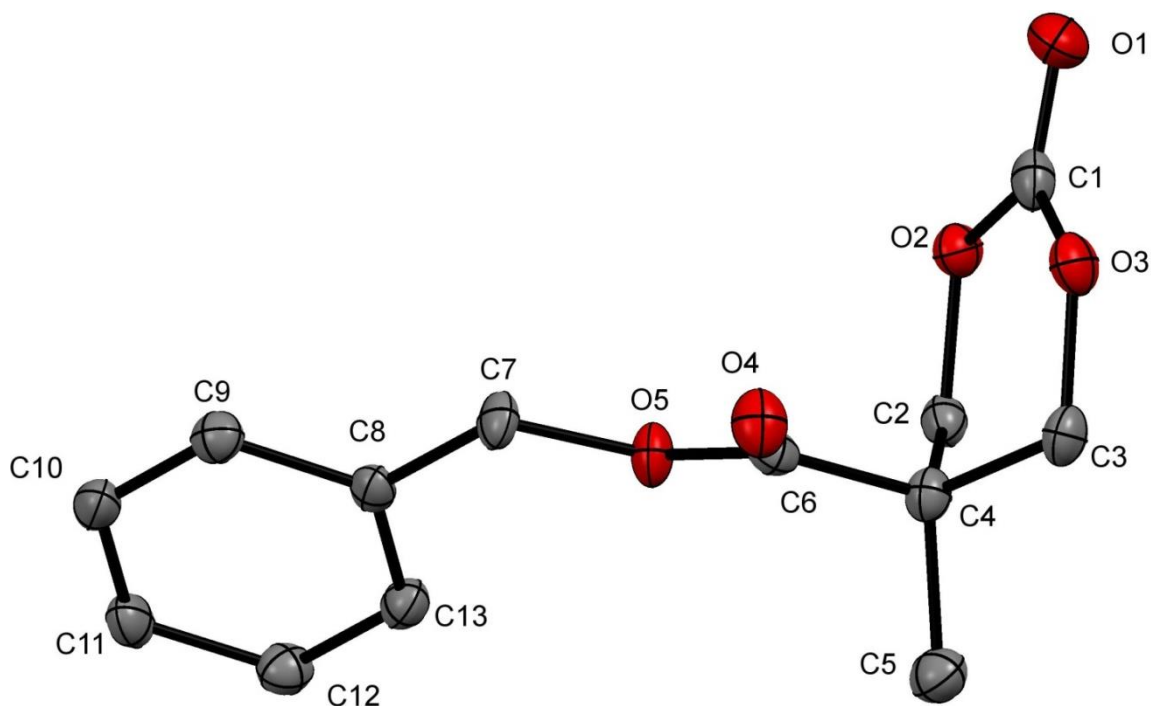
Table D-6. Crystal data and structure refinement for zzz.

Identification code	zzz
Empirical formula	C13 H14 O5
Formula weight	250.24
Temperature	110(2) K
Wavelength	1.54178 Å
Crystal system	Monoclinic
Space group	P21/c
Unit cell dimensions	a = 13.687(2) Å a= 90°.
	b = 5.8122(8) Å b= 91.729(7)°.
	c = 14.776(2) Å g = 90°.
Volume	1175.0(3) Å^3
Z	4
Density (calculated)	1.415 Mg/m^3

Absorption coefficient	0.918 mm^{-1}
F(000)	528
Crystal size	0.18 x 0.08 x 0.04 mm^3
Theta range for data collection	3.23 to 60.00°.
Index ranges	-15<=h<=13, -6<=k<=6, -16<=l<=16
Reflections collected	8823
Independent reflections	1725 [R(int) = 0.0375]
Completeness to theta = 60.00°	98.5 %
Absorption correction	Semi-empirical from equivalents
Max. and min. transmission	0.9642 and 0.8521
Refinement method	Full-matrix least-squares on F^2
Data / restraints / parameters	1725 / 0 / 164
Goodness-of-fit on F^2	1.117
Final R indices [I>2sigma(I)]	R1 = 0.0346, wR2 = 0.0920
R indices (all data)	R1 = 0.0442, wR2 = 0.1072
Largest diff. peak and hole	0.200 and -0.277 e.Å^{-3}

Table D-7. Atomic coordinates (x 10^4) and equivalent isotropic displacement parameters (Å ^{2}x 10^3) for zzz. U(eq) is defined as one third of the trace of the orthogonalized U^{ij} tensor.

	x	y	z	U(eq)
C(1)	966(1)	10920(3)	8022(1)	23(1)
C(2)	1621(1)	8091(3)	6981(1)	19(1)
C(3)	679(1)	11310(3)	6387(1)	22(1)
C(4)	1596(1)	9923(3)	6258(1)	19(1)
C(5)	1551(1)	8782(3)	5317(1)	26(1)
C(6)	2487(1)	11504(3)	6317(1)	19(1)
C(7)	4205(1)	11634(3)	6548(1)	20(1)
C(8)	5059(1)	10076(3)	6389(1)	17(1)
C(9)	5999(1)	10861(3)	6617(1)	21(1)
C(10)	6808(1)	9539(3)	6426(1)	22(1)
C(11)	6693(1)	7401(3)	6026(1)	23(1)
C(12)	5761(1)	6589(3)	5818(1)	23(1)
C(13)	4952(1)	7921(3)	5995(1)	20(1)
O(1)	811(1)	11545(2)	8779(1)	31(1)
O(2)	1523(1)	9078(2)	7880(1)	22(1)
O(3)	619(1)	12141(2)	7315(1)	24(1)
O(4)	2463(1)	13542(2)	6192(1)	26(1)
O(5)	3308(1)	10311(2)	6502(1)	21(1)

Table D-8. Bond lengths [Å] and angles [°] for zzz.

_____

C(1)-O(1)	1.200(2)
C(1)-O(2)	1.335(2)
C(1)-O(3)	1.339(2)
C(2)-O(2)	1.456(2)
C(2)-C(4)	1.508(3)
C(3)-O(3)	1.457(2)
C(3)-C(4)	1.509(2)
C(4)-C(6)	1.527(3)
C(4)-C(5)	1.541(3)
C(6)-O(4)	1.199(2)
C(6)-O(5)	1.342(2)
C(7)-O(5)	1.449(2)
C(7)-C(8)	1.503(3)
C(8)-C(13)	1.387(3)
C(8)-C(9)	1.396(3)
C(9)-C(10)	1.384(3)
C(10)-C(11)	1.382(3)
C(11)-C(12)	1.385(3)
C(12)-C(13)	1.383(3)
O(1)-C(1)-O(2)	120.52(18)
O(1)-C(1)-O(3)	119.89(17)
O(2)-C(1)-O(3)	119.51(17)
O(2)-C(2)-C(4)	111.54(14)
O(3)-C(3)-C(4)	111.50(14)
C(2)-C(4)-C(3)	106.80(15)
C(2)-C(4)-C(6)	112.57(15)
C(3)-C(4)-C(6)	109.66(15)
C(2)-C(4)-C(5)	109.59(15)
C(3)-C(4)-C(5)	109.45(15)
C(6)-C(4)-C(5)	108.72(15)
O(4)-C(6)-O(5)	124.08(16)

O(4)-C(6)-C(4)	124.63(16)
O(5)-C(6)-C(4)	111.27(15)
O(5)-C(7)-C(8)	109.56(15)
C(13)-C(8)-C(9)	118.78(17)
C(13)-C(8)-C(7)	122.45(16)
C(9)-C(8)-C(7)	118.73(16)
C(10)-C(9)-C(8)	120.40(18)
C(11)-C(10)-C(9)	120.28(17)
C(10)-C(11)-C(12)	119.58(17)
C(13)-C(12)-C(11)	120.31(18)
C(12)-C(13)-C(8)	120.62(17)
C(1)-O(2)-C(2)	121.91(14)
C(1)-O(3)-C(3)	122.01(14)
C(6)-O(5)-C(7)	116.00(14)

Symmetry transformations used to generate equivalent atoms:

Table D-9. Anisotropic displacement parameters $(\mathring{A}^2 \times 10^3)$ for zzz. The anisotropic displacement factor exponent takes the form: $-2p^2[\,h^2\,a^{*2}U^{11} + ... + 2\,h\,k\,a^*\,b^*\,U^{12}\,]$

	U^{11}	U^{22}	U^{33}	U^{23}	U^{13}	U^{12}
C(1)	14(1)	22(1)	33(1)	-2(1)	1(1)	-2(1)
C(2)	15(1)	19(1)	23(1)	-3(1)	2(1)	0(1)
C(3)	15(1)	25(1)	27(1)	1(1)	-3(1)	1(1)
C(4)	16(1)	19(1)	23(1)	0(1)	0(1)	1(1)
C(5)	26(1)	26(1)	24(1)	-2(1)	-1(1)	-4(1)
C(6)	20(1)	18(1)	18(1)	-1(1)	2(1)	4(1)
C(7)	14(1)	18(1)	28(1)	-2(1)	-1(1)	-5(1)
C(8)	16(1)	22(1)	14(1)	4(1)	1(1)	-2(1)
C(9)	22(1)	19(1)	20(1)	0(1)	1(1)	-3(1)
C(10)	17(1)	30(1)	19(1)	0(1)	0(1)	-4(1)
C(11)	16(1)	30(1)	22(1)	1(1)	1(1)	5(1)
C(12)	24(1)	21(1)	22(1)	-2(1)	0(1)	2(1)
C(13)	19(1)	22(1)	20(1)	0(1)	-2(1)	-4(1)
O(1)	27(1)	38(1)	28(1)	-9(1)	5(1)	3(1)
O(2)	18(1)	24(1)	23(1)	-2(1)	-1(1)	5(1)
O(3)	18(1)	25(1)	31(1)	0(1)	2(1)	6(1)
O(4)	23(1)	18(1)	38(1)	1(1)	1(1)	1(1)
O(5)	13(1)	19(1)	32(1)	2(1)	0(1)	0(1)

Table D-10. Hydrogen coordinates (x 10^4) and isotropic displacement parameters ($\mathring{A}^2$x 10^3) for zzz.

	x	y	z	U(eq)
H(2A)	1093	7007	6863	23
H(2B)	2233	7256	6959	23
H(3A)	671	12611	5976	27
H(3B)	112	10364	6241	27
H(5A)	2145	7949	5225	38
H(5B)	1472	9946	4859	38
H(5C)	1006	7741	5279	38
H(7A)	4281	12356	7138	24
H(7B)	4180	12837	6092	24
H(9)	6082	12282	6899	25
H(10)	7432	10091	6566	27
H(11)	7237	6513	5899	27
H(12)	5680	5142	5558	27
H(13)	4330	7367	5848	24
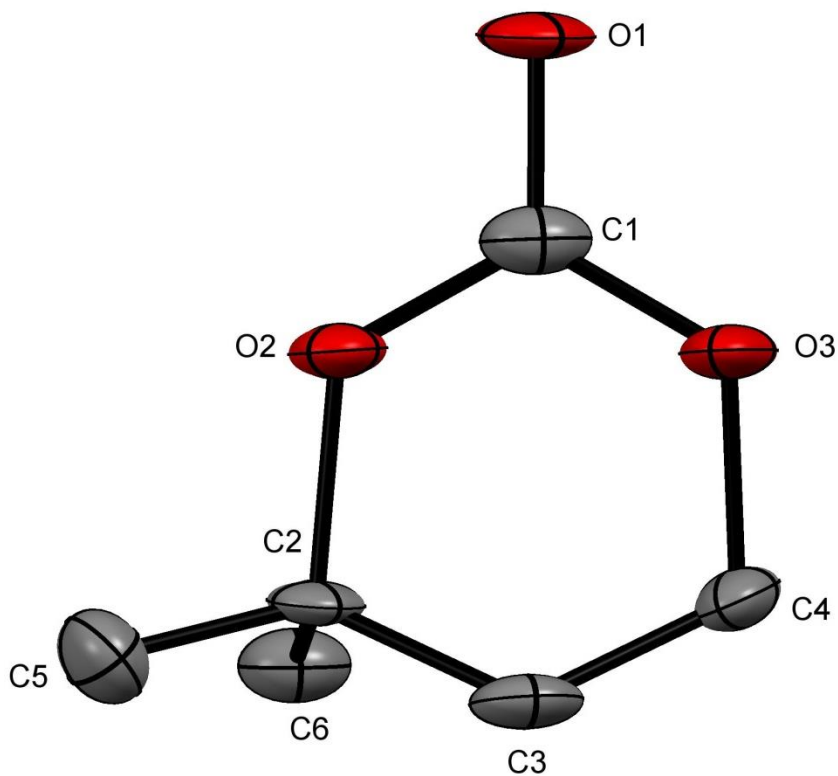
Table D-11. Crystal data and structure refinement for 1.

Identification code	1
Empirical formula	C6 H10 O3
Formula weight	130.14
Temperature	110(2) K
Wavelength	0.71073 Å
Crystal system	Orthorhombic
Space group	P2(1)2(1)2(1)
Unit cell dimensions	a = 6.178(12) Å a= 90°.
	b = 7.403(14) Å b= 90°.
	c = 13.76(2) Å g = 90°.
Volume	629(2) Å^3
Z	4
Density (calculated)	1.373 Mg/m^3
Absorption coefficient	0.110 mm^{-1}
F(000)	280
Crystal size	0.40 x 0.20 x 0.10 mm^3

Theta range for data collection   2.96 to 25.03°.

Index ranges   -7<=h<=2, -7<=k<=8, -15<=l<=15

Reflections collected   1493

Independent reflections   993 [R(int) = 0.0328]

Completeness to theta = 25.03°   96.2 %

Absorption correction   Semi-empirical from equivalents

Max. and min. transmission   0.9891 and 0.9574

Refinement method   Full-matrix least-squares on F^2

Data / restraints / parameters   993 / 0 / 84

Goodness-of-fit on F^2 1.153

Final R indices [I>2sigma(I)]   R1 = 0.0611, wR2 = 0.1696

R indices (all data)   R1 = 0.0684, wR2 = 0.1789

Absolute structure parameter   -4(3)

Largest diff. peak and hole   0.258 and -0.346 e.Å^{-3}

Table D-12. Atomic coordinates (x 10^4) and equivalent isotropic displacement parameters (Å^{2}x 10^3) for 1. U(eq) is defined as one third of the trace of the orthogonalized U^{ij} tensor.

	x	y	z	U(eq)
C(1)	2052(6)	10905(5)	4728(3)	28(1)
C(2)	2863(6)	9013(5)	6167(3)	24(1)
C(3)	1435(6)	10363(6)	6674(3)	28(1)
C(4)	1837(6)	12214(5)	6320(3)	27(1)
C(5)	2142(7)	7131(5)	6315(3)	34(1)
C(6)	5207(6)	9224(6)	6405(3)	30(1)
O(1)	1929(4)	11040(4)	3867(2)	33(1)
O(2)	2634(4)	9337(3)	5115(2)	27(1)
O(3)	1535(4)	12272(4)	5278(2)	31(1)

Table D-13. Bond lengths [Å] and angles [°] for 1.

_____

C(1)-O(1)	1.192(5)
C(1)-O(3)	1.303(5)
C(1)-O(2)	1.327(5)
C(2)-O(2)	1.475(5)
C(2)-C(5)	1.476(6)
C(2)-C(6)	1.492(6)
C(2)-C(3)	1.504(6)
C(3)-C(4)	1.475(7)
C(4)-O(3)	1.448(5)
O(1)-C(1)-O(3)	119.8(4)
O(1)-C(1)-O(2)	119.3(4)
O(3)-C(1)-O(2)	120.9(3)
O(2)-C(2)-C(5)	105.0(3)
O(2)-C(2)-C(6)	106.9(3)
C(5)-C(2)-C(6)	111.2(4)
O(2)-C(2)-C(3)	106.9(3)
C(5)-C(2)-C(3)	112.7(4)
C(6)-C(2)-C(3)	113.5(4)
C(4)-C(3)-C(2)	111.5(4)
O(3)-C(4)-C(3)	109.4(3)
C(1)-O(2)-C(2)	124.2(3)
C(1)-O(3)-C(4)	121.4(3)

_____

Symmetry transformations used to generate equivalent atoms:

Table D-14. Anisotropic displacement parameters ($\text{Å}^2\text{x }10^3$) for 1. The anisotropic displacement factor exponent takes the form: $-2p^2[\ h^2\ a^{*2}U^{11} + ... + 2\ h\ k\ a^*\ b^*\ U^{12}\ ]$

	U^{11}	U^{22}	U^{33}	U^{23}	U^{13}	U^{12}
C(1)	22(2)	45(3)	16(2)	2(2)	0(2)	0(2)
C(2)	30(2)	35(2)	7(2)	4(2)	-3(1)	3(2)
C(3)	26(2)	47(3)	10(2)	2(2)	2(2)	0(2)
C(4)	36(2)	30(2)	14(2)	-6(2)	-2(2)	6(2)
C(5)	43(2)	28(2)	32(3)	7(2)	0(2)	-1(2)
C(6)	27(2)	45(3)	19(2)	2(2)	-1(2)	-1(2)
O(1)	38(2)	53(2)	8(1)	4(1)	-2(1)	6(2)
O(2)	36(2)	36(2)	10(2)	1(1)	-1(1)	3(1)
O(3)	47(2)	37(2)	10(2)	2(1)	1(1)	8(1)

Table D-15. Hydrogen coordinates (x 10^4) and isotropic displacement parameters (Å^2x 10^3) for 1.

	x	y	z	U(eq)
H(3A)	-101	10044	6560	33
H(3B)	1707	10312	7382	33
H(4A)	824	13065	6639	32
H(4B)	3332	12584	6485	32
H(5A)	634	7009	6103	51
H(5B)	2253	6821	7005	51
H(5C)	3059	6315	5934	51
H(6A)	5447	8919	7089	46
H(6B)	5648	10477	6288	46
H(6C)	6063	8415	5993	46
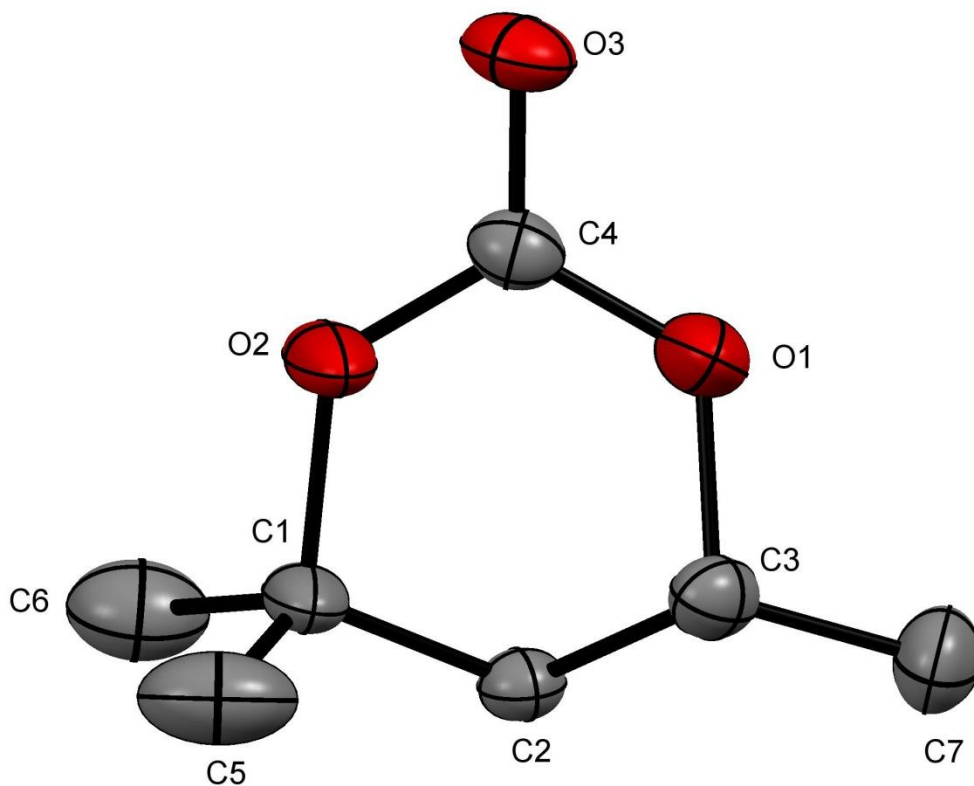
Table D-16. Crystal data and structure refinement for mp21c.

Identification code	mp21c	
Empirical formula	C7 H12 O3	
Formula weight	144.17	
Temperature	110(2) K	
Wavelength	0.71073 Å	
Crystal system	Monoclinic	
Space group	P2(1)/c	
Unit cell dimensions	a = 7.162(5) Å	a= 90°.
	b = 8.323(6) Å	b= 92.747(8)°.
	c = 12.984(9) Å	g = 90°.
Volume	773.1(10) Å^3	
Z	4	
Density (calculated)	1.239 Mg/m^3	

Absorption coefficient	0.096 mm^{-1}
F(000)	312
Crystal size	0.25 x 0.23 x 0.18 mm^3
Theta range for data collection	2.85 to 27.50°.
Index ranges	-9<=h<=9, -10<=k<=10, -16<=l<=16
Reflections collected	8566
Independent reflections	1778 [R(int) = 0.0363]
Completeness to theta = 27.50°	100.0 %
Absorption correction	Semi-empirical from equivalents
Max. and min. transmission	0.9829 and 0.9764
Refinement method	Full-matrix least-squares on F^2
Data / restraints / parameters	1778 / 5 / 105
Goodness-of-fit on F^2	1.084
Final R indices [I>2sigma(I)]	R1 = 0.0619, wR2 = 0.1499
R indices (all data)	R1 = 0.0689, wR2 = 0.1548
Largest diff. peak and hole	0.401 and -0.420 e.Å^{-3}

Table D-17. Atomic coordinates (x 10^4) and equivalent isotropic displacement parameters ($\mathring{A}^2$x 10^3) for mp21c. U(eq) is defined as one third of the trace of the orthogonalized U^{ij} tensor.

	x	y	z	U(eq)
O(1)	10112(2)	8673(2)	6108(1)	51(1)
O(2)	9415(2)	11002(2)	6910(1)	53(1)
O(3)	12298(2)	10346(2)	6636(1)	40(1)
C(1)	7363(2)	10772(2)	6800(2)	37(1)
C(2)	6931(3)	9417(3)	6013(2)	26(1)
C(3)	8225(3)	8030(3)	6251(2)	31(1)
C(7)	8020(30)	6652(10)	5499(16)	42(1)
C(2A)	6955(8)	8930(5)	6684(4)	26(1)
C(3A)	8057(6)	8476(8)	5774(5)	31(1)
C(7A)	8010(80)	6700(30)	5530(40)	42(1)
C(4)	10657(2)	10017(2)	6559(1)	29(1)
C(5)	6715(3)	10653(4)	7869(2)	58(1)
C(6)	6637(3)	12272(3)	6280(2)	55(1)

Table D-18. Bond lengths [Å] and angles [°] for mp21c.

_____

O(1)-C(4)	1.313(2)
O(1)-C(3)	1.474(3)
O(1)-C(3A)	1.523(4)
O(2)-C(4)	1.307(2)
O(2)-C(1)	1.482(2)
O(3)-C(4)	1.206(2)
C(1)-C(5)	1.488(3)
C(1)-C(6)	1.500(3)
C(1)-C(2)	1.544(3)
C(1)-C(2A)	1.567(5)
C(2)-C(3)	1.503(3)
C(2)-H(2A)	0.9900
C(2)-H(2B)	0.9900
C(3)-C(7)	1.509(8)
C(3)-H(3)	1.0000
C(7)-H(7A)	0.9800
C(7)-H(7B)	0.9800
C(7)-H(7C)	0.9800
C(2A)-C(3A)	1.501(5)
C(2A)-H(2AA)	0.9900
C(2A)-H(2AB)	0.9900
C(3A)-C(7A)	1.509(9)
C(3A)-H(3A)	1.0000
C(7A)-H(7AA)	0.9800
C(7A)-H(7AB)	0.9800
C(7A)-H(7AC)	0.9800
C(5)-H(5A)	0.9800
C(5)-H(5B)	0.9800
C(5)-H(5C)	0.9800
C(6)-H(6A)	0.9800
C(6)-H(6B)	0.9800
C(6)-H(6C)	0.9800

C(4)-O(1)-C(3)	120.51(15)
C(4)-O(1)-C(3A)	118.7(3)
C(3)-O(1)-C(3A)	28.0(2)
C(4)-O(2)-C(1)	125.00(15)
O(2)-C(1)-C(5)	105.70(16)
O(2)-C(1)-C(6)	104.91(17)
C(5)-C(1)-C(6)	110.99(19)
O(2)-C(1)-C(2)	108.93(14)
C(5)-C(1)-C(2)	120.47(19)
C(6)-C(1)-C(2)	104.85(18)
O(2)-C(1)-C(2A)	108.4(2)
C(5)-C(1)-C(2A)	87.6(3)
C(6)-C(1)-C(2A)	135.4(3)
C(2)-C(1)-C(2A)	36.0(2)
C(3)-C(2)-C(1)	108.85(18)
C(3)-C(2)-H(2A)	109.9
C(1)-C(2)-H(2A)	109.9
C(3)-C(2)-H(2B)	109.9
C(1)-C(2)-H(2B)	109.9
H(2A)-C(2)-H(2B)	108.3
O(1)-C(3)-C(2)	104.79(18)
O(1)-C(3)-C(7)	104.7(8)
C(2)-C(3)-C(7)	114.3(8)
O(1)-C(3)-H(3)	110.9
C(2)-C(3)-H(3)	110.9
C(7)-C(3)-H(3)	110.9
C(3A)-C(2A)-C(1)	102.7(4)
C(3A)-C(2A)-H(2AA)	111.2
C(1)-C(2A)-H(2AA)	111.2
C(3A)-C(2A)-H(2AB)	111.2
C(1)-C(2A)-H(2AB)	111.2
H(2AA)-C(2A)-H(2AB)	109.1
C(2A)-C(3A)-C(7A)	114(2)

C(2A)-C(3A)-O(1)	106.6(4)
C(7A)-C(3A)-O(1)	100(2)
C(2A)-C(3A)-H(3A)	111.8
C(7A)-C(3A)-H(3A)	111.8
O(1)-C(3A)-H(3A)	111.8
C(3A)-C(7A)-H(7AA)	109.5
C(3A)-C(7A)-H(7AB)	109.5
H(7AA)-C(7A)-H(7AB)	109.5
C(3A)-C(7A)-H(7AC)	109.5
H(7AA)-C(7A)-H(7AC)	109.5
H(7AB)-C(7A)-H(7AC)	109.5
O(3)-C(4)-O(2)	120.33(17)
O(3)-C(4)-O(1)	119.85(16)
O(2)-C(4)-O(1)	119.81(15)
C(1)-C(5)-H(5A)	109.5
C(1)-C(5)-H(5B)	109.5
H(5A)-C(5)-H(5B)	109.5
C(1)-C(5)-H(5C)	109.5
H(5A)-C(5)-H(5C)	109.5
H(5B)-C(5)-H(5C)	109.5
C(1)-C(6)-H(6A)	109.5
C(1)-C(6)-H(6B)	109.5
H(6A)-C(6)-H(6B)	109.5
C(1)-C(6)-H(6C)	109.5
H(6A)-C(6)-H(6C)	109.5
H(6B)-C(6)-H(6C)	109.5

_____

Symmetry transformations used to generate equivalent atoms:

Table D-19. Anisotropic displacement parameters ($\mathring{A}^2$x 10^3) for mp21c. The anisotropic displacement factor exponent takes the form: $-2p^2[\,h^2\,a^{*2}U^{11} + ... + 2\,h\,k\,a^*\,b^*\,U^{12}\,]$

	U^{11}	U^{22}	U^{33}	U^{23}	U^{13}	U^{12}
O(1)	27(1)	49(1)	78(1)	-24(1)	13(1)	-4(1)
O(2)	19(1)	54(1)	84(1)	-36(1)	1(1)	-3(1)
O(3)	21(1)	56(1)	42(1)	-2(1)	0(1)	-2(1)
C(1)	17(1)	37(1)	56(1)	-16(1)	0(1)	0(1)
C(2)	21(1)	29(1)	28(1)	1(1)	-1(1)	-2(1)
C(3)	28(1)	27(1)	36(1)	5(1)	2(1)	-1(1)
C(7)	45(1)	31(1)	51(1)	-8(1)	1(1)	1(1)
C(2A)	21(1)	29(1)	28(1)	1(1)	-1(1)	-2(1)
C(3A)	28(1)	27(1)	36(1)	5(1)	2(1)	-1(1)
C(7A)	45(1)	31(1)	51(1)	-8(1)	1(1)	1(1)
C(4)	24(1)	35(1)	26(1)	3(1)	-1(1)	1(1)
C(5)	35(1)	87(2)	51(1)	18(1)	-1(1)	-13(1)
C(6)	38(1)	73(2)	53(1)	10(1)	-4(1)	-4(1)

Table D-20. Hydrogen coordinates (x 10^4) and isotropic displacement parameters ($\mathring{A}^2$x 10^3) for mp21c.

	x	y	z	U(eq)
H(2A)	5616	9066	6054	31
H(2B)	7110	9813	5305	31
H(3)	8101	7648	6975	37
H(7A)	8233	7040	4801	63
H(7B)	6761	6201	5519	63
H(7C)	8944	5819	5688	63

H(2AA)	7392	8333	7309	31
H(2AB)	5604	8725	6547	31
H(3A)	7707	9146	5155	37
H(7AA)	8746	6499	4923	63
H(7AB)	6710	6371	5374	63
H(7AC)	8529	6095	6117	63
H(5A)	7235	9681	8198	87
H(5B)	5347	10600	7848	87
H(5C)	7137	11599	8265	87
H(6A)	6998	13208	6703	82
H(6B)	5271	12217	6198	82
H(6C)	7168	12371	5601	82